HELMUT SCHMIDT UNIVERSITÄT
Universität der Bundeswehr Hamburg

Karl Frederik Blender

Adsorption Process Development for the Separation of Toxic Gaseous Components

Adsorption Process Development for the Separation of Toxic Gaseous Components

Von der Fakultät für Maschinenbau

der Helmut-Schmidt-Universität / Universität der Bundeswehr Hamburg

zur Erlangung des akademischen Grades eines Doktor-Ingenieurs

genehmigte

DISSERTATION

vorgelegt von

Karl Frederik Blender

aus Eckernförde

Hamburg 2020

Tag der mündlichen Prüfung:	16. Dezember 2019
Erster Gutachter:	Univ.-Prof. Dr.-Ing. Bernd Niemeyer Helmut-Schmidt-Universität / Universität der Bundeswehr Hamburg
Zweiter Gutachter:	Univ.-Prof. Dr.-Ing. Karsten Meier Helmut-Schmidt-Universität / Universität der Bundeswehr Hamburg

Adsorption Process Development for the Separation of Toxic Gaseous Components

Doctoral Thesis

approved by the

Department of Mechanical Engineering

of the

Helmut-Schmidt-University

University of German Federal Armed Forces

for obtaining the academic degree of

Doktor Ingenieur (Dr.-Ing.)

presented by

Karl Frederik Blender

from Eckernförde, Germany

Hamburg 2020

Day of completion of the oral examination:	December 16th, 2019
First referee:	Univ.-Prof. Dr.-Ing. Bernd Niemeyer Helmut-Schmidt-University / University of German Federal Armed Forces
Second referee:	Univ.-Prof. Dr.-Ing. Karsten Meier Helmut-Schmidt-University / University of German Federal Armed Forces

Acknowledgements

This dissertation was developed in the course of my work as a scientific assistant at the Chair of Process Engineering with Focus on Separation Technology at Helmut-Schmidt-University / University of the Bundeswehr Hamburg.

My special thanks go to Professor Dr.-Ing. Bernd Niemeyer for the challenging topics and the extraordinarily intensive and instructive scientific supervision.

I would like to thank Professor Dr.-Ing. Karsten Meier for taking over the co-lecture and his dedication on this project.

Furthermore, my thanks to my colleagues Helena Horn, M Sc., Christian Hermann, M. Sc., Dr. rer. nat. Stephan Lassen and Johann Puerta, M. Sc. for an uncountable number of discussions and the notably friendly and accommodating atmosphere.

For the support in the laboratory I would like to thank Tatjana Distel and the tireless student assistants Max Egbers, M.Sc., Tristan Eden, M.Sc., and Markus Schwarz, M.Sc.

Thanks also go to the numerous students who contributed significantly to the results listed here with their student research papers, bachelor and master theses. Representative for all of them, especially Daniel Dorn, M.Sc., and Chris Boysen, M.Sc. should be mentioned here.

Big thanks also to my wonderful family for giving me the freedom and the necessary support without which it would have not been possible to pursue my scientific researches.

Table of Contents

Latin minuscules

Symbol	Unit	Meaning
c	ppm_v	Concentration
$c\ (t)$	ppm_v	Concentration to a certain time
c_0	ppm_v	Initial concentration
c_{LC}	ppm_v	Lethal concentration
c_r	[-]	Relative concentration
d	M	Thickness
f_{le}	µg mol^{-1}	Substance quantity-related efficiency of a bound ligand
k	$mol^{1-n}\ (L^{n-1}\ s)^{-1}$	Rate constant
l	M	Length
m_a	g	Mass of adsorptive
m_{ad}	g	Mass of a dried and unloaded adsorbent
m_{al}	g	Mass of an adsorbent after adsorption
m_{bad}	g	Mass of weighing glass incl. cap and dried, unloaded adsorbent
m_{bal}	g	Mass of weighing glass with cap and loaded adsorbent
m_l	g	Mass of adsorpt bound onto the adsorbent
n	mol	Amount of substance
n_a	mol	Substance amount of an adsorptive
n_i	mol	Share of a corresponding total amount of substance

n_l	mol	Amount of substance loaded onto an adsorbent
n_l	mol	Amount of substance loaded onto adsorbent
n_{tot}	mol	Total amount of substance
p	Pa	Pressure
p_0	kPa	Vapour pressure
p_i	kPa	Share of a corresponding total pressure
p_{tot}	kPa	Overall pressure
q	µg g^{-1}	Relative load per weight onto an adsorbent
$q_{l;A}$	µmol m^{-2}	Ligand's density on adsorbent's surface relative to surface
$q_{l;w}$	mmol g^{-1}	Ligand's density on adsorbent's surface relative to weight
q_m	µg	Monolayer load
q_{max}	g g-1	Maximal possible load
q_r	g m^{-2}	Relative load per surface on an adsorbent
q_{r+}	g m^{-2}	Additional relative load per surface onto an adsorbent
r	m	Coordinate on a radius
r_a	(µg m^{-2}) min^{-1}	Mean adsorption rate
$\bar{t}$	s	Average resting time of particles in a reactor

Latin majuscules

Symbol	Unit	Meaning
A, B, C	[-]	Empirical, substance-specific parameters for the Antoine equation
A_{BET}	$m^2\ g^{-1}$	Specific surface calculated by BET-method
A_S	m^2	Adsorbent's surface
D	$m^2\ s^{-1}$	Diffusion coefficient
$F(t)$	[-]	Cumulative distribution function
$K_A; K_B$	[-]	Equilibrium constants
K_{BET}	[-]	BET adsorption coefficient
K_F	[-]	Freundlich adsorption coefficient
K_H	[-]	Henry adsorption coefficient
K_L	[-]	Langmuir adsorption coefficient
L	$g\ L^{-1}$	Solubility product
M	$g\ mol^{-1}$	Molar mass
T	K	Temperature
T_{Des}	°C	Desorption temperature
V	m^3	Volume
$\dot{V}$	$m^3\ s^{-1}$	Volume flow
V_p	$cm^3\ g^{-1}$	Pore volume

Greek minuscules

Symbol	Unit	Meaning
$\alpha_{A,B}$	$[-]$	Selectivity
δ	µm	Thickness of boundary layers
ε_p	$[-]$	Porosity
λ	m	Wavelength
ρ_a	kg m^{-3}	Seeming density
ρ_s	kg m^{-3}	Apparent density
ρ_w	kg m^{-3}	True density
σ_i	[-]	Fraction of surface covered with gases
τ	s	Fluid dynamic resting time
φ	[-]	Saturation degree
φ_{rh}	% rh	Relative humidity

Greek majuscules and other symbols

Symbol	Unit	Meaning
Θ	[-]	Covering degree
∂_{eff}	m^2 s^{-1}	Transport coefficient

Abbreviations

Abbreviation	Meaning
AC	Active Carbon
BET	Isotherm model of Brunauer, Emmet and Teller
DIN	Deutsches Institut für Normung (German Institute for Industrial Standards)
FID	Flame Ionisation Detector
GC	Gas chromatography
GDP	Gross domestic product
HSU	Helmut-Schmidt-University / University of German Federal Armed Forces
MS	Mass spectrometry
PPE	Personal protective equipment
ppb	Parts per billion
ppm_v	Parts per million (volumetric)
TIC	Toxic Industrial Compound
VOC	Volatile Organic Compound

1 Introduction

There are different reasons why certain components should be separated from the ambient air or other gas mixtures. In addition to the recovery of recyclable materials, in many cases this involves the removal of pollutants that are dangerous for humans and the environment.

Since 1990, the German Federal Environment Agency has been publishing the emission levels of certain pollutants for public information. Figure 1 shows the values for carbon monoxide, ammonia, and volatile organic compounds without methane (VOC).

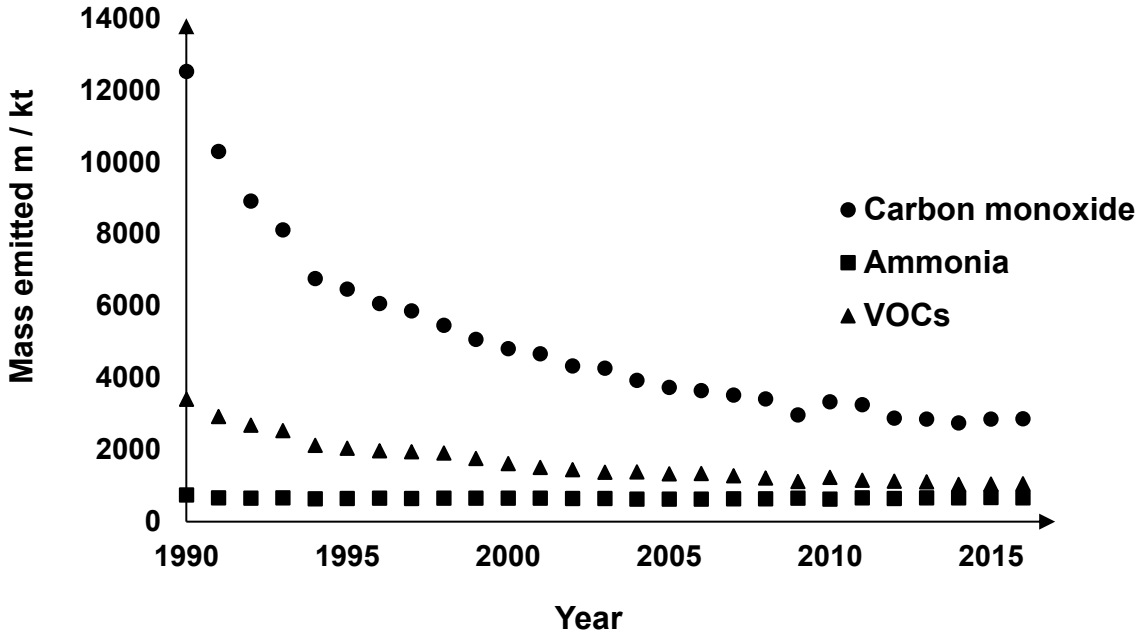

Figure 1: Emissions of carbon monoxide, ammonia and volatile organic compounds except methane in Germany from 1990 to 2016 (1)

It is essential in all these considerations that it has been possible to significantly reduce emissions of carbon monoxide and volatile hydrocarbon compounds since 1990. Ammonia emissions fell by slightly more than 10% between 1990 and 2016, volatile organic compounds by 69% and carbon monoxide emissions by 77% over the same period. On the other side, for all three pollutants considered, there has also been a contrary trend latest since 2014, with the total balance of pollutants emitted rising again. But independent of this slight increase, stagnation can be observed for all three emissions. This has been the case for volatile organic compounds and carbon monoxide since 2009. In 2010, all investigated values increased again. Ammonia has

been emitted to a comparably constant extent since 1991. No significant progress can therefore be discerned here.

It is noteworthy that the largest share of each emission can always be attributed to industrial processes. The economy therefore plays an important role in this context. The drop of pollutants emitted in 2009 can also be seen in the reduced economic output in line with the gross domestic product of the same year as shown in Figure 2.

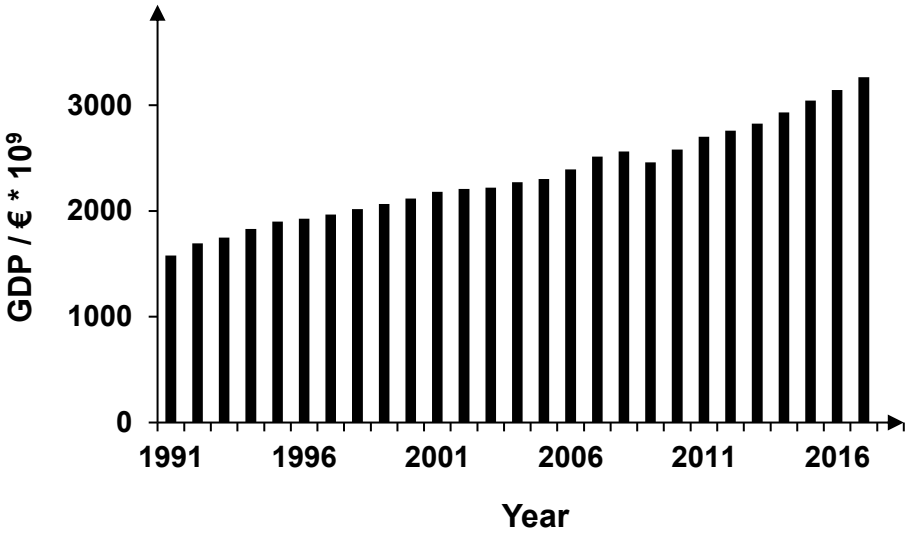

Figure 2: German annual gross domestic product (GDP) from 1991 to 2017 (2)

The graph also reveals another trend. In recent decades, despite an increase in economic output, emissions of these pollutants have been reduced. This is no longer the case in the current decade. On the contrary, it can be assumed that the pollution load increases with production. This leads to the necessity of new and improved approaches to exhaust gas purification, if necessary, also via post-processing of the already conventionally purified exhaust gases. In addition, the protection of the individual human being is of utmost importance.

The goal of the engineering sciences of our time must be to combine two opposing requirements. On the one hand, it is important to maintain and, if possible, improve the standard of living achieved. A reduction will not be accepted by the population. On the other hand, the focus must be on protecting people and the environment. Increasing productivity and the associated prosperity must not lead to an increasing threat to them. The goal must be environmentally and resource-neutral production. Stagnation in the improvement of one of the two parameters endangers prosperity and must be approached creatively.

The aim of the present work is to achieve performance increases in the separation of certain pollutants, in particular carbon monoxide, ammonia, hydrogen sulphide and cyclohexane, from the air by skilfully adapting certain adsorbents with the aid of selected functionalisation methods. In addition, it is shown which analytical methods can be used to characterise the performance of the adsorbents investigated.

At the beginning, the work deals with the theoretical basics of adsorption from the gas phase. In a further section, the starting materials used for this as well as their functionalisation and characterisation are explained. Finally, extensive series of experiments determine the performance of individual materials for adsorption and their improved versions in the separation of various gaseous pollutants.

2 Adsorption

In general, adsorption is a highly effective separation method. It also offers a high potential for removing gaseous components from the ambient air, even for low concentrations (3 pp. 1-2). Different types of coal are utilised in the gas phase for the reduction of displeasing odours since the 18th century, at the latest. With the beginning of the 20th century, industrial plants were built to produce activated carbon. When the Bayer process was developed in 1916, activated carbon found wide use for the separation of organic vapours from exhaust gases. Since the 1970s, the environmental protection regulations became more stringent. Therefore, adsorption has come back into focus as a separation technique, e.g. in odour intensive industries like the chocolate and cocoa production (4 p. 4; 5 p. 12; 6 p. 117 ff.; 7 p. 31 ff.; 8 p. 239 ff.).

2.1 Fundamentals of Adsorption

Adsorption is a thermal separation process by the binding of molecules out of a fluid phase, i.e. liquid or gaseous, onto the surface of a solid phase and can be described as

$$A + B + S \rightleftharpoons A + B \vdots S \qquad (1)$$

where A and B are parts of such a fluid phase and S represents the surface of a solid phase. The affinity between component B and the active surface S is higher compared to the affinity between the other component A and S. Thus, it is possible to separate B from A by this technique. The binding of component B onto the surface S is symbolised by three dots at the right side of the equation. The back reaction is called desorption. In Figure 3, the normed vocabulary is presented.

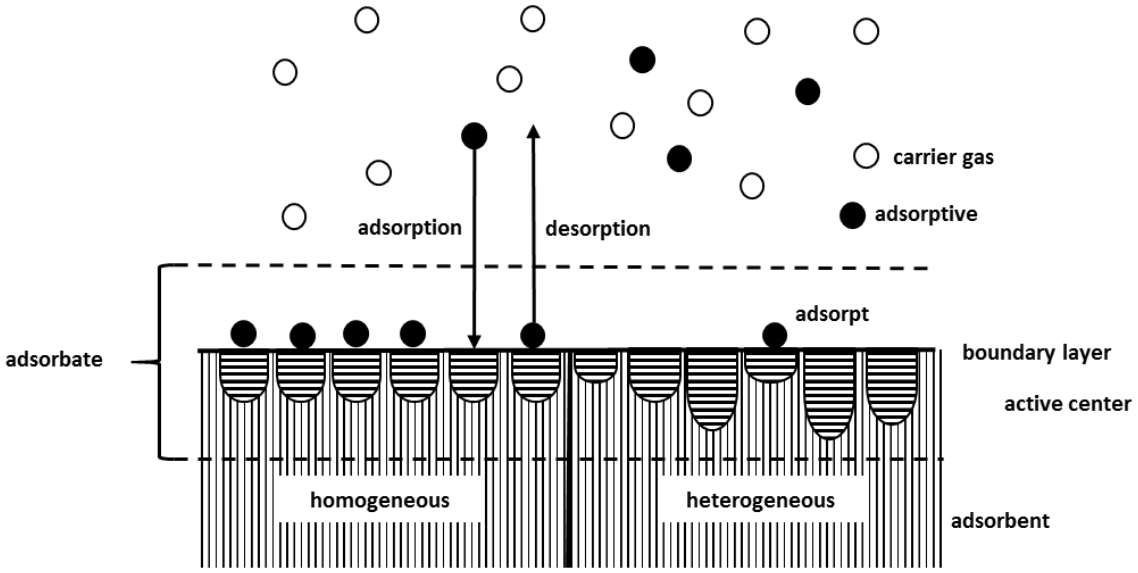

Figure 3: Vocabulary for adsorption processes in a schematic depiction (4 p. 5)

In the depiction, a carrier gas (white dots) transports another phase, which is to be separated and called adsorptive (black dots). Between adsorptive and adsorbent, which is the solid material for the separation, physical interaction and, sometimes, chemical forces, lead to a drawing force. As soon as the adsorptive is bound onto the boundary layer, it is further called adsorpt. The combination of adsorbent and adsorpt bound on the active surface is called adsorbate. The structure of the surface of the adsorbent can be homogeneous or heterogeneous (3 p. 1; 9 p. 19; 10 p. 467; 11 pp. 2-6). As measurements have shown, only heterogeneous surfaces are of interest in this book. These are different to homogeneous surfaces. The heterogeneity results from different pore widths and pore depths.

According to Wedler, a distinction can be made between several forces that play a role in adsorption. These are the repulsion forces, and the relatively far-reaching dispersion forces, which are both largely independent from polarity. If polarity nevertheless played a role, dipole interactions and valence forces should also be mentioned. In addition, with increasing loading, interactions between the adsorptive molecules or atoms also become relevant (12 pp. 15-16). These forces depend on the chemical nature of the adsorbent and adsorptive, the special properties of the surface of the adsorbent and, in particular, the pressure of the adsorptive in the gas phase and the adsorption temperature. Further, the presence of other adsorptives in the gas phase plays a decisive role (13 pp. 387-388). In its entirety, the process is fundamentally exothermic. Consequently, the adsorption capacity decreases progressively as the temperature rises, until it finally reverses, and desorption occurs. This effect can also be seen when

the ambient pressure is reduced (4 p. 4 f.; 10 p. 499 ff.). These two desorption techniques play an important role in the following scientific research.

2.1.1 Equilibrium

The first main parameter for the characterization of adsorption processes is the equilibrium as already mentioned in equation (1). It occurs when the flow of adsorbed molecules equals the flow of desorbed molecules. Therefore, the relative load of the adsorbent q_r is a function of temperature T and the equilibrium pressure p. Consequently, the following relation applies

$$q_r = q_r(T, p) \tag{2}$$

and for T = const, what depicts an isotherm

$$q_r = q_r(p) \tag{3}$$

Literature mostly names a certain temperature, at which, depending on different given concentrations c of the adsorptive, or alternatively different partial pressures p/p_0, the mass of adsorptive adsorbed per surface of the adsorbent q after an infinite time is investigated. Especially in the standards of adsorption, Henry, Freundlich and Brunauer, Emmet and Teller defined the load as the mass of the bonded adsorptive m_a over the weight of the unloaded adsorbent m_{ad}. Thus, it defines a dimensionless quantity. The results are depicted then in a diagram displaying the load over the saturation degree φ of the adsorptive. This results in an isotherm, which shows the performance of an adsorbent in the separation of a specific component. Such a diagram is given in Figure 4, where the dimensionless loads q of different models of adsorption isotherms are plotted over a saturation degree φ. In scientific history until today, several researchers modelled mathematically different phenomena they found during different adsorption processes (14 p. 16). The most important ones are explained below.

The simplest equation describing an isotherm was derived by Henry (15 pp. 41-42). Several factors were not considered. This concerns the finiteness of adsorption spaces as well as reactions between the molecules of the adsorptive or energetically different levels of the adsorption spaces, or a potential multilayer coverage, respectively. For the Henry model, a space of endless and constant adsorption conditions is assumed, which leads to a linear correlation between the load q and the saturation degree φ. For

the proportionality, K_H - a dimensionless Henry constant, must be introduced. The isotherm can then be modelled mathematically by

$$q = K_H \cdot \varphi \qquad (4)$$

This correlation applies in particular at extremely low concentrations, as linear regressions of the measurement data are sufficiently precise in this range.

In comparison to Henry, the Langmuir isotherm respects the finiteness of active spaces for adsorption on the surface of the adsorbent. Here, it is assumed that the surface is covered by a monomolecular layer, for the fluid phase, the ideal gas law is valid and there are no mutual reactions between the adsorpt molecules and the molecules of the fluid phase. The equation for the isotherm can then be written as

$$q = \frac{K_L * q_{max} * \varphi}{1 + K_L * \varphi} \qquad (5)$$

where q_{max} describes the maximal possible load and K_L the Langmuir-coefficient. The model applies, if the covering degree $\Theta = \frac{q}{q_{max}}$ is smaller than one (3 p. 23).

Markham and Benton postulated, that the inverted equation, written as

$$\frac{1}{q} = \frac{1}{K_L\, q_{max}} \frac{1}{\varphi} + \frac{1}{q_{max}} \qquad (6)$$

should ideally result in a line, when the inverted load is plotted against the inverted concentration of the adsorbent (16 p. 502). This is a very practical method to verify, whether the assumption that an isotherm is of Langmuir type, is correct or not. On the other hand, there is the disadvantage of distortion. For smaller values of concentration and, more decisive, loads, small deviations have a much larger impact compared to higher values.

Contrary to the isotherm modelled by Langmuir, the isotherm model derived by Freundlich

$$q = K_F \cdot \varphi^n \qquad (7)$$

is not identical with the Henry isotherm at lowest concentrations. The exponent n in combination with the adsorption coefficient K_F allows a more complex description of an isotherm compared to the latter model. Furthermore, it respects the fact that for high covering degrees Θ, the load increase becomes progressively slower and does not ignore the possibility of a multilayer loading onto the adsorbent.

Brunauer, Emmett and Teller (BET) focused on multi-layer adsorption and explored a possibility to describe these processes with multiple layers mathematically (17 p. 312 f.). For this purpose, a further adsorption coefficient K_{BET} as well as the monolayer load q_m are required.

$$q = \frac{\varphi}{1-\varphi} \cdot \frac{q_m \cdot K_{BET}}{1+(K_{BET}-1)\cdot\varphi} \qquad (8)$$

However, supplementary limiting factors like pore volume do not affect the calculations, which could lead to unwanted deviations and inappropriate predictions of the possible loads. Additionally, the model does not work well for high adsorptive concentrations.

In Figure 4, the courses of the described isotherm models are depicted over the whole range of possible saturations φ. This way, they can be compared.

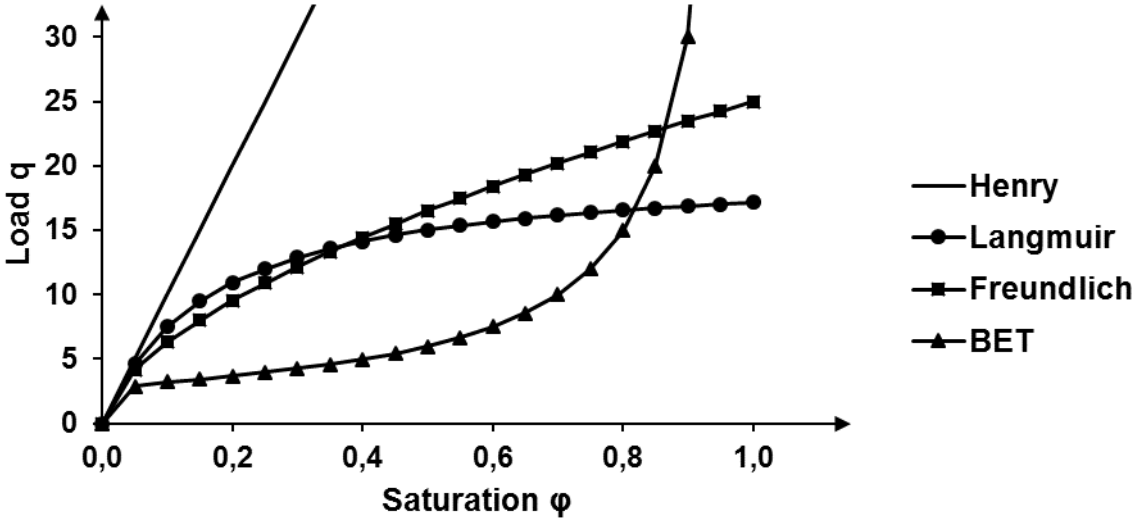

Figure 4: Qualitative course of different models of isotherms

From the figure, it becomes clear that the Henry isotherm describes a straight line. Thus, the isotherm is essentially valid for extremely low degrees of saturation. By contrast, the Langmuir and Freundlich models consider the finite number of active centres to which the adsorptive can be attached. For both functions applies that the load increases progressively weaker at higher saturations. The BET function provides a possibility to model the transition from monolayer to multilayer loading. This is due to the turning point, which indicates the completion of the single-molecule loading and at the same time describes the beginning of multilayer loading up to pore condensation.

2.1.2 Transportation and Kinetics

Kinetics are defined as the rate of a reaction. In the case of adsorption, it is the velocity at which a thermodynamic equilibrium between the fluid phase and the adsorbent is established (10 p. 489). This mainly depends on the transportation processes within the pores of the adsorbent (18 p. 131 ff.). In Figure 5, the main steps are depicted. For this purpose, an adsorbent grain with only one pore is shown as a model. The adsorption starts with the film diffusion, which is represented by the arrow numbered with 1, where the adsorptive passes through the boundary layer with its thickness of δ. After that, symbolised by number 2, pore diffusion occurs, which strongly depends on the tortuosity of the pores. In the last step, numbered with 3, the adsorption process itself, binds the component onto the surface. The desorption process works in the opposite direction, symbolised by the arrows 4 to 6 (11 p. 4; 19 p. 408; 20 p. 110 f.).

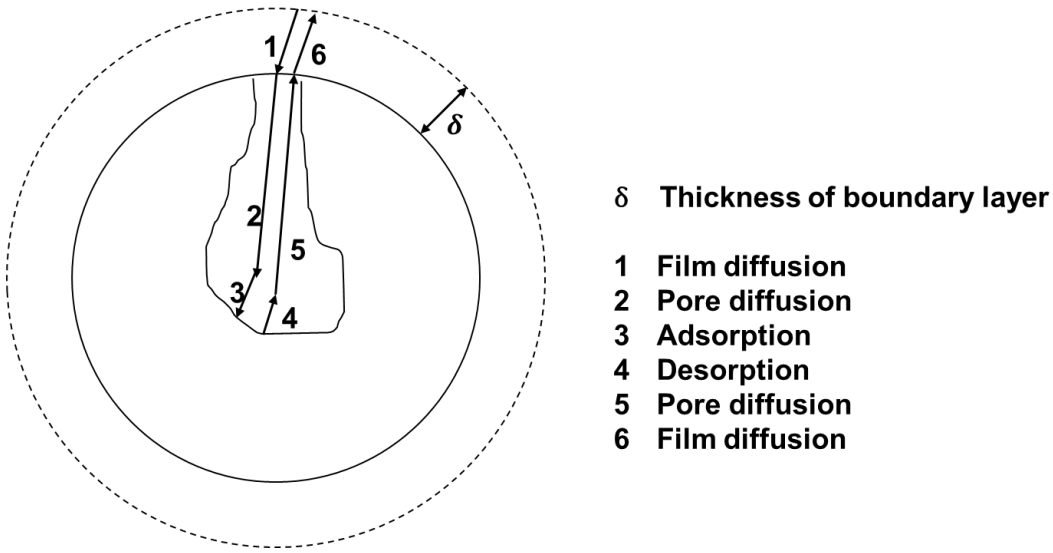

Figure 5: Steps of the transportation process during adsorption and desorption of a target substance (11 p. 4; 19 p. 408)

The most limiting factor for kinetics is the diffusion sub-step with the slower transportation process. This could be the film diffusion, as the adsorbent grain could be very small, and the boundary layer is relatively large. But mostly, pore diffusion is the rate-determining factor. Compared to the outer size of the adsorbent, the inner fissure is usually very large and thus has a larger impact. (19 p. 401 f.; 21 p. 42)

The transport during adsorption and desorption is carried out by diffusion, flow and molecular movement depending on pore size, partial pressure, and transportation

processes. Thus, the mathematical description is complex, as can be seen from the equation

$$\frac{1}{r^2} \cdot \frac{\partial}{\partial r}\left(\partial_{eff} \cdot r^2 \cdot \frac{\partial q}{\partial r}\right) = \frac{\partial q}{\partial t} \qquad (9)$$

which is based on Fick's law and describes adsorption as a kinetic process. Here, r defines the coordinate inside the radius of a grain of adsorbent, which, for reasons of simplifying the complexity, must be assumed to have the form of a sphere. The aforementioned q is the load of an adsorptive on the surface of an adsorbent. The time is described by t. The transport coefficient ∂_{eff} is suitable to describe various transport modes and, thus, is a complex factor of the equation (3 p. 86; 10 p. 490; 22 p. 66). As a result, the adsorption kinetics depend not only on the coordinate itself but also on the already existing load on its surface, and on time.

The solution of the equation relies on the knowledge about the boundary conditions. These, eventually, must be determined by several experiments with different efforts and subsumed under the known equation. The research described below is application-oriented. For this reason, the kinetic behaviour of the respective adsorbent-adsorptive pairing must be considered first and foremost. Then, the equation with the unknown transport coefficient ∂_{eff}, can be traced back, given that the remaining parameters are known.

As the research mainly focuses on finding absorbents which provide maximum retention with minimum material usage, kinetics is of major importance, as fast adsorption requires a shorter time for the adsorptive to reside in the adsorber. This results in the possibility to utilise a smaller (less material) or faster removal (less time) of Toxic Industrial Compounds (TICs) for the benefit of the breathing air.

2.1.3 Breakthrough

The description of mass transport effects is necessary for the determination of the component's breakthrough curves, which describe the course of the load on the adsorbent depending on layer and time. The maximum load as described in section 2.1.1, as well as kinetics, limit the breakthrough behaviour of an adsorbent. Kinetics is of special interest since it restricts the possible loading per time even for a completely unaffected adsorber bed. This limiting effect even increases as soon as the loading begins, and kinetics becomes slower with time. Thus, the breakthrough calculation, dependent on time and location in the adsorber, always leads to a

differential equation. Thinking the other way around, with the knowledge of the associated boundary conditions, breakthrough curves also allow the investigation of the kinetics of adsorbent-adsorptive combinations (23 p. 337).

Figure 6 shows two breakthrough curves, which represent the possible two extrema of a desired (DKG) and undesired (DKS) curve form. The ordinate of the coordinate system represents the relative concentration

$$c_r = c\, c_0^{-1} \qquad (10)$$

of a component to be separated after an adsorber bed. Here, c_0 is the input and c the absolute concentration measured after the adsorber bed. The abscissa represents the time. The concentration after the adsorber bed relative to time is depicted by both graphs DKG and DKS. If one assumes that both graphs, whose summed integrals have the same value, represent the breakthrough of different adsorbents with identical maximum loading, the great influence of kinetics on the breakthrough behaviour becomes clear.

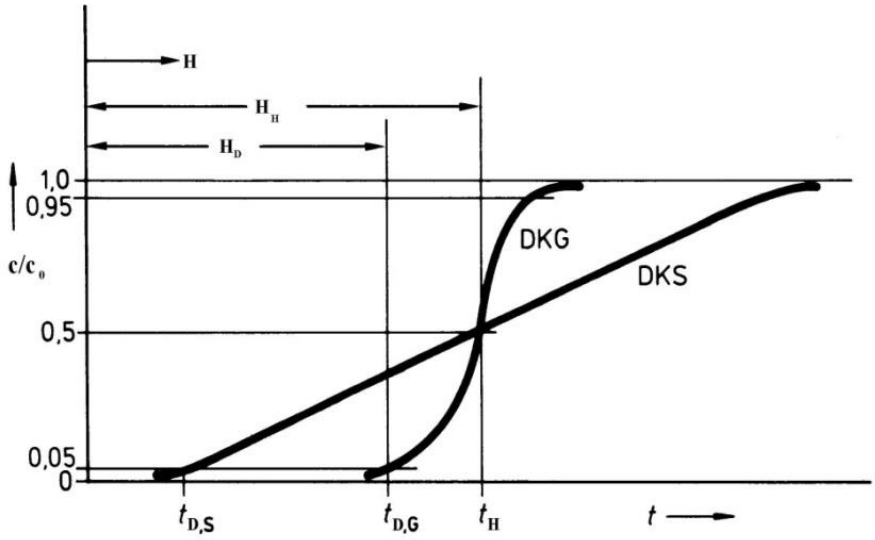

Figure 6: Model depiction of good (DKG) and bad form (DKS) of breakthrough curve (19 p. 411)

The adsorbent causing the very steep DKG curve offers very fast, the adsorbent causing the DKS curve comparably slow kinetics. For this reason, the concentration in the case of DKG starts rising so early compared to DKG. As a model representation, kinetics is a chance for a molecule to be adsorbed by a certain free space. If the chance to be adsorbed by each free space is lower, the possibility to pass through the adsorber bed is getting higher. The successful passes are then depicted in the Figure as an

elevating concentration. The free adsorption spaces in this model are of the same number, and the adsorptives of the same quantity. This means, that the last adsorption spaces are free for a significantly longer time, and the passing air is longer but with less efficiency cleared than with a fast kinetics adsorber bed. In most cases, relative concentrations of $c_r \geq 0.05$ are already critical. Thus, adsorption that proceeds longer with a comparably flat form (like the DKS curve) provides no benefits for applications in air cleaning. For analytical methods for the detection and determination of certain substances, such as chromatography, however, both maximum expressions of the breakthrough curve may be useful.

2.1.4 Multi-Component Adsorption

Compared to single-component adsorption, the complexity of multi-component adsorption is significantly higher. In the gas phase, there normally is at least humidity beneath the surrounding air. To avoid any uncertainties, authors often decide to choose nitrogen or another nearly inert or even inert gas as carrier for the gas phase to be separated. But even then, there are difficulties in leaving out humidity and thus multi-component adsorption (24 pp. 935-937).

To get multi-component adsorption process results, mostly investigations for two or more single-component adsorptions are conducted and then combined using a model or theory for multi-component adsorption. These theories are considered to be sufficiently accurate (25 p. 75). On the other hand, there is little experimental data to confirm this predication. However, Markham and Benton developed a model based on the ideas of Langmuir, as discussed in Chapter 2.1.1, to simulate results of multi-component adsorption processes. For their further calculations, they defined σ_i as the fraction of the adsorbent's surface covered with gases of the same index i, where in this case the indices stand for i = 1 and i = 2. This leads to

$$\sigma_1 = \frac{K_{L1}\,\varphi_1\,(1-\sigma_2)}{1+K_{L1}\,\varphi_1} \qquad (11)$$

or

$$\sigma_2 = \frac{K_{L2}\,\varphi_2\,(1-\sigma_1)}{1+K_{L2}\,\varphi_2} \qquad (12)$$

via

$$\sigma_1 = \frac{K_{L1}\,\varphi_1}{1+ K_{L1}\,\varphi_1+ K_{L2}\,\varphi_2} \qquad (13)$$

and

$$\sigma_2 = \frac{K_{L2}\,\varphi_2}{1+ K_{L2}\,\varphi+ K_{L1}\,\varphi_1} \qquad (14)$$

respectively. And with the help of the adsorbent's load q_i and its monolayer load q_{mi}, as indicated:

$$\sigma_i = \frac{q_i}{q_{mi}} \qquad (15)$$

the load regarding each of the adsorptives can be calculated as

$$q_1 = \frac{K_{L1}\,q_{m1}\,\varphi_1}{1+ K_{L1}\,\varphi_1+ K_{L2}\,\varphi_2} \qquad (16)$$

and

$$q_2 = \frac{K_{L2}\,q_{m2}\,\varphi_2}{1+ K_{L2}\,\varphi_2+ K_{L1}\,\varphi_1} \qquad (17)$$

The restrictions in this model rely on the fact that only adsorbates which strictly comply with the Langmuir isotherm can be calculated. Even the authors admit, that there are areas of incompleteness (16 p. 504 f.). Nevertheless, this model is in use and was later written universally as

$$q_i = \frac{K_{L,i}\,q_{max,i}\,\varphi_i}{1+ \sum_{j=1}^{N} K_{L,j}\,\varphi_j} \qquad (18)$$

in case of a multi-component adsorption with N different adsorptives (9 p. 10; 26 p. 147).

2.2 Adsorbents

For the following research, the focus was on silica gels, which were functionalised differently. The basic silica supports were different in particle size, pore size and manufacturer. Pore structure and functionalising success, on the other side, were analysed during the investigations. These processes are described later in the book. For a theoretical understanding of the processes, primarily the effects of different structures and possibilities of functionalisation are explained.

At first, an overview of the most common adsorption materials is given, some of which were also investigated in this research. This, however, should not distract from the fact

that silica gels are the most promising basis for the objectives of the research described here.

2.2.1 Basic Materials

Five basic materials were considered as adsorbents, as they are commercially available, can be delivered in high qualities and have extremely low deviations even between different charges. These are activated carbon, zeolites, clay minerals, aluminium oxides and silica gels. Table 1 gives an overview of the typical physical characteristics of the materials. In addition to the true density, this also includes the seeming density and the apparent density. Furthermore, the porosity and the parameters of the specific surface, the associated pore volume and the desorption temperatures, which are of utmost importance for further investigations, are presented.

Table 1: Physical data of different adsorption materials (3 p. 11 ff.; 11 p. 19; 19 p. 407)

Measurement	Formula symbol	Silica gels	Activated carbon	Zeolites	Clay minerals	Aluminium oxide
True density	ρ_w / kg m^{-3}	2200	1880-2100	2100-2600	2200	3000-3100
Seeming density	ρ_a / kg m^{-3}	750-1250	440-850	1100-1500	1600-1700	1200-2400
Apparent density	ρ_s / kg m^{-3}	300-850	250-550	400-900	500-700	700-950
Porosity	ε_p	0.45-0.65	0.45-0.77	0.5-0.6	0.2-0.35	0.13-0.6
Specific surface	A_{BET} / m² g^{-1}	100-850	500-1800	350-1100	120-300	100-400
Pore volume	V_p / cm^3 g^{-1}	0.35-0.95	0.7-1.5	0.2-0.7	0.25-0.35	0.35-0.6
Desorption temperature	T_{Des} / °C	100-150	120-250	100-500		150-320

From the Table, it becomes obvious that clay minerals and aluminium oxides have a relatively high density compared to their specific surface which does not exceed 300 m² g^{-1} for clay minerals and 400 m² g^{-1} for aluminium oxides, and porosity with values not larger than 0.35 and 0.6, respectively. For clay minerals and aluminium

oxides, the seeming densities with maximum values of 1700 kg m^{-3} and 2400 kg m^{-3} are considerably higher than the values achieved by silica gels and activated carbon of 1250 kg m^{-3} and 850 kg m^{-3}, respectively. This makes them particularly less attractive for applications which prefer less weight. Silica supports, activated carbon and zeolites seem to be the more appropriate choice in this case. Although zeolites are relatively heavy, as can be seen from the high apparent density, which is higher than 1100 kg m^{-3}, the porosity ($0.5 < \varepsilon_p < 0.6$) and specific surface ($350\ m^2\ g^{-1} < A_{BET} < 1100\ m^2\ g^{-1}$) is at least comparable to activated carbon with typical specific surface sizes of 500 $m^2\ g^{-1}$ to 850 $m^2\ g^{-1}$ and silica supports, which are characterised by specific surfaces between 100 $m^2\ g^{-1}$ as a minimum, 850 $m^2\ g^{-1}$ as a maximum and porosities between 0.45 and 0.65. However, the latter two are the most promising materials for further research, whereas silica-supports offer a more uniform pore-size distribution (27 p. 717).

2.2.2 Pore Size, Particle Size and Selectivity

The pore size of an adsorbent obviously influences its selectivity, especially for bigger molecules. But this effect is also investigated to be utilised with molecular sieves for the separation of nitrogen from oxygen out of the surrounding air (28 p. 1680). Thus, it remains interesting for very small molecules and a topic for scientific research in the field of different adsorptives (29 p. 720). The resulting separation effect is called steric mechanism, even if scientific literature sometimes relates it to the kinetic mechanism.

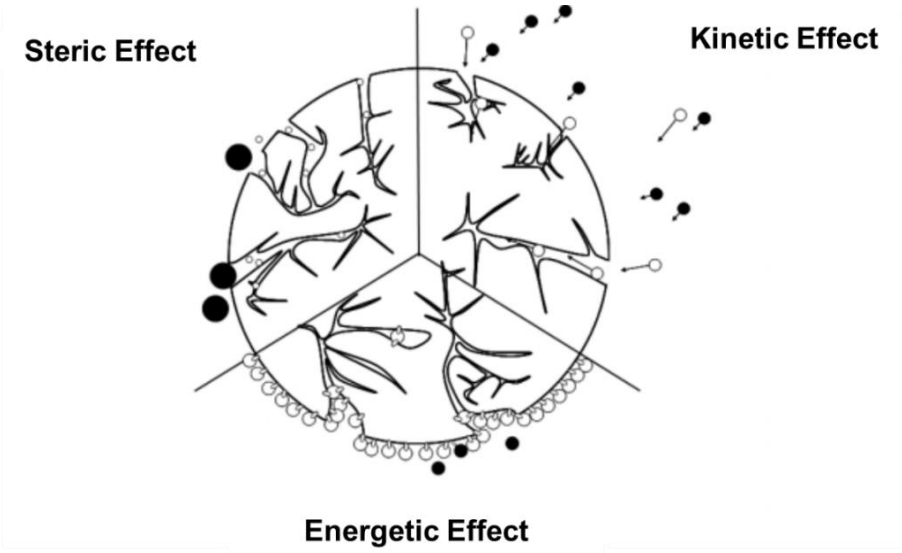

Figure 7: Mechanisms of selectivity (30 p. 1230)

This kinetic effect occurs in particular on the inner surface of the adsorbents. Here, the free spaces for the adsorptives are occupied by those types of molecules which diffuse faster into the pores of the adsorbent. This factum is of importance, as equilibrium states mostly progress very slowly.

The energetic mechanism, which can also be explained as affinity, shall be mentioned here finally. This is the only effect which is significantly influenced by the energetic condition of the adsorbent-adsorptive pair. For this, the binding of the adsorptive, which leads to the lowest energy level possible after the execution of the adsorption process, runs with priority. This effect is therefore also important for multi-component adsorption when a single-adsorption process already took place before. The difference in the energetic levels leads to a desorption of the previously bound adsorpt.

The success of the selectivity can be seen as a fraction

$$\alpha_{A,B} = \frac{K_A}{K_B} \qquad (19)$$

where $\alpha_{A,B}$ represents the selectivity between the components A and B, and K_A the equilibrium constant of the target component A, whereas K_B is the equilibrium constant of the components not wished to be adsorbed (30 p. 1231).

The selectivity can be improved by utilizing functionalisation methods. The most common principles are described in the following Chapter 2.2.3.

2.2.3 Selection of Functionalization Method and Development of Ligands

Silica gels as adsorbent basis material can be functionalised by different methods. For the following research, especially silanisation was applied.

Silanisation is a widely researched and employed option for the functionalisation of adsorbents, especially for activated carbon and silica gels. In these studies, silica supports were silanised with different ligands, but with a well-known and approved procedure, which can be retraced (31 pp. 42-52; 32 p. 128). Although the functionalisation principle remains the same, the utilised ligands were newly composed, and the reaction conditions were slightly adapted for the different silane reactions. In principle, for the functionalisation method of silanisation, the corresponding silane is placed in a suitable solvent for functionalisation, in which it is then activated by the traces of water present in the solvent. This takes place by splitting

off an alcohol. The activated silane can then bind to the silanol group on the surface of the silica gel and thus is immobilised.

With the aim to increase the affinity of the adsorbent to the adsorptive, suitable ligands were specifically sought. The selection was based on knowledge, either experience with similar adsorptives or theoretical knowledge about the reaction behaviour of the target substances. The used ligands are listed in Table 2.

Table 2: Ligands applied for the improvement of adsorption behaviour towards certain adsorptive substances

Designation	Brief description	Target substances
-430	Multiphenolic derivative	Acetone Chlorobenzene Cyclohexane
-07	Amino derivative	Cyclohexane
-10	Sulphur derivative	Hydrogen sulphide
.01	Chlorine complexed ligand (low concentration)	Carbon monoxide
.02	Chlorine complexed ligand (high concentration)	Carbon monoxide

It is striking that ligands bound on the adsorbents' surfaces, which are similar to the target substance, provide better adsorption results compared to an unfunctionalised adsorbent. Silane -430 used for acetone, chlorobenzene, and cyclohexane, for instance, contains cyclic hydrocarbon structures. Ligand -10 is another example for similarities, as hydrogen sulphide in particular is successfully bound with this sulphur derivative.

The ligand -07, which is also used as an amino derivative for the adsorptive binding of cyclohexane, has no chemical similarities to the targeted adsorptive. Here, the special reaction behaviour between the target substance and the silane plays the decisive role. Ligands .01 and .02 are basically identical, as they rely on complexed chlorine. The difference between those lies in the coating of the surface. The .01-functionalisation is considerably lower concentrated than the .02-functionalisation, as discussed in detail in Chapter 3.1.2. This ligand also increases the adsorption performance due to its reactivity with the target substance.

2.3 Adsorptives

Six different adsorptives were mainly used for the investigations:

- Cyclohexane (C_6H_{12})
- Chlorobenzene (C_6H_5Cl)
- Acetone (C_3H_6O)
- Carbon monoxide (CO)
- Hydrogen sulphide (H_2S)
- Ammonia (NH_3)

With hydrogen sulphide, ammonia and cyclohexane, three of these are test substances according to the norm DIN EN 14387 for the accreditation of mask filters (33 p. 12). The others were analysed additionally. Table 3 on the next page lists the materials with their chemical and physical properties, which are of main interest for the further research, such as the empirical formula of the individual adsorptive, which provides information about its chemical composition. This information is particularly important for the selection of the functionalisation of the adsorbent. Further, the molecular weight is considered. In later chapters, it will be shown that certain masses of the adsorptive are bound to the adsorbent. In order to evaluate the adsorbed substance quantity, the molecular weight is indispensable as a quantity for converting the substance mass into a substance quantity. The state of aggregation of the adsorptive is of particular interest for the experimental set-up, which depending on whether the adsorptive is already gaseous or still liquid, must be adapted as can be seen in Chapter 4. For multi-component experiments in combination with humidity, the solubility in water is also relevant. The concentration in the air that is lethal to humans or laboratory animals is also given as a safety parameter for handling the adsorptives and for evaluating the breakthrough curves.

Table 3: Material properties of investigated adsorptives (34)

Name	Empirical formula	Molecular weight M / g mol^{-1}	Phase at standard conditions	Lethal concentration in air c_{LC} / ppm$_v$	Solubility in water L / g L^{-1}
Cyclohexane	C_6H_{12}	84.16	liquid	26 600 after 60 minutes for rabbits	0.06
Chlorobenzene	C_6H_5Cl	112.56	liquid	no data	0.4
Acetone	C_3H_6O	58.08	liquid	76 $mg\ L^{-1}$ after 240 minutes for rats	fully soluble
Carbon monoxide	CO	28.01	gaseous	1500 after 60 minutes	30
Hydrogen sulphide	H_2S	34.08	gaseous	1000 immediately	6.72
Ammonia	NH_3	17.03	gaseous	5000 after 5 minutes	541

With these adsorptives, six different compounds with completely different behaviours are investigated. Regarding the topics of adsorption of the mentioned liquid substances and H_2S, there is already plenty of scientific work done, e.g. (23 p. 325 ff.; 35 p. 563 ff.; 36 p. 541 ff.; 37 p. 275 ff.; 38 p. 620). The same is true for the adsorption of ammonia, e.g. (39; 40; 41; 42 p. 87 ff.; 43 p. 201 ff.) and carbon monoxide, e.g. (44 p. 206 ff.; 45 p. 14287 ff.; 46 p. 747 ff.; 47 p. 2103 ff.; 48 p. 9350 ff.), respectively.

The molecules of the organic substances cyclohexane, acetone and chlorobenzene consist of more atoms than the also employed inorganic compounds carbon monoxide, hydrogen sulphide and ammonia. This also leads to significant differences in molecular weight. For ammonia, it is 17.03 g mol^{-1} and thus only 15% of the molecular weight of chlorobenzene with 112.56 g mol^{-1}. Consequently, an equal adsorbed weight of the two substances causes a considerably higher adsorbed amount of ammonia compared to cyclohexane. The solubility in water shows, among other things, that chlorobenzene

with 0.4 g L^{-1} and especially cyclohexane with 0.06 g L^{-1} are hardly soluble in water. Ammonia, on the other hand, dissolves very well in water up to 541 g L^{-1}. Because of this high solubility, the experiments on multi-component adsorption of water and ammonia are carried out with ammonia water, as discussed in Chapter 5.2.4.

2.4 Potential Hazardous Scenarios

There are two ways of causing a hazardous scenario. On the one hand, intended threats are possible. These could be caused by the utilisation of chemical weapons in a symmetric combat situation or a terroristic attack. On the other hand, there are unintended threats possible, ranging from respiring polluted air at a highly frequented street to the explosion of a chemical plant caused by human error. In order to get an idea of the actual danger of becoming a victim of a threat caused by TICs, it is useful to have a look at historical scenarios, realistic threats in our times and how such a cloud could possibly spread.

2.4.1 Historical Scenarios

Looking at the described TICs, so far none of them has been used as combat weapon. But chemical warfare is not the most threatening danger concerning toxic substances in the ambient air for most individuals in the world. This has been the case at least since 1997, when the Chemical Weapons Convention became valid (49 p. 4). The use of TICs in the industry is much more substantial. Here, although the companies try to make production and use as safe as possible, and the legislator always improves the rules for safe handling, accidents occur from time to time. Three historical scenarios, showing the unintended or accidental release of these toxic substances, are shown in Table 4.

Table 4: Historic scenarios of unintended release of TICs in chemical incidents

Incident	Date	Released substance	Cause of accident	Victims
Flixborough disaster (50; 51)	June 1st, 1974	cyclohexane	Explosion of bypass-pipe	28 fatalities 36 injured
Explosion in Toulouse (52 p. 6)	September 21st, 2001	ammonia	Explosion at dumping ground	31 fatalities approx. 2500 injured
Gas-explosion of Chuandongbei (53)	December 23rd, 2003	natural gas and hydrogen sulphide	Explosion of pipeline	> 200 fatalities > 1000 hospitalised

Presumably, these accidents were not the only ones that happened with these substances, but they were the most tragic and found a place in collective history. All these incidents occurred in chemical plants. During the disaster of Flixborough, GB, in a plant producing polyamide, a bypass pipe between two reactors exploded and caused 28 fatalities. In 2001 in Toulouse, FRA, an ammonia nitrate plant exploded causing 31 casualties. Large amounts of ammonia were released, and the health of people and animals in the area was threatened. In 2003, the most tragic of these accidents occurred in Chuandongbei, CHI, when a pipeline exploded and natural gas with a high concentration of hydrogen sulphide was released, resulting in the deaths of more than 200 people. Although the victims had little chance of escaping their fate in these disasters, the number of injured and killed underlines the importance of effective Personal Protective Equipment (PPE) for first responders to protect them from the dangerous atmosphere. As the references show, there are official investigation reports with lessons learned, that resulted in new laws. But these incidences still emphasise that there is a realistic threat caused by the named substances.

2.4.2 Realistic Threats

In Chapter 2.4.1, disasters that attracted worldwide attention are reported. However, it is usually minor incidents rather than these major disasters that pose a threat to the population or first responders. Especially in the case of carbon monoxide, there has never been a disaster of this magnitude in history. On the other hand, nobody would doubt the dangers of CO.

Carbon monoxide (CO)

In the year 2015, a total of 648 German citizens died in minor incidents from CO. In comparison, only 77 persons in the same area and time died from electric shocks (54 p. 28), which in the mindsets of most people might be the much more present threat. This emphasises the danger of carbon monoxide. The number of fatalities even increased in comparison to the years 2000 – 2009, where on average 374 persons in Germany died from CO poisoning per year (55 p. 429). CO is produced in nearly every combustion process, especially when there is not enough oxygen (O_2) for the oxidation of the involved carbon. The stoichiometric reaction is depicted here as follows

$$C + \frac{1}{2}\, O_2 \longrightarrow CO \qquad (20)$$

Main sources of CO are industrial firing and domestic fuel (56 pp. 126, 140), but also road traffic, mainly caused by light-duty vehicles (57 p. 3), especially in emerging countries (58 p. 53 ff.; 59 p. 37 ff.). For first responders, particularly the accruement during fires is of major interest. Here, different situations could be considered. Measurements showed that smouldering beech wood emits 716 ppm_v CO (60 p. 133). This is particularly interesting information when fighting forest fires which are a main contributor of CO to the atmosphere beneath fine dust pollution (61 p. 143 ff.; 62 p. 213). Other research showed the accruement of CO during fires in houses. Therefore, a modelled living room was ignited and the concentration of CO, beneath other gases, measured in an altitude of 10 m right above the fire. The concentration did not exceed a value of 5,100 ppm_v in these experiments but 4,000 ppm_v were exceeded for at least three minutes. A concentration of emitted CO could be measured for 20 minutes overall (63 p. 46). But, even tobacco is a serious source of CO. Data of research from Switzerland gives a hint, that there is a linear correlation between

cigarettes smoked in a room and the concentration of CO. Five burning cigarettes in a 30 m² room led to a concentration of 11 ppm_v. If ten cigarettes are burned, the concentration increases to 22 ppm_v in the same room (64 pp. 268, 277). This even exceeds the EC occupational 8 hours limit value, which is defined as 20 ppm_v (34).

Hydrogen Sulphide (H_2S)

Hydrogen sulphide results from putrefaction and constitutes a part of sour gas (65 p. 556) as well as biogas (66 p. 1723). Further, it is a main constituent of the resulting odour emission after wastewater treatment (67 p. 345) and odour emission caused by livestock production facilities (68 p. 47). Tanneries, furriers, adhesives factories, slaughterhouses, waste disposal plants and sugar refineries produce large quantities of hydrogen sulphide as a by-product. This also applies to the production of paper and viscose fibres and the vulcanisation of rubber. For residents in the immediate vicinity of such industrial plants, this is equivalent to a temporary increase in odour nuisance. For employees working in such establishments, an urgent need for appropriate protective facilities and equipment emerges in order to preserve their physical integrity (69 p. 99 f.).

In contrast to CO, H_2S smells intensively, with a threshold in the range of ppb (70 p. 69), which is a functional warning signal, but stuns olfactometry at concentrations higher than 100 ppm_v. This increases the danger of H_2S and emphasises the importance to reduce the concentration of H_2S to a measure below this limit, as the lethal concentration of 1000 ppm_v (34) cannot be smelled anymore, proving the real danger of H_2S as a toxic compound.

Ammonia (NH_3)

Ammonia is a product of volcanic eruptions (71 p. 107) and, comparable to hydrogen sulphide, of agriculture. In Germany, agricultural industry produces 96 % of the emitted ammonia. Most of it comes from cattle farming, but also from pig and chicken farming and is a result of microbial conversion processes of excrements (72 p. 9). For the reduction of ammonia in the air, scientists try to design animal feed with a lower potential for ammonia formation (73 p. 4). The material is also produced intentionally, mainly as fertilizer (74 p. 233), which results in connected risks. Liquid ammonia in particular could evaporate during the synthesis process. In history, it seems to be proven, that severe impacts are confined to a radius up to 60 m with a corresponding

explosion around the leak (74 p. 225). Such leaks might also be a risk of cooling systems, which are based on liquid ammonia (75 pp. 108-109). Moreover, ammonia is a product of wood fires, which probably spreads over a large area, as can be seen from wood fires in Greece (61 p. 143).

Cyclohexane and Volatile Organic Compounds

Cyclohexane is widely used in the industry as a solvent and basic product for the fabrication of nylon (76 p. 179). If cyclohexane leaks, there is a high risk of detonation, caused by its explosion limits. If there is no ignition, the atmosphere could be filled with cyclohexane, where a concentration of 26,600 ppm is lethal, at least for rabbits (34). With an overpressure in a leaky pipe-system, this concentration could be reached.

Cyclohexane and further acetone and chlorobenzene represent the large variety of volatile organic compounds. All the typical behaviours of the different organics cannot be covered here. However, VOC are health suppressing and, comparably to CO, a present danger, especially in industrial areas or near roads (57 p. 4; 77 p. 311 ff.), but also during hydrocarbon extractions (78 p. 629 ff.).

2.4.3 Requirements Depending on Infrastructure

The main incentive for the described research is the protection of persons who could absorb the considered substances cyclohexane, carbon monoxide, hydrogen sulphide and ammonia via the respiratory tract during a stay in a correspondingly polluted atmosphere. During this exposure, they may be located both in a building shielded from the external atmosphere by air purification systems and outdoors. Outside protective installations in an appropriately contaminated atmosphere, a gas mask must be worn by persons exposed to this atmosphere for their own safety. This also means that in the event of outdoor exposure, only the protection of one person needs to be calculated. For buildings shielded from the outside air, a varying number of people must be assumed in the interior, which makes it more difficult to calculate the material requirements for adsorbents. However, the basic approach for determining this is the same in both cases.

For an evaluation of the needed material for a successful separation of these compounds from the breathing air, it is necessary to know the basic information about the personnel to be protected. In case of a hazardous release, the first fundamental information is the threatening concentration of the harmful compound. Then, the

parameters, particularly the concentration of the substance to be separated in the air and the necessary air exchange for a sufficient oxygen supply of the personnel are crucial for the calculation of possible protection times for the affected personnel. This supply depends on the number of people and the work intensity they face. In European standards, a physical working individual needs an air flow of approximately 95 $m^3 min^{-1}$, which is a quite large amount compared to a person who does mental work. This person needs approximately 30 $m^3 min^{-1}$ of air for respiration (33). With the knowledge of the labour, done by the personnel inside, the number of persons in the facility and the composition of the threatening atmosphere, it is possible to calculate, what amount of adsorbent is likely to protect the people inside for a certain time.

In addition to this data and the knowledge of which hazardous substance pollutes the ambient air, its concentration is another decisive parameter. From these factors, it is possible to calculate the necessary amount of adsorbent for the protective system or to calculate the time span of a possible secure air purification. Therefore, the performance of the adsorbent regarding loading amount, adsorption kinetics and consequently breakthrough behaviour represent the relevant data.

3 Characterization of Adsorbents and Adsorptives

Before the start of any research, suitable adsorptives and adsorbents had to be selected. As the adsorptives were predefined, the major topic in this project was to choose and develop an experimental set-up for the evaluation of the important data. Another challenge was posed by the different aggregate states of the adsorptives. The adsorbents, on the other side, had to be selected considering characteristics like particle and pore size. Further, the type of ligands, which are coupled onto the silica supports' surface, had to be chosen. Then, the functionalised adsorbents had to be analysed. These analyses must be explained as well, as this is a specific scientific topic.

3.1 Analysis of Adsorbents' Structure and Coating

Compared to activated carbon, only silica gels are comparably effective in adsorption. The other materials mentioned in Chapter 2.2.1 are not powerful enough (79 p. 27 ff.). Therefore, these studies focus on silica supports, which also offer some advantages compared to activated carbon and can be functionalised effectively (80 p. 889; 81 p. 1634 f.). As basis material, different silica supports with different pore and particle sizes were used. For comparison purposes, measurements were also carried out with a specific activated carbon, which is already being utilised very successfully in agriculture and industry.

3.1.1 Structure Investigation

Although the manufacturers provide some data of the basic materials, the pore size often is not or imprecisely specified. Therefore, measurements with the Belsorp Mini II (Bel Corp., Osaka, JPN) were conducted to get precise information, especially about the pore size and active surface of the adsorbents. As every functionalisation might influence the surface as well, such as e.g. pores might be narrowed by a bound ligand, all functionalised adsorbents were analysed regarding surface per weight and pore sizes as well.

In order to determine the corresponding values, the system works both with liquid nitrogen for cooling and with gaseous nitrogen as adsorptive. Pressure sensors are integrated in the system as detectors, and the software itself records the associated time. The adsorption temperature can be reduced to values below -196 °C with the aid of liquid nitrogen. Below this temperature, the gaseous nitrogen condenses, making it

possible to measure its adsorption up to pore condensation. Using the BET model, the BelMaster software (version 6.1.0.4, Bel Corp., Osaka, JPN) can calculate the corresponding values for the specific surface as well as the mean pore radii from the collected measurement results. Table 5 shows the results obtained for the specific surface and average pore diameter. The indicated particle size is based on data provided by the respective manufacturer. For HSU 9000-2 all given data is provided by the manufacturer.

Table 5: Physical characteristics of selected adsorbents

Adsorbent	Particle size d_K / µm	Specific surface A_{BET} / m² g⁻¹	Average pore diameter d_P / Å
Industrial AC	300 - 400	535 ± 13	29 ± 1
HSU 031-279	200 - 500	414 ± 1	76 ± 1
HSU 031-295	2000 – 5000	577 ± 5	33 ± 1
HSU 031-295.1	2000 – 5000	554 ± 11	28 ± 1
HSU 031-295.2	2000 – 5000	480 ± 17	27 ± 1
HSU 001-075	200 – 500	275 ± 5	100 ± 5
HSU 001-075.1	200 – 500	246 ± 3	116 ± 2
HSU 001-075.2	200 – 500	222 ± 4	103 ± 2
HSU 101-075-07	200 – 500	252 ± 8	179 ± 80
HSU 101-075-10	200 – 500	255 ± 5	103 ± 2
HSU 9000-2	200 – 500	53	300

Overall, it can be observed that the specific surface area of the adsorbents decreases as a result of functionalisation. Depending on the immobilised ligand, this may even occur to a large extent. The functionalised adsorbent HSU 031-295.2 has a surface area of 480 ± 17 Å, which is only 83 % of the surface area of the starting material HSU 031-295, which reaches a value of 577 ± 5 Å. HSU 001-075.2 provides with 222 ± 4 Å only 80 % of the surface reached by HSU 001-075 with a value of 275 ± 5 Å. But these are the extrema, although approximately 10 % of the active surface should be expected to be lost, as the executed measurements show. For example, the loss of active surface for the silanised variants HSU 101-075-07 and HSU 101-075-10 with values of 252 ± 8 Å and 255 ± 5 Å, respectively, is slightly less than 10 %. For HSU 001-075.1 with values of 246 ± 3 Å the decrease of the surface is a little higher.

For the finer-pored HSU 031-295, these effects seem to be less pronounced. Thus, the values of HSU 031-295.1 with 554 ± 11 Å decrease by 4 %, of HSU 031-295.2 with 480 ± 17 Å by 17 % of the initial value of HSU 031-295 with 577 ± 5 Å.

For the pore sizes, all silica gels listed here are in the mesoporous range between pore diameters of 2 nm and 50 nm (82 p. 325). With pore diameters of approx. 30 Å or 3 nm at least the considered activated carbon and HSU 031-295 as well as its functionalised variants are even close to the microporous range. For the pore volumes, although the pore diameter fundamentally changes during functionalisation, by contrast it cannot be assumed that it will fundamentally decrease or increase. This might be caused by the agglomeration of molecules around the existing pores. Two possible effects are probable. On the one hand, the ligands are bound inside the pores. This would result in a smaller pore diameter and further in a smaller pore volume. On the other hand, the ligands could be bound before entering the pores. This would cause a larger pore volume, as the pores are getting longer. But it could also cause both, a larger and a smaller pore diameter in the beginning, which would have a significant effect on the average pore diameter calculated by the BET model. This can be seen especially with HSU 101-075-07. Here, the measurements had a relatively large deviation of ± 80 Å with an average measured pore diameter of 179 Å. This is a result gained from different measurements, where in the one half, the pore sizes decreased and in the other half, the pore sizes grew significantly. With other functionalisations, the pore size seems to be almost unchanged. E.g. for both, HSU 101-075-10 and HSU 001-075.2, the mean pore diameter is 103 ± 2 Å compared to a pore diameter of 100 ± 5 Å for the starting material HSU 001-075. Thus, the values for these two functionalised silica gels are within the standard deviation of the pore sizes of the base material. However, for HSU 001-075.2 this effect could be misleading, if assumed with this state of knowledge, that the associated functionalisation has no effect on the pore sizes. The functionalisation to HSU 001-075.1 carried out with the same material but with less loading leads to an enlargement of the mean pore diameter to 116 ± 2 Å. This value is clearly outside the standard deviation of the starting material and is thus a clear indication of the considerable change in the surface due to corresponding functionalisations.

It should be assumed, that the ligands are attached to the outside and on the inside of the pores. From this, it can also be deduced that the ligand obviously tethers at the

outer edge of the pores before entering them and attaching to the wall. Depending on the basis material, the one or the other effect has a greater effect and leads to larger or smaller pore diameters.

3.1.2 Analysis of Functionalisation Success

The functionalisation of silica gels, regardless of the method used, involves a certain amount of energetic and material effort. This effort must be in proportion to the benefit achieved by functionalisation. For this purpose, it is necessary to gain knowledge not only of the additional adsorption success achieved by functionalisation, but also of the quantity of the corresponding ligands required for this.

For the determination of the functionalisation success, elementary analysis was employed. With the help of an elementary analyser, the amount of carbon, hydrogen, nitrogen, and sulphur could be detected. Therefore, the functionalised adsorbents are pyrolyzed inside a combustion chamber under an oxygen rich atmosphere at a temperature of approximately 1800 °C, where carbon is converted to carbon dioxide (CO_2), hydrogen to water (H_2O), nitrogen to nitrogen oxides (NOx) and sulphur to sulphur dioxide (SO_2). The formed gases then are swept out of the chamber by helium or another inert gas and lead above heated copper of high purity. By this step, oxygen, which was not consumed, is removed, and nitrogen oxides are reduced to pure Nitrogen (N_2). The flue gases CO_2, H_2O, SO_2 and N_2 then are led through a GC-column, divided by the purge & trap process and quantified by a thermal conductivity sensor (83 p. 570 ff.). A flow chart to explain such a system is shown in Figure 8.

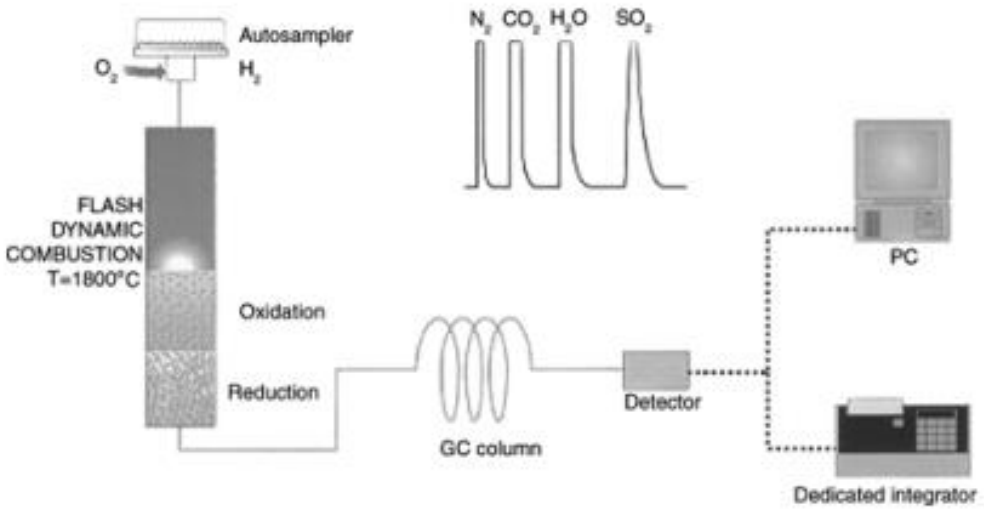

Figure 8: Flow chart of elementary analyser (83 p. 570)

The connected computer program displays the mass fraction of the elements carbon, hydrogen, nitrogen, and sulphur. With these, it is possible to calculate the substance quantity of the ligands bound onto the silica gels surface per weight, and with the knowledge of the results from Chapter 3.1.1, the substance quantity per surface of the adsorbent. Further, it is possible to trace back the elemental formula of the bound molecules, which gives an indication of the surface coverage of the basic support material. For comparison, earlier thermogravimetric measurements showed that the analysis results are very similar (9 p. 40), which proves that this analysis method is of high reliability.

In Table 6, the functionalisation success as a density of the ligand on the adsorbent in relation to weight ($q_{l;w}$) and surface ($q_{l;A}$) is listed.

Table 6: Determination of functionalisation success of selected materials

Adsorbent	Functionalisation density compared to mass $q_{l;w}$ / mmol g^{-1}	Functionalisation density compared to surface $q_{l;A}$ / µmol m^{-2}
HSU 031-295.1	1.65 ± 0.29	2.86 ± 0.50
HSU 031-295.2	6.46 ± 0.04	11.20 ± 0.07
HSU 001-075.1	1.61 ± 0.21	5.85 ± 0.76
HSU 001-075.2	7.24 ± 0.07	26.32 ± 0.25
HSU 001-075-07	0.44 ± 0.03	1.61 ± 0.12
HSU 001-075-10	0.24 ± 0.01	0.86 ± 0.04

While for HSU 031-295.1 and HSU 001-075.1, the functionalisation with respect to the adsorbent mass $q_{lig;w}$ with 1.65 ± 0.29 mmol g^{-1} or 1.61 ± 0.21 mmol g-1 hardly differs and the respective standard deviations overlap considerably, this does not apply to the surface. In this context, HSU 031-295.1 with 2.86 ± 0.50 µmol m^{-2} could only be functionalised half as well as HSU 001-075.1 with 5.85 ± 0.76 µmol m^{-2}. For HSU 031-295.2 with 11.20 ± 0.07 µmol m^{-2} and HSU 001-075.2 with 26.32 ± 0.25 µmol m^{-2}, this effect has an even stronger impact. The degree of surface-related functionalisation for HSU 001-075.2 is more than 2.3 times as strong as the functionalisation of HSU 031-295.2. The smaller pore sizes and larger particle sizes obviously have a considerable influence on the functionalisation. For HSU 031-295,

the pore sizes are significantly smaller, but the particle sizes are on average ten times as large as those of HSU 001-075 as already shown in Table 5.

It is probable, that the ligands, which represent a comparably large molecule, do not coat the inner pores of the adsorbent, because the molecules cannot pass through the pore entrances. Further, the inner length of the pores and thus the interweaving of the adsorptives' path is increasing with the particle size. This intensifies the mentioned effect. Reference is made here to Chapter 5, in which the effects of the different functionalisations on the adsorption success of the individual adsorbent are further discussed.

3.2 Appropriation of Adsorptives

The appropriation of the adsorptives has a direct impact on the experimental set-up described in Chapter 4. Therefore, two different aggregate states are possible. On the one hand, they can be in the liquid state. Then the material must be vaporised, assuring that no droplets pass the gasification device and get in contact with the adsorbent (84). In the other case, the adsorptive is already gaseous under the given conditions.

Vaporised Adsorptives

Cyclohexane as well as all other investigated organic adsorptives are liquid under the measurement conditions and must be vaporised. The given vapour pressure allows that air can be loaded with the adsorptive. The quality of the disposed liquids corresponds to the "per analysis" standard, i.e. with a purity of at least 99.5 % for the investigated hydrocarbons. Regarding the deviations to be expected in adsorption, the quality is sufficiently high. The same quality was employed in case of liquid ammonia, which had to be diluted. Pure water was used for dilution. There should also be no effect that overlaps the standard deviations caused by the adsorption process.

Gaseous Adsorptives

The used gas mixtures, CO, H_2S or NH_3 in synthetic air, were provided by Linde (Pullach, GER) in pressurised gas cylinders from alloy with a volume of 40 L and a filling pressure of 150 bar, which results in a volume of 6000 L of atmosphere under standard conditions. These atmospheres were delivered in different concentrations, as can be seen in Table 7.

Table 7: Composition of different hazards in synthetic air as used for the research

Gas phase dissolved in synthetic air	Utilised concentrations c / ppm_v
Carbon monoxide (CO)	0.9; 8.5; 85; 170; 1,000; 10,000; 100,000
Hydrogen sulphide (H_2S)	10; 70; 140; 5,000
Ammonia (NH_3)	137; 274; 10,000

The selected gas mixtures cover an as wide as possible range of concentrations. These are limited on the one hand by the existing explosion limits under the corresponding pressure, and on the other hand, by the stability of the atmosphere, which is considerably restricted especially at lower concentrations. For carbon monoxide concentrations, values from 0.9 ppm_v up to 100,000 ppm_v are possible. Higher concentrations were not used due to the hazardous nature of the gas. On the other hand, lower concentrations than the utilised minimum do not lead to a more intensive gain of knowledge. For hydrogen sulphide, volume concentrations of less than 7 ppm_v mean that they are not stable long enough in synthetic air, and hydrogen sulphide as target substance would have to be added to a pure nitrogen atmosphere instead. This would, admittedly, embezzle the possible influence of oxygen, which could not be avoided in a later industrial application of the research results. Concentrations with values higher than 5,000 ppm_v cannot be filled into pressurised gas cylinders under the specified pressure, as their contents then form an explosive atmosphere. For ammonia, a concentration below 130 ppm_v means a reduced shelf life of the gas mixture, too. The concentration of 100,000 ppm_v is also an arbitrary upper limit to keep the hazard low during the experiments.

The manufacturer guarantees that the quality of the gas mixtures complies with the certified quality level 1, representing the highest quality classification which is commercially available. The allowed manufacturing tolerances and relative measuring inaccuracies for the gas production at this standard of individual concentrations are depicted in Table 8 below. The related data is specified by the gas manufacturers. The column “Adsorptive concentration” represents the value ranges of the desired concentration of the target substance in synthetic air. The manufacturing tolerance indicates the accuracy; the manufacturer can achieve a certain adsorptive concentration with. Finally, the gas mixtures are analysed by the manufacturer; the

associated measurement deviations at the respective concentration can be taken from the column with the relative measuring inaccuracy.

Table 8: Test gas characteristics regarding basic parameters of adjusted atmospheres as used in the experiments (85 p. 123)

Adsorptive concentration	Manufacturing tolerance	Relative measuring inaccuracy
< 10 ppm_v	± 20 % rel.	± 5 % rel.
10 – 99 ppm_v	± 10 % rel.	± 2 % rel.
100 – 999 ppm_v	± 5 % rel.	± 2 % rel.
1 – 4.9 vol.-%	± 2 % rel.	± 2 % rel.
5 – 50 vol.-%	± 1 % rel.	± 1 % rel.

Every single gas cylinder was analysed gravimetrically after it was filled with the correctly adjusted atmosphere (85 p. 123 f.). Thus, the concentrations of the adsorptives are as precise as possible. Even at concentrations below 10 ppm_v, they do not deviate more than 1 ppm_v from the required concentration. This slightly inaccurate concentration can then be determined very precisely with a maximum deviation of ± 5 % rel. The higher the concentration of the adsorptive, the smaller the possible deviations during production and later determination. For example, the deviation in the production of a gas mixture with an adsorptive content of more than 5 vol.-% is only ± 1 % rel. The same value is achieved with the measurement inaccuracy.

Thus, uncertainties only have a minor impact on measurement deviations. As the atmospheres were as exact as possible, there was no need to analyse them internally. On the other hand, it is possible to calibrate employed measurement devices in this project under the unaffected atmosphere from the pressurised gas cylinders.

4 Measurement Methods

For the measurements of equilibrium loading, two mainly different methods were applied, dependent from the adsorptive. The equilibria of carbon hydroxides could be investigated by the utilization of a volumetric sorption measurement device. A gravimetric measurement method was developed for the other adsorptives, as for all kinetics investigations.

The measurements of breakthrough curves, which are a function of equilibrium load and kinetics, were conducted by a new established measurement set-up since a breakthrough could not be investigated with the other installations, as described in more detail below.

4.1 Gravimetric Measurements

Two different methods were used for gravimetric measurements. One method is used with a precisely adjusted atmosphere inside the measuring chamber, but no further exchanges of the atmosphere during the adsorption process, which means a decreasing concentration of the aimed gaseous component in the atmosphere. This set-up is further called static. The second set-up is used with a constant gas flow. In this version, the concentration of the adsorptive remains stable, as the atmosphere is exchanged constantly with fresh and unaffected, precisely adjusted gas mixtures.

4.1.1 Static Set-Up

The static set-up as described in the following or in variations was widely used in earlier research. Therefore, a measuring chamber, a container with an adsorptive which is vaporising over time and weighing glasses with the adsorbent were employed (86 p. 25 f.; 79 pp. 17-24). The adsorbents and the adsorptives are placed in the measuring chamber, which is then closed. There are two significantly influencing factors for the duration of the experiment. On the one hand, the atmosphere must adjust within the research room. For this purpose, the adsorptive which was introduced as a liquid in the test chamber evaporates. Depending on the vapour pressure of the respective liquid to be investigated, this takes a few hours to a few days. At the same time, the used silica gels start to adsorb the target material, which is formed as a gas phase, in order to create an equilibrium. Notably, the vaporisation causes the necessity for longer experimental times. Comparison measurements with different adsorptives

showed, that five days are sufficient for fully loading the atmosphere inside the chamber with the adsorbent (9 p. 43; 79 p. 21).

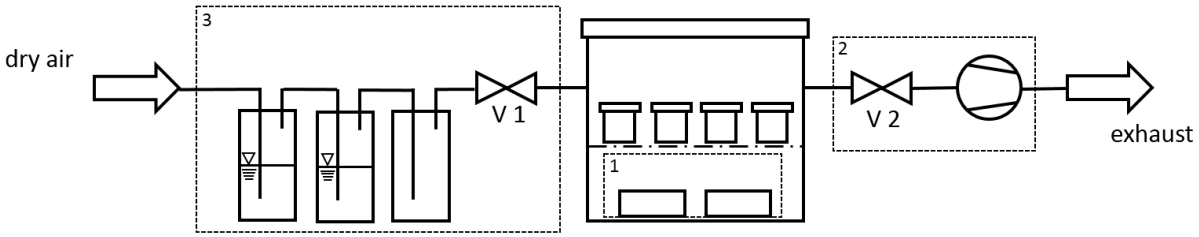

Figure 9: Different set-up options for static equilibrium measurements

Figure 9 shows possible set-ups for establishing a static atmosphere. These have the desiccator with weighing glasses inside in common. The basic and commonly utilised set-up is marked with number 1, where the adsorptive is in small bowls inside the desiccator. For an adjustment of the humidity, it is further possible to put in a small bowl with a saturated mixture of salt and water. This way, a defined degree of humidity is evaporated into the ambient atmosphere. During the experiments, the salt was sodium chloride. The adjustment of the equilibrium can be accelerated by adding a diaphragm pump after an additionally installed valve (V 2), as box number 2 shows. Thus, the pressure inside the desiccator can be lowered, the adsorptive is evaporating faster and the atmosphere is saturated earlier. This possibility has the disadvantage that the atmosphere inside the desiccator is difficult to adjust.

One way of further optimising the test set-up is to remove the vials with the adsorptive to be evaporated shown in box 1 and instead connect the gas washing bottles with the adsorptive as shown in box 3. Of the three vessels shown, the first two are filled with the respective liquid, while the third bottle serves as a droplet separator for preventing entire droplets from entering the measuring chamber and falsifying the measurement results. This measuring set-up attracts room air via the resulting vacuum. It is advisable to install a dry column upstream of the gas washing bottles so that the air drawn in is freed as far as possible from humidity and other undesirable components. Valve V1 ensures a connection between the gas washing bottles and the desiccator.

Now, the adsorbent in the weighing glasses can be placed in the desiccator, which then is sealed. The pump can be started, and valve V 2 opened until a vacuum is established. Then, valve V 2 is closed, and valve V 1 is opened. Via pressure equalization, the desiccator is filled with a completely loaded atmosphere. The

adsorbents can then be exposed to the adjusted atmosphere for a predetermined period. Then, the loading success results from the weight difference of the adsorbent before and after loading, as described in more detail in Chapter 4.1.3.

4.1.2 Set-Up with Constant Gas Flow

Although the experimental set-up for experiments with a constant gas flow is largely similar to the sophisticated closed atmosphere experimental set-up described in the previous chapter, it is fundamentally different in parts. The correspondingly adjusted atmosphere is not supplied, as was previously the case, by balancing the negative pressure prevailing in the test chamber. Instead, the adjusted atmosphere is fed into the test chamber by means of overpressure and purged during the experiments so that the adsorptive concentration is always identical. This experimental set-up is particularly suitable, if adsorptives are to be investigated, that are already present in compressed gas cylinders as a gas phase. Otherwise, experiments with liquid adsorptives that must be vaporised can also be investigated. A flow diagram of the corresponding test set-up can be found in Figure 10. It shows both, the possibility of introducing a test gas as a pre-set gas mixture into the test chamber and of evaporating a liquid adsorbent, as already explained in the previous chapter, and then feeding it to the adsorbent in the test chamber. The main difference is that it is not ambient but synthetic air from the compressed gas cylinder that is loaded with the adsorptive. Both, the synthetic air and the test gas are passed through a pressure reducer and a Mass Flow Controller (MFC) made by Bronkhorst (Ruurlo, NL), which sets the volume flow to 300 mL min $^{-1}$. The corresponding atmosphere is fed into the test chamber via valve V 1 and can escape via valve V 2. A PC Vario 3001 diaphragm vacuum pump (Vacuubrand, Wertheim, GER) is connected by valve V 3, as is the case for experiments without constant exchange of the test atmosphere. With the aid of the vacuum pump, it is possible to adjust the atmosphere within the test chamber more quickly than by purging. For this purpose, the valves V 1 and V 2 are closed, a vacuum is created via the open valve V 3, which is then replaced again by the desired atmosphere after closing V 3 and opening valve V 1. This process is repeated a total of three times. Valve V 3 is then closed, and V 1 and V 2 are opened.

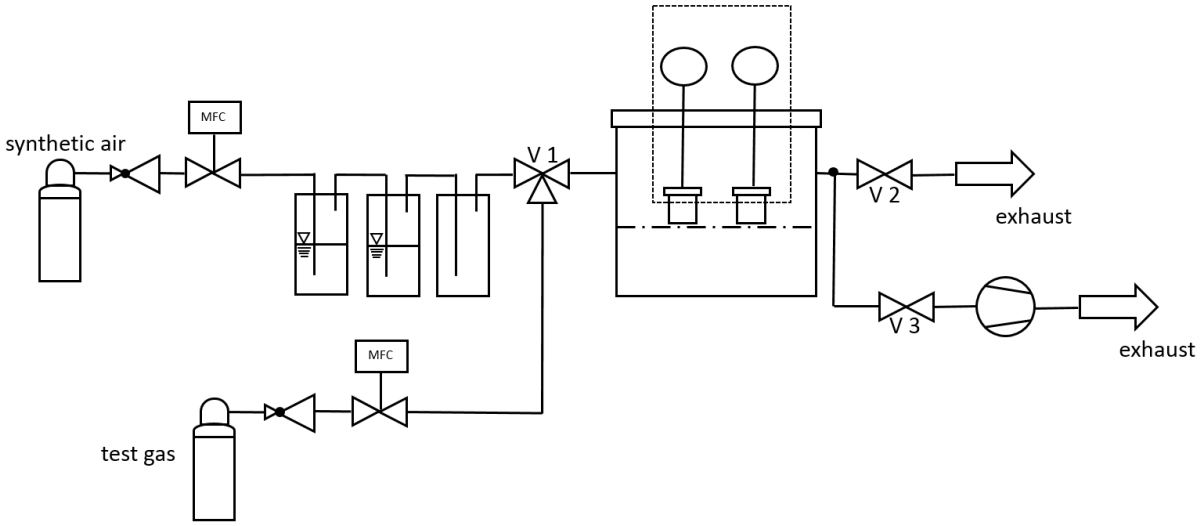

Figure 10: Set-up for equilibrium and kinetics measurements with constant gas flow

The major advantage of the test set-up described is the possibility to protect the adsorbents from an external atmosphere until it is precisely adjusted. For this purpose, a possibility was developed to open and close sealable bottles containing the adsorbent by a mechanism from outside the test chamber. This is highlighted by the dotted box in Figure 10. The vials are hermetically sealed as soon as they are closed. Thus, it is possible to expose adsorbents exclusively to the exactly defined atmosphere required and to precisely determine this time of exposure. In addition to measurements of the maximum load, the kinetics of the corresponding adsorbent-adsorptive pairing can also be determined.

4.1.3 Mathematical Operations for Single Component Measurements

The necessary computations for the evaluation of the measurement results from the experimental set-ups without exchange and with constantly flowing atmosphere are basically identical. For the calculation of the relative load q_r onto the adsorbent, it is crucial to know the adsorbed mass m_l, or substance quantity n_l, respectively, of the adsorptive and the mass of the vacuum-dried adsorbent m_{ad}.

With the knowledge of m_{ad} and the determined mass of the loaded adsorbent m_{al}, the mass of the adsorpt m_l can be calculated:

$$m_l = m_{al} - m_{ad} \qquad (21).$$

With this and the knowledge of the calculation of substance quantities, it is also possible to compute n_l.

As different basis materials with different pore sizes and active surfaces were used during the research, it was decided to measure the adsorption success relative to the absolute surface A_s of each adsorbent. Therefore, the relative surface of the adsorbent A_{BET}, investigated as described in Chapter 3.1, can be multiplied with the mass of the dry and uncharged adsorbent as

$$A_S = A_{BET} \cdot m_{ad} \qquad (22).$$

Finally, it is possible, to determine the relative load q_r onto the adsorbent as:

$$q_r = \frac{m_l}{A_s} \qquad (23).$$

The last two calculations are also valid for an adsorbed substance quantity, where m_l is translated into n_l.

With this result, a comparison of adsorbents independent from their pore and particle size is possible. The indispensable measurements of the associated relative surfaces as well as their results have already been described in Chapter 3.1.1.

4.1.4 Multi Component Measurements

Multi-component measurements are a further development of the set-up and especially of the measurement procedure with a constant gas flow. When adsorbing several components, it is not possible with the previous experimental set-up to decide which component binds to the adsorbent in which ratio. For this reason, the procedural design presented in Chapter 4.1.2 was modified.

The experimental set-up shown in Figure 11 differs from the previous one shown in Figure 10, especially by the possibility to allow two different gas phases to flow simultaneously into the test chamber. The experimental set-up shown here is designed for the use of an evaporated liquid as adsorptive besides the additionally added target substance. Via valve V 1, it can be decided whether dry synthetic air from the same gas pressure cylinder or the atmosphere with the target substance flows into the test chamber in addition to the synthetic air loaded with the previously mentioned liquid. The two MFCs can also be used to precisely adjust the gas phase composition.

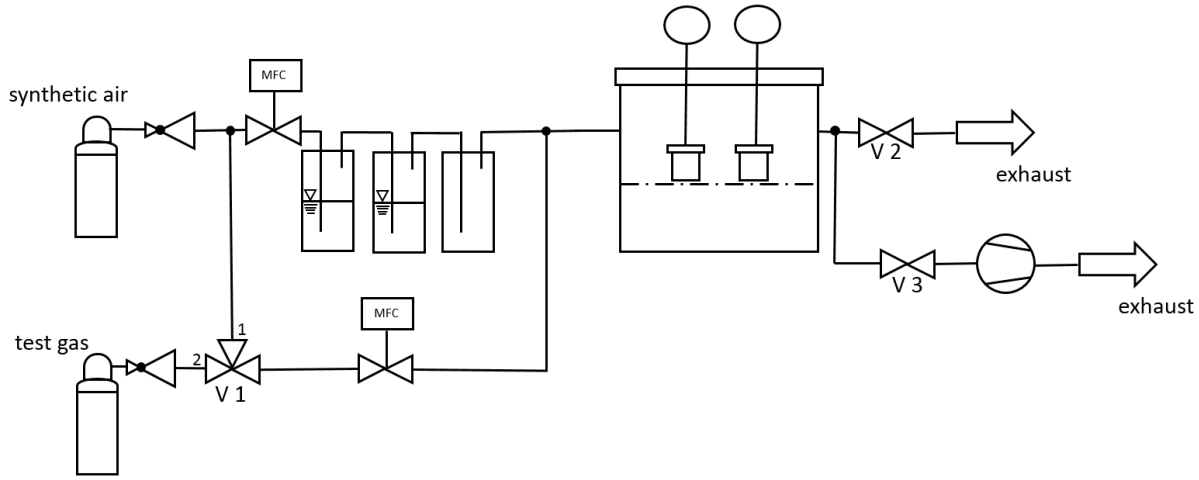

Figure 11: Measurement set-up for multi-component measurements of kinetics and equilibrium

Now, it is possible to determine the adsorption success for both adsorptives in two steps. Therefore, the adsorbent was first fully loaded with adsorptive A, which in this example should be the evaporated substance. In parallel, cleaned synthetic air was also led onto the adsorbent. Then, the weight of the adsorbent was ascended to obtain the mass of adsorptive A on the adsorbent as explained in the previous chapters and mentioned in the next equation:

$$m_{l,A} = m_{al;A} - m_{ad} \qquad (24)$$

In the second step, the adsorbent was loaded with an atmosphere containing the same concentration of adsorptive A plus a specific concentration of adsorptive B, which in this example is the test gas. Both components must be part of the incoming atmosphere. If only component B was in the atmosphere, but A was omitted, there would be the possibility of desorbing component A from the surface, which would lead to deviations in the results that cannot be investigated. Therefore, the synthetic air was either loaded via gas washing bottles or the pressurised gas cylinder was exchanged with one containing the correctly defined atmosphere. This was conducted over five hours. In the end, the weight of the adsorbent was ascertained again, as follows, to determine the extra load caused by component B.

$$m_{l;+B} = m_{al;A,B} - m_{al;A} \qquad (25)$$

If the weight increased after this second step, this must be caused by the second adsorptive, as the adsorbent is assumed to be maximally loaded by the first

component A. This were a sign of successful multi-component adsorption. Then, the resulting relative load per surface can be calculated as

$$q_{r;+B} = \frac{m_{l;+B}}{A_S} \qquad (26)$$

In this research, component A was humidity, component B was the defined atmosphere with a target compound. For reasons of readability, the possibility of heating the chamber containing the adsorbent is not mentioned. This was a further step to make the measurement results more precise and repeatable. As can be seen in the figure, there is a three-way valve to decide between a loading with synthetic air or an adjusted atmosphere. For the pre-loading, the line indexed with 1 is opened, for the loading with the second component, it is the line indexed with 2. In the case of this figure, the used adsorptives are liquid and gaseous, respectively. Other combinations with two liquid phases or two gaseous phases are possible as well after an appropriate adaption.

4.2 Volumetric Measurements

Volumetry is of another complexity than gravimetry. It is important to understand the main advantages and disadvantages in comparison to gravimetric measurements, the knowledge of the principle and the necessary preparations.

4.2.1 Measurement Principle

The volumetric measurements were conducted with a Belsorp Aqua 3 (Bel Corp., Osaka, JPN) and the related BelMaster analysis software, which was already mentioned in Chapter 3.1.1. Its principle relies on the ideal gas law

$$p \cdot V = m \cdot R_S \cdot T \qquad (27)$$

which is assumed to be known. The equipment itself is only able to detect and control its inner pressure and temperature at different places inside the system. This data are recorded and can be interpreted by the analysis software. Compared to other sorption measurement methods, its data per time productivity is very efficient (87 p. 277). Figure 12 depicts a flow chart of the Belsorp Aqua 3.

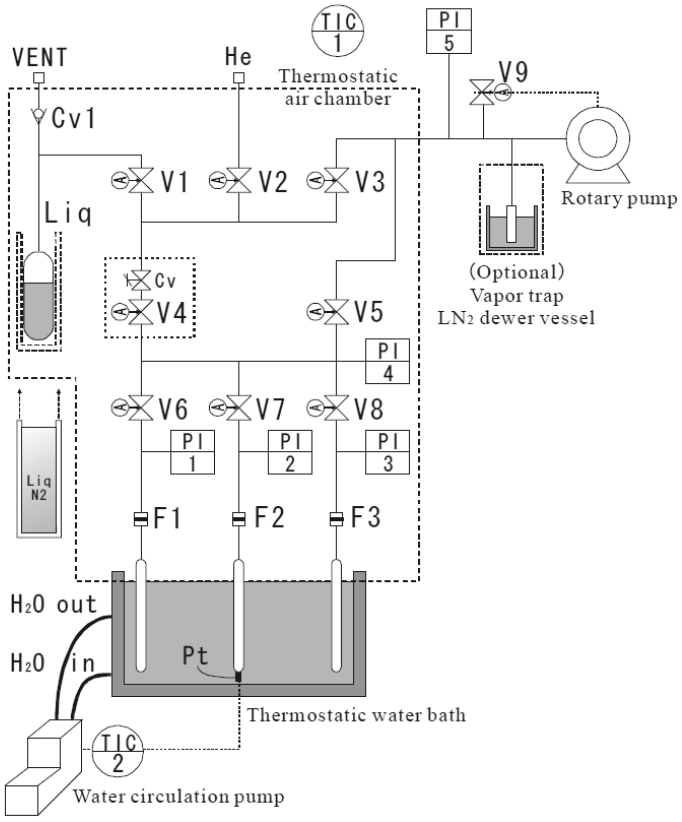

Figure 12: Flow chart of Belsorp Aqua 3 as depicted in (88 p. 19)

Additional equipment is attached to the Belsorp Aqua 3 system. To create an inert atmosphere, it is connected to a Helium supply. Furthermore, for establishing a vacuum inside the system, it is connected to a rotary pump, which, in this case, has a connection to a vapour trap. The entire system is specified for the adsorption of vapours. Therefore, liquids can be filled in the adsorptive tank, which is labelled as “Liq” in Figure 12. Using a defined underpressure up to a vacuum and the thermostatic air chamber, which can be heated up to 50 °C, the poured in liquid is transferred into the gas phase. The adsorption temperature can be controlled by the thermostatic water bath, also labelled in Figure 12 at the bottom and connected to a heating and cooling system (Julabo GmbH, Seelbach, GER). Inside the sample cells, certain atmospheres can be set in terms of pressure and temperature using the pressure sensors.

In sum, the system principle is the following: the inner volume V of the equipment is known as well as the specific gas constant R_S of the vaporised adsorbent. The adsorption temperature T and the pressure p are controlled by the system using the corresponding sensors. Only one parameter, the adsorbed mass m_l or as a substitute the amount of substance n_l of the separated component, must be calculated.

With Dalton's law, where the sum of all partial pressures is the total pressure, it can be assumed that

$$\frac{n_i}{n_{tot}} = \frac{p_i}{p_{tot}} \qquad (28),$$

where n and p are the substance quantity and pressure, respectively. The indices i and tot are for a defined part and the sum of all parts. During an adsorption measurement, the only parameter changed is the pressure p, which affects the saturation degree φ. Consequently, it is possible to determine an isotherm for every sample over the equivalent of a broad range of adsorptive concentrations.

4.2.2 Measurement Preparation

The adsorptives, described in Chapter 3.2, were prepared in a defined way according to the manual of the Belsorp Aqua 3 system (88). Liquids were degassed by cooling down to a temperature of -196 °C, followed by the establishment of a vacuum, where every gas phase was removed. Hereafter, the vacuum was broken by the helium supply, so an inert atmosphere was given, and the adsorptive melted. By repeating this procedure three times, it could be guaranteed that no gaseous inclusions were solved in the adsorptive.

Next, drying under vacuum, utilising a BelPrep II device (Bel Corp., Osaka, JPN) for at least three hours at a temperature of 120 °C to remove humidity and other adsorbed compounds from the surface was executed for the adsorbent to be investigated. Approximately 10 % of the adsorbent's weight in general vanished through this procedure, as it was caused by humidity from the air, which also could be observed before (89 p. 11).

The samples of the adsorbent had a weight as close as possible to 100 mg after the drying process, depending on the particle composition. For the experiments, the temperature for the vaporisation was always set to 50 °C, whereas the adsorbing temperature was set in a range of 10 °C to 35 °C, depending on the objective of the investigation. By using the Antoine equation

$$log_{10}(p) = A - \frac{B}{T+C} \qquad (29)$$

where A, B and C are parameters, which must be looked up for every adsorptive, the vapour pressure could be calculated.

In addition, partial pressures and thus degrees of saturation were specified at which the associated maximum loads should be set. Therefore, 14 measuring points were defined at which an equilibrium should be established. This was accepted by the system if it was stable for more than 800 s.

After these measurements, the experimental data was analysed with the BelMaster software (Bel, Osaka, JPN) and translated into load over adsorbents' mass.

4.3 Breakthrough Measurements

Breakthrough experiments require a certain atmosphere, a separation cell with the adsorbent through which the atmosphere passes, and a suitable analytical device to measure the composition of the atmosphere after the adsorbent has passed the exhaust. These constituents must be scientifically considered for successful investigations. Although these are only three parameters, each of them offers different difficulties. In particular, the handling under different pre-settings of the experimental set-up and the use and permissibility of the measurement devices should be explained.

4.3.1 Measurement Set-Up and Analysis Methods

The set-up for the measurements of the breakthrough behaviour is depicted in Figure 13. Comparably, like for the gravimetric measurement methods for the maximum load, it is possible to attach sources for liquid or gaseous adsorptives, respectively. In front of the adsorption cell, samples can be drawn from the incoming gaseous composition using a special valve, which is marked with a small arrow. The samples can then be investigated by an appropriate analysis device, such as a chromatograph with mass spectrometer (GC / MS), which was employed during research in the form of an Agilent 6890 GC / 5973 MSD system (Agilent Technologies, Santa Clara, CA, USA) for the investigated hydrocarbons. Furthermore, as the pressure drop is of major interest in process engineering (90 p. 171 f.), it can be determined by a pressure difference measurement. Depending on the adsorptives, which are loading the adsorbent, an appropriate analysis device is installed at the exhaust for the investigation of the exiting gas composition.

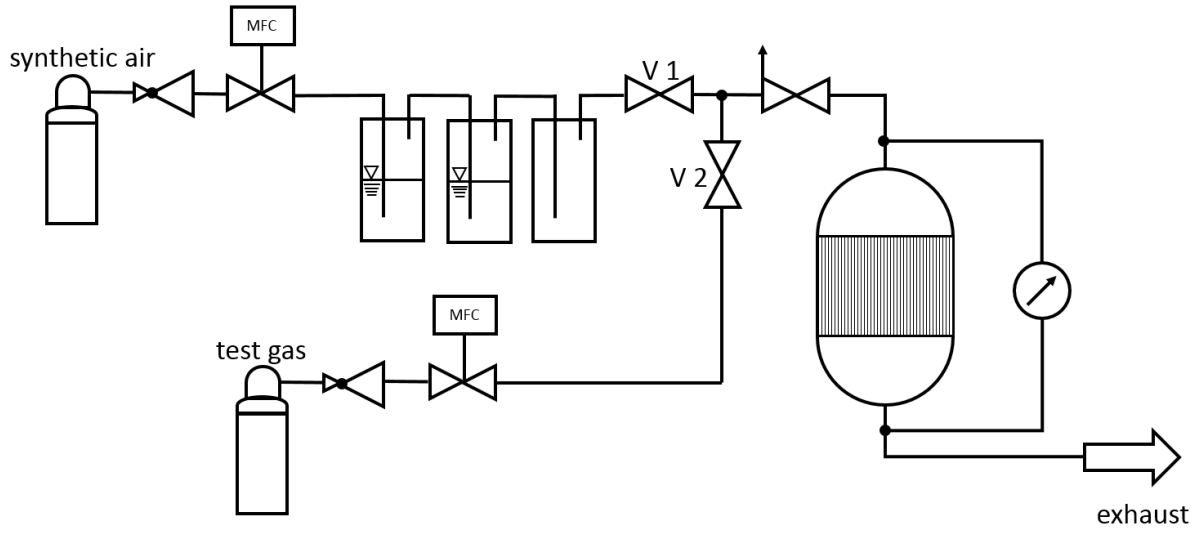

Figure 13: Flow chart for breakthrough measurements of single components

The depicted arrangement is also functional for multi-component measurements. It is possible to open valves V 1 and V 2 singularly or both at the same time. If both are opened in parallel, two different gaseous phases can flow through the adsorber cell. The sources of the adsorptives can also be replaced. E.g., it is possible to attach two pressurised gas cylinders with an adjusted test gas or two lines with liquid vaporisable adsorptives.

The incoming and outgoing gaseous mixtures must be known for a valid analysis and rating of the separation process. The incoming atmosphere therefore was determined by Flame Ionization Detection (FID) (FID 2110 µP, Amluk, Oberaudorf, GER), GC / MS as already mentioned, other commercially available detection devices, mainly based on electro chemical methods (PAC 7000, Dräger, Lübeck, GER; BW Clip Real Time, Honeywell, Morris Town, NJ, USA), or by the knowledge about the engaged gaseous composition in the experiment. A corresponding adsorption success is represented by the difference in concentration between the adsorptive before and after the fixed bed of adsorbent. In principle, the outgoing atmosphere can be analysed by the same means as the incoming gas mixture, except for the knowledge-based approach.

4.3.2 Influence of Adsorption Cell on Breakthrough

Two different adsorption cells were engaged for the research described. Both have significantly different diameters and volumes. The larger one is even modular, so that with one cell different bed lengths and customised inner volumes are provided.

At the beginning of an experiment, the cell is full of ambient air, which is displaced by the adjusted atmosphere that is fed into the adsorption cell. This can be understood as displacement marking, which is also known from stirred tank reactors, but also applies to all apparatuses through which flow occurs (91 p. 233). Therefore, the adsorption cell itself is the tank reactor. If the diameter of the cell were nearly or exact identic in its diameter compared to the tubes, the system represented a tubular reactor and the scientific laws would behave accordingly different. For the deceleration of the gas flow, a widened diameter of the adsorption cell, intentioned and designed for a longer residence time of the gaseous phase, is reasonable. For the resulting reactor, the cumulative distribution function $F(t)$ of any volume element is valid as

$$F(t) = \frac{c(t)}{c_0} \qquad (30)$$

where $c(t)$ is the trace concentration inside the reactor at a certain time and c_0 the input concentration (92 p. 7). As soon as the atmosphere inside the reactor is completely replaced by the displacing gas composition, the gas concentration in the reactor $c(t)$ will reach the equivalent value of the applied gas phase concentration c_0. Mathematically, the total residence time function then approaches $F(t)$ = 1.

A volume element passing the reactor needs a certain time for this process. This time is statistically distributed and unpredictably long. The average retention period of a volume element in the reactor is written as $\bar{t}$ and calculated as follows:

$$\bar{t} = \int_0^1 t \; dF(t) \qquad (31)$$

Here the cumulative distribution function plays a role, again. If it is considered, that

$$\bar{t} = \tau \qquad (32)$$

where τ is the fluid dynamic residence time, and

$$\tau = \frac{V}{\dot{V}} \qquad (33)$$

where V is the volume of the reactor and $\dot{V}$ is the volume flow of the fluid (91 pp. 234-237), this concludes into

$$\frac{V}{\dot{V}} = \int_0^1 t \; dF(t) \qquad (34).$$

The variables in this equation are the reactor volume V, which is determined by the set-up of the adsorption cell and its resulting reactor size, on the left side and the time

t on the right side. Consequently, a larger reactor interior inevitably leads to a longer residence time t. Thus, the volume V of the reactor is decisive for the function of the concentration over time. This function represents the system response of the empty adsorption cell. Consequently, the fixed adsorber bed inside the cell also has an important impact on the system response. It occupies space inside the reactor, which reduces the effective volume V and leads calculatively to a shortened residence time t. This shortens the possible time period for adsorption as well, and reduces the probable adsorption success in relation to the amount of adsorbent applied.

5 Results and Discussion

The results of the executed experiments can be divided into three different parts. Similar to earlier chapters, first the results of equilibrium and kinetics are reported. Then, the equilibria of the target substances in relation to humidity are presented, followed by the results of breakthrough measurements, which embody the subsumtions of the earlier named.

5.1 Kinetics and Equilibrium Measurements

In the following, the adsorption of cyclohexane as well as of acetone and chlorobenzene is discussed. In a next step, the adsorption of carbon monoxide, hydrogen sulphide and ammonia are described. The measurements concerning hydrogen sulphide and, even more, carbon monoxide were particularly complex and difficult, which is due to comparably small loads. Minor deviations in the measurements of carbon monoxide and hydrogen sulphide had a much larger effect than deviations in the measurements of the organic substances, where the achieved loads, measured as weight per surface, were in dimensions of 10^2 times higher.

5.1.1 Cyclohexane

The isotherms of cyclohexane were measured volumetrically with the Belsorp Aqua 3 device. Overall, 13 different ligands, immobilised onto the adsorbent's surface were investigated. Four of these are of special interest, as they performed very well with cyclohexane or were successful with the other investigated adsorptives. The adsorption isotherms of these ligands and the base support HSU 001-075 for cyclohexane as adsorptive are depicted in Figure 14. Therefore, the relative load q_r in units of µg m^{-2} is represented as a function of the partial pressure p in the dimensionless quantity of the factorised vapour pressure p_0. Other shown functionalised adsorbents, carrying different immobilised ligands, are HSU 101-075-07, HSU 101-075-10, HSU 101-075-430 and HSU 001-075.2 introduced and explained in Chapter 2.2.3. All measurements were conducted at least three times. As the results of all three measurements for each of the investigated samples were nearly the same, no deviations are marked in Figure 14. Such a high repeatability was found to be typical for measurements with organic solvents using the Belsorp Aqua 3 device.

Figure 14 can be divided into three different parts of adsorption success. It is clearly shown that at low partial pressures, which can be translated into low concentrations of the compound in the air, every investigated functionalised adsorbent is superior to the base material HSU 001-075, except HSU 101-075-430. This functionalised material behaves identical to its base support, which must be considered as not successful for low concentrations. Only for partial pressures above 0.75 p_0, the performance of HSU 101-075-430 is the highest.

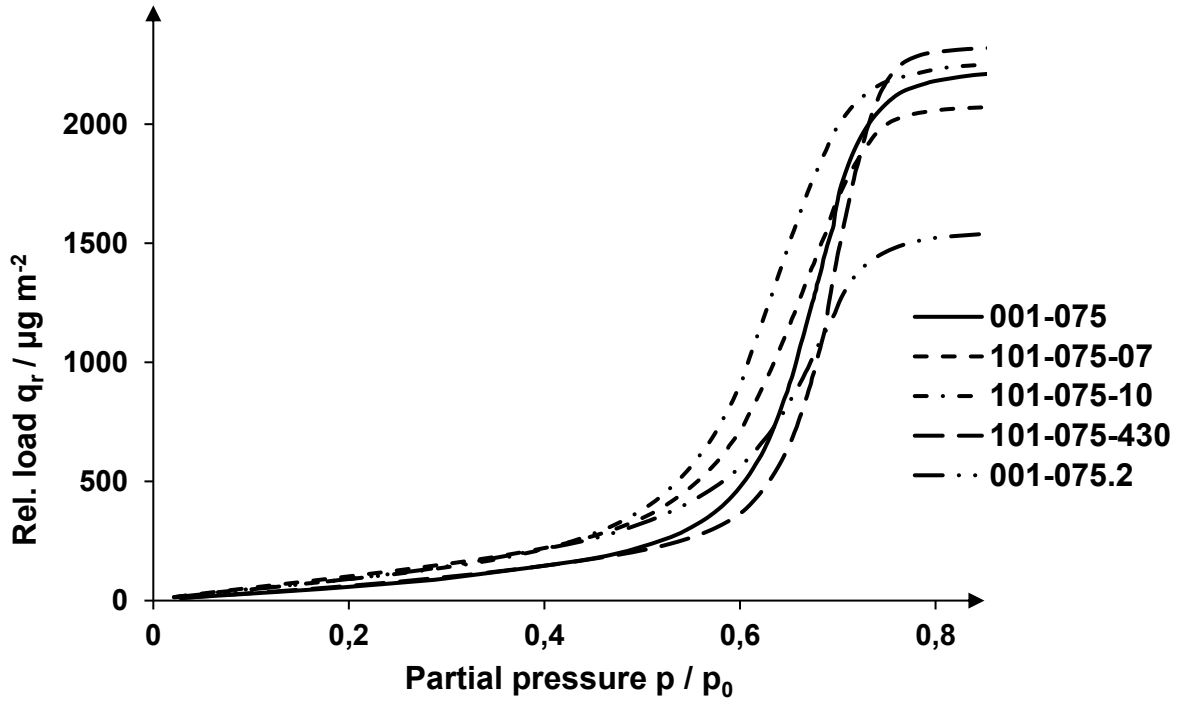

Figure 14: Isotherms of cyclohexane on silica supports with different ligands immobilised onto the surface

At partial pressures between 0.5 p_0 and 0.75 p_0, multi-layer adsorption begins, which leads to pore condensation. Consequently, the loads increase very quickly. For the following consideration, the gradients at low partial pressures are of outstanding interest, as they are a measure for the effectiveness of the adsorbent at lower concentrations. As can be seen from Figure 15, the adsorbents HSU 101-075-07 and HSU 101-075-10 provide a relatively steep isotherm at lower partial pressures. At lowest concentrations, HSU 101-075-07 is the most effective. However, this ratio changes fundamentally and to an increased extent at elevated partial pressures from 0.4 p_0. Above partial pressures of 0.7 p_0, even the basic material HSU 001-075 is more efficient than the functionalised variant HSU 101-075-07. Accordingly, HSU 101-075-10 is regarded as the most efficient adsorbent for separating

cyclohexane, whereas HSU 101-075-07 is considered the second most effective despite its initial superiority. HSU 001-075.2, however, in this case is the least effective. As it is especially developed for the separation of carbon monoxide, this is, on the other hand, a valuable signal for selectivity. At the most elevated partial pressures, HSU 101-075-430 offers the highest gradient. Its isotherm is in the named area the steepest, resulting in the highest loading at higher concentrations, although multi-layering and pore condensation in this case even begins the latest, as can be seen from Figure 14. Thus, at maximum concentrations, HSU 001-075-430 is the material with the highest capacity, whereas HSU 001-075.2 offers the lowest capacity.

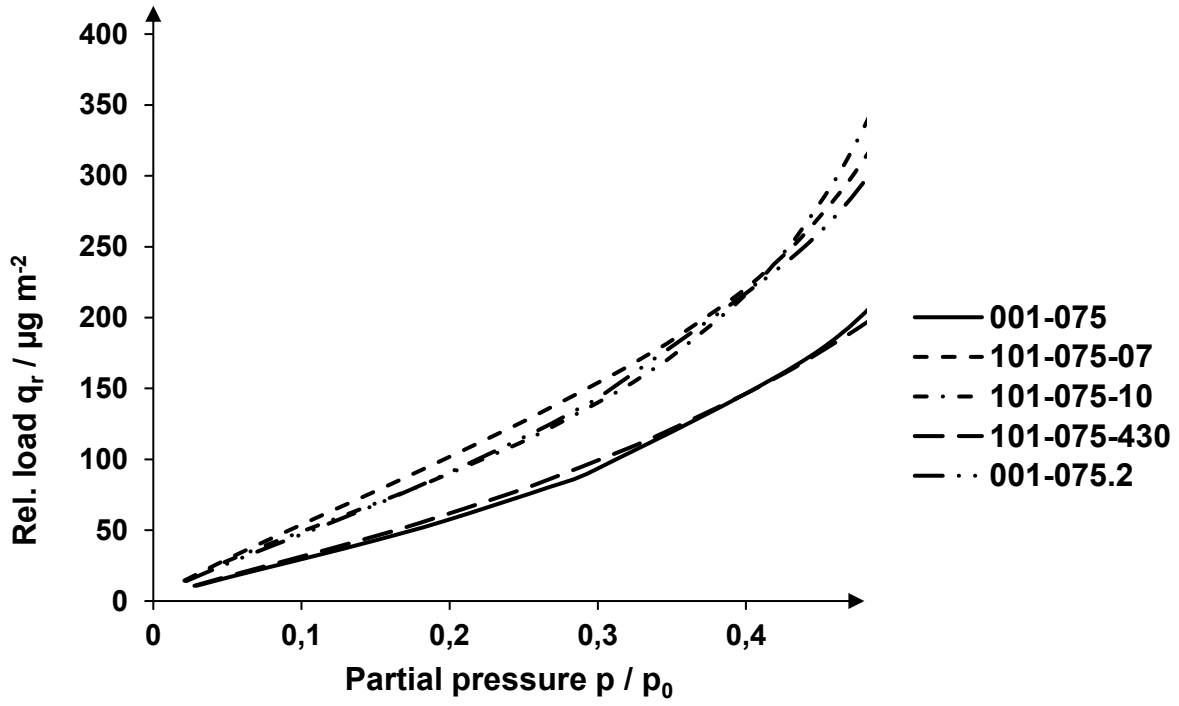

Figure 15: Isotherms of cyclohexane on silica supports with different ligands immobilised onto the surface at lowest partial pressures

Up to a partial pressure of 0.5 p_0, the isotherms of the adsorbents shown are almost linear. Consequently, the relative loads were interpolated at a partial pressure of 0.5 p_0 and plotted in Table 9 to establish comparability. Furthermore, the additional adsorption success achieved by the respective functionalisations compared to HSU 001-075 was calculated and listed as q_{r+}. Due to the almost linear course of the isotherms up to this point, it is possible to draw conclusions about the quality of the performance increase through functionalisations in the particularly relevant low concentration range.

Table 9: Relative load of cyclohexane on differently functionalised adsorbents and benefit of functionalisation in comparison to the base material at 0.5 p_0

Adsorbent	Relative load q_r / µg m^{-2}	Additional relative load q_{r+} / µg m^{-2}
HSU 001-075	232	-
HSU 101-075-10	381	149
HSU 101-075-07	347	115
HSU 101-075-430	211	-21
HSU 001-075.2	325	103

With an average additional loading of 149 µg m^{-2}, the functionalised HSU 101-075-10 is 64 % more efficient than the initial adsorbent HSU 001-075. An increase in performance also occurs for HSU 101-075-07, which adsorbs 115 µg m^{-2} and thus almost 50 % more than the base material. HSU 001-075.2 adsorbs a total of 325 µg m^{-2} at the corresponding partial pressure, which is also equal to an increase of 40 %, but, as already mentioned, drops back significantly at higher partial pressures. HSU 101-075-430, the most successful adsorbent at highest partial pressures, is also the least effective at low partial pressures. With an average relative loading of 211 µg m^{-2}, it is 21 µg m^{-2} or just under 10 % weaker than the base material. Compared to the most promising adsorbent, it is thus 81 % weaker at the prevailing partial pressure and adsorbs 170 µg m^{-2} less of the target substance. Thus, the outstanding quality gain by functionalising the base material to HSU 101-075-10 becomes clear.

The influence of the temperature at the lower and thus more interesting partial pressures was also investigated. Figure 16 depicts the relative loading of cyclohexane onto HSU 101-075-10 as the most promising adsorption material at different temperatures. Furthermore, only the results for lower partial pressures and consequently the equivalents for lower concentrations are shown. The experimental adsorption temperatures were also adjusted between 10 °C and 35 °C, respectively. The relative loading for these temperatures only differs in a negligible extent. This was not expected, because adsorption is an exothermic process. Hence, at higher temperatures, the binding of the adsorptive onto the adsorbent was expected to be considerably less favoured.

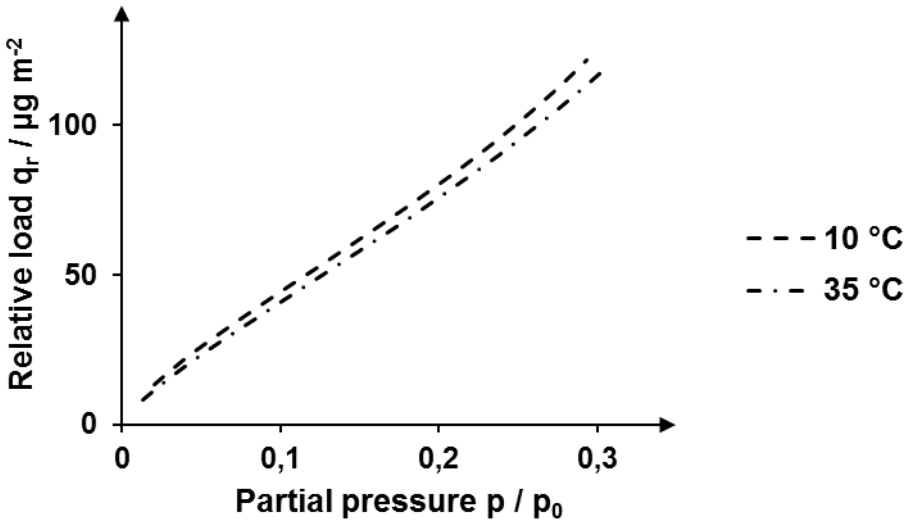

Figure 16: Relative loading of HSU 101-075-10 with cyclohexane under different temperature conditions depending on the partial pressures

Referring to the relative concentration of the adsorptive in the ambient air, the prevailing temperature obviously plays no role during the adsorption. For a deeper understanding, it is important to highlight the fact that this consideration does not take into account the importance of partial pressure and its dependence on temperature. The vapour pressure curve of cyclohexane is not linear, as shown in Figure 17, where the vapour pressure between 7 °C and 62 °C can be seen. The data for the graph was calculated using equation (30) from Chapter 4.2.2 with data from (93 p. D41).

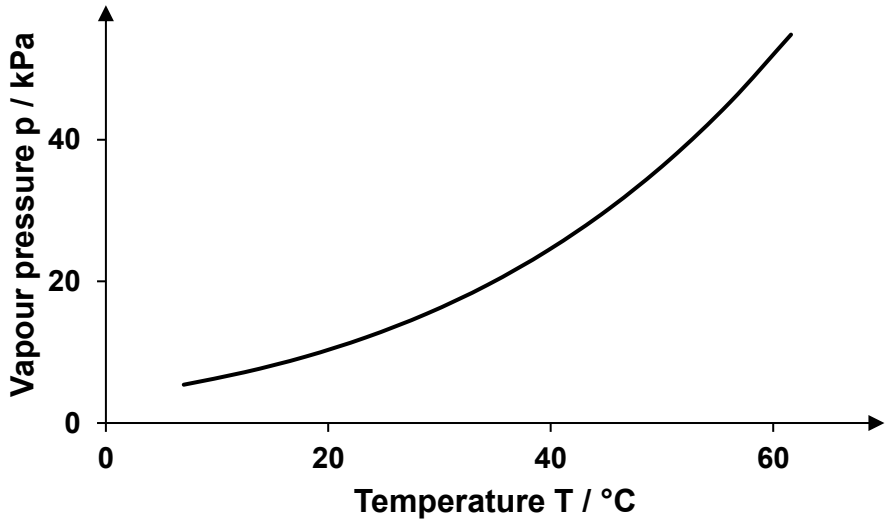

Figure 17: Vapour pressure curve of cyclohexane in a temperature range of 7 °C to 62 °C

The vapour pressure is clearly increasing in an exponential way. A possible surrounding atmosphere of nitrogen and oxygen, on the other hand, behaves at least nearly as an ideal gas. If the volume keeps the same, the pressure of air increases nearly linearly depending on the temperature.

Accordingly, these results must be proven by obeying the law of Dalton

$$p_{tot} = \sum_{i=1}^{k} p_i \qquad (35),$$

where the total pressure is the sum of the partial pressures. In fact, the calculated fraction of cyclohexane in the air rises significantly. In a predefined room, taking the ideal gas law for the air and the known data for cyclohexane into account, the total volumetric fraction of cyclohexane ascents from approximately 6.1 vol.-% at 10 °C to ca. 15.9 vol.-% at 35 °C, which is more than double. Following this argumentation, it is reasonable to value the absolute pressure and the resulting relative loading of HSU 101-075-10, which can be seen in Figure 18.

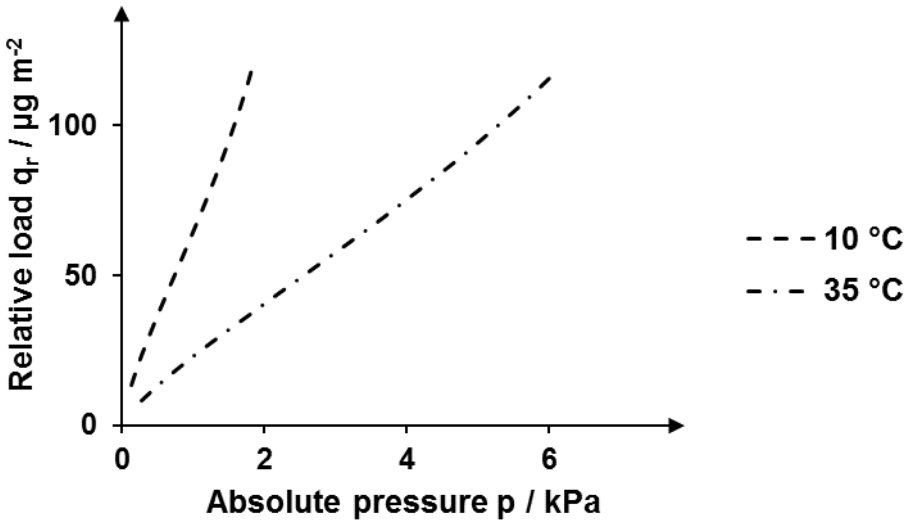

Figure 18: Relative loading of cyclohexane at HSU 101-075-10 under different temperatures over the absolute pressure of the adsorptive

The course of the isotherm represented as relative loading over the absolute partial pressure is much steeper for an adsorption temperature of 10 °C than for an adsorption temperature of 35 °C. This means, that at low temperatures for relatively low absolute pressures, a comparably large amount of the respective adsorptive is bound onto the surface of the adsorbent. For the shown example of cyclohexane, which is exposed to a temperature of 10 °C, a relative loading of 50 µg m^{-2} at a pressure of 0.739 kPa is achieved. At 35 °C, the same loading is only achieved at a pressure of 2.547 kPa. It

can also be assumed that the corresponding absolute pressures are reached more quickly at the higher temperature. But then, there is also more adsorptive in the atmosphere. Consequently, a smaller proportion of the total content of the adsorptive can be separated from the atmosphere with a constant amount of adsorbent, regardless of the relative loading the adsorbent achieved.

This demonstration makes it clear that temperature indeed is an important factor in scientific and applied adsorption, even at relatively low temperatures such as those set for these experiments.

5.1.2 Further Measurements with Liquid Organic Solvents

For acetone and chlorobenzene, data concerning maximum loading and isotherms was recorded as well. Especially for the understanding of the influence of the vapour pressure, a comparison of the relative loading as a function of the partial pressure is helpful. The vapour pressures of selected adsorptives at a temperature of 20 °C are given in Table 10.

Table 10: Vapour pressures of acetone, chlorobenzene and cyclohexane at 20 °C

Hazardous compound	Vapour pressure p / kPa
Acetone	24.6
Chlorobenzene	1.2
Cyclohexane	10.4

From the values shown for 20 °C, it becomes clear that acetone with a vapour pressure of 24.6 kPa evaporates to a greater extent than cyclohexane, whose vapour pressure of 10.4 kPa is less than half as high. Chlorobenzene, by contrast, has a much lower vapour pressure. A higher vapour pressure is equivalent to a higher concentration in a surrounding atmosphere. In Figure 19, the adsorption isotherms, which refer to the partial pressure as a fraction of the vapour pressure at a temperature of 20 °C of acetone, chlorobenzene and cyclohexane onto HSU 001-075, are shown as graphs.

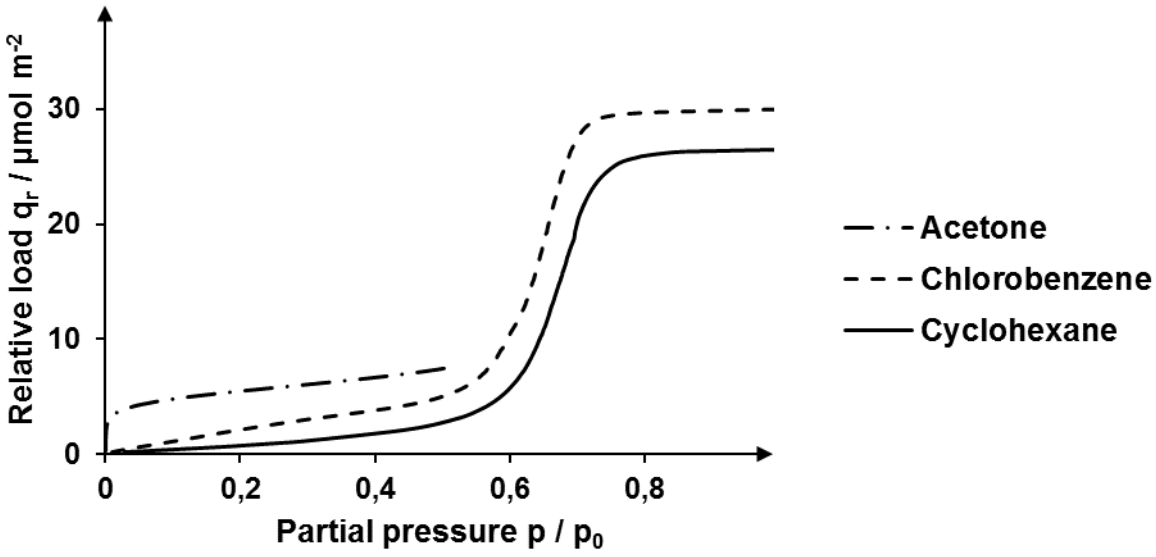

Figure 19: Relative load on HSU 001-075 with different organic adsorptives over the partial pressure

Because of the different molar masses M, q_r is specified in this case as the substance quantity per area in µmol m^{-2}. This representation makes the adsorption processes comparable, as for every chemical reaction, not the pure mass is decisive, but the number of molecules bound on the adsorbents' surfaces. For the comprehension of Figure 19, it is necessary to mention the possible maximum vapour pressure of 12.5 kPa, which can be handled by the utilised Belsorp Aqua 3 device. Thus, it is understandable, why the graph of acetone is not shown up to a partial pressure of 1 like the other two compounds. The vapour pressure of acetone is with 24.6 kPa nearly twice as high as the highest value feasible for the equipment. Consequently, the isotherm of acetone cannot be measured and depicted completely. Therefore, it cannot be concluded, whether further pore condensation occurs at higher concentrations. Cyclohexane and chlorobenzene, on the other hand, are measured over the complete range of possible partial pressures from 0 % to 100 % of the vapour pressure. Basically, the isotherms of cyclohexane and chlorobenzene are very similar, although chlorobenzene is obviously always adsorbed at a higher level than cyclohexane at the determined partial pressures. For both substances, pore condensation begins slowly above half of their corresponding vapour pressure. For acetone, where the measurement stops much earlier, this cannot be experimentally determined. In this case, the very steep increase of the isotherm at lowest partial pressures is remarkable. It is rather unlikely that pore condensation is already present here. The form speaks for a very steep Henry isotherm which changes into a Freundlich isotherm. The long

slight increase after the Freundlich bend supports this assumption as well. After pore condensation, a plateau would be expected, as this occurs both for chlorobenzene and cyclohexane, as can be seen in the figure at highest concentrations.

Figure 20 shows the same data related to absolute pressure. Thus, it becomes clear that the three substances investigated have completely different vapour pressures and consequently result in completely different concentrations in a contaminated atmosphere. For chlorobenzene, a partial pressure of 1.2 kPa already results in a completely saturated atmosphere; for acetone, a partial pressure of 24.6 kPa would be necessary. For these contemplations, it is essential to understand that vaporisation always is in an equilibrium with the surrounding atmosphere (94 p. 201).

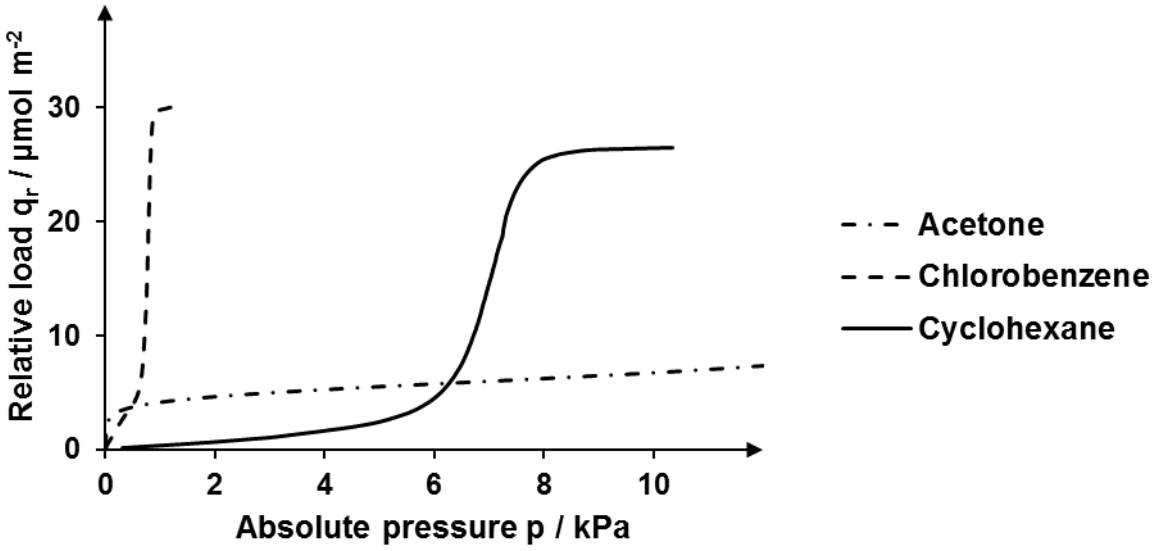

Figure 20: Relative loading at HSU 001-075 with different organic adsorptives over the absolute pressure

Consequently, for already very low concentrations of chlorobenzene, the adsorption performance of the used adsorbent is superior in comparison to the adsorption of acetone and cyclohexane. Only at the lowest concentrations, the amount of bound acetone is higher. This trend is also valid for all other investigated functionalised adsorbents. It is omitted to show all these results here. The possible improvement of the investigated base materials for each compound does not overlay or even exceed this effect caused by the choice of the adsorptive. This should not obscure the fact that functionalisation by means of ligands immobilised on the adsorbents' surface is equivalent to a considerable increase in performance.

The pore sizes also have a decisive impact on the adsorption behaviour (3 p. 72 f.; 76 f.). To clarify the extent of influence, further measurements were conducted in this set-up with acetone, comparing the equilibrium results of three different pore sizes from 100 Å over 300 Å to 500 Å. These results were compared regarding their relative load per surface. A selection of the most relevant graphs can be seen in Figure 21. The adsorbents for these experiments were of the same particle size, produced by the same factory, with the aim to guarantee a high degree of comparability.

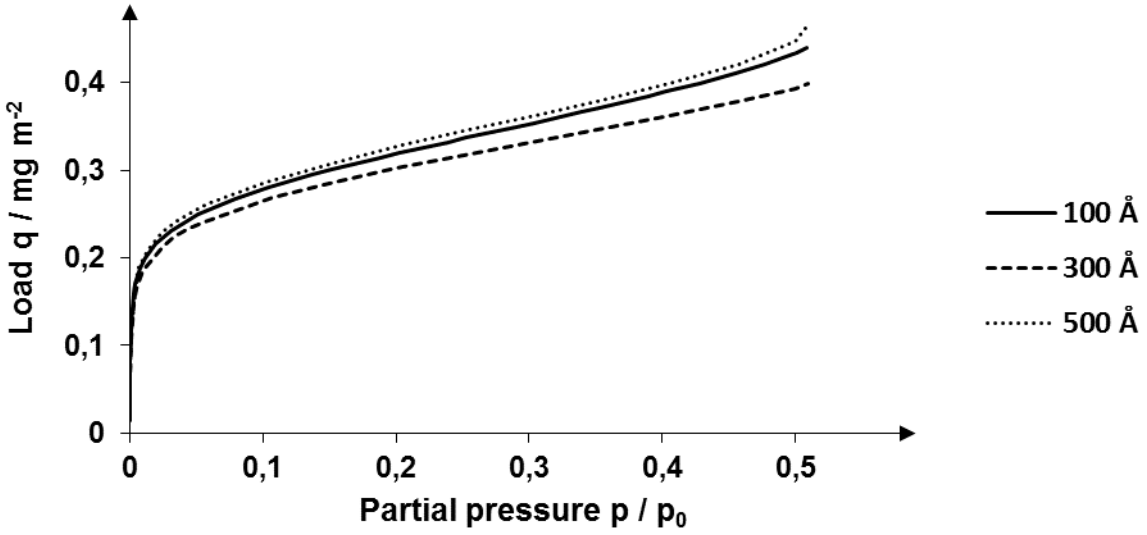

Figure 21: Equilibrium loading on adsorbents with different pore sizes with acetone as adsorptive

It is noticeable, that the adsorbents with 100 Å and 500 Å behave in a nearly identical way. On the other hand, the mid-size with pore diameters of 300 Å is less effective relative to its surface. This might be due to deviations within the production process of Silicycle. For the experiments, three different samples of the same charge were investigated. Remarkably, the distances of the different graphs are in a scaled ratio to each other, which supports the above thesis. With these results, it has been proven that a comparison of different adsorbents on the basis of the separation performance via the relative load per surface is a valuable method even for supports, which differ greatly in pore size and particle size.

5.1.3 Carbon Monoxide

Mainly HSU 031-295 and HSU 001-075 with their functionalised versions were investigated for the separation of carbon monoxide. As reported in Chapter 3.1.1 in

Table 5, these two materials differ in pore size as well as in particle size. The comparison of the separation results achieved by them as well as their functionalised versions should give an insight in the successful improvement that a functionalisation process offers and can be extrapolated to other silica supports.

In Figure 22, four points of the isotherms for HSU 001-075 and HSU 001-075.2 as well as for HSU 031-295 and HSU 031-295.2 are depicted. The improvement with the .2-ligand was chosen, because it offered the most promising results of all developed functionalisation methods. Shown is the relative load per surface q_r over the concentration c. For HSU 001-075 and its functionalised version HSU 001-075.2, two facts are obvious and important, as can be seen in Figure 22. For the lowest concentrations of 0.9 ppm_v and 8.5 ppm_v of CO, the relative load for both materials can be considered as equal. The measuring deviation for HSU 001-075.2, especially for the lowest concentration, is much higher compared to the deviation for the base material HSU 001-075. Overall, they are in the same range in terms of their adsorption performance with lower precision. Higher deviations may occur, because the functionalisation method was newly developed and is thus in the prototype state. Consequently, the reproducibility is not of a standard as in an automated industrial process.

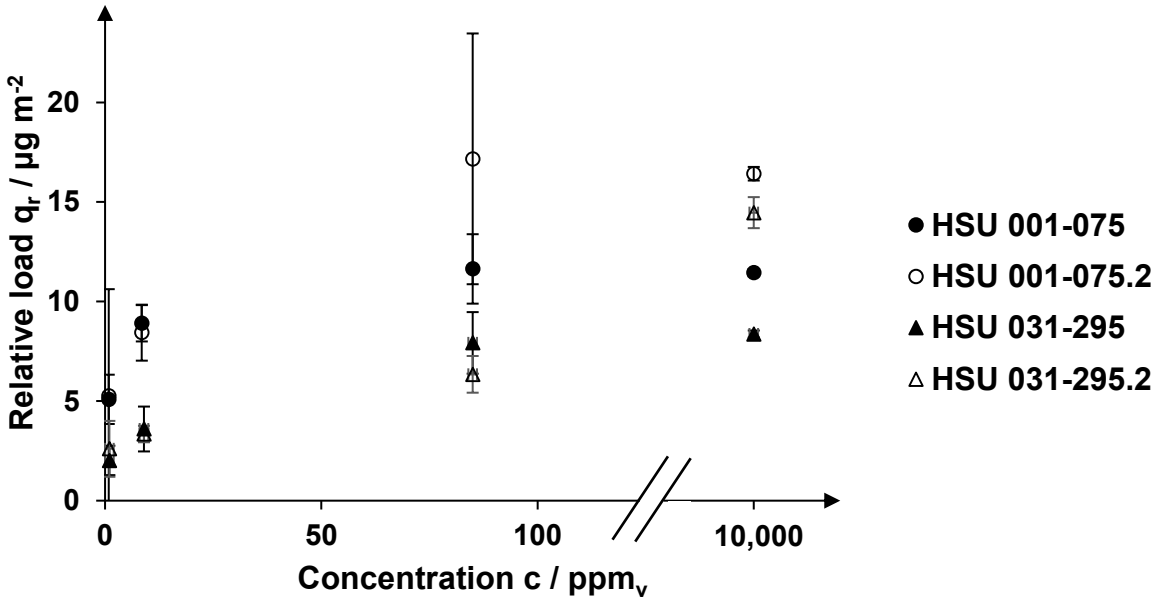

Figure 22: Maximum loads by CO under different concentrations on HSU 001-075 and HSU 031-295 as well as their functionalised versions HSU 001-075.2 and HSU 031-295.2, respectively

For the higher concentrations of 85 ppm$_v$ and moreover for 10,000 ppm$_v$, the difference in the possible loading quantities of the adsorbents with CO as adsorptive is remarkable. The relative load of the silica support with the immobilised ligand on its surface is in average more than 40 % higher compared to the load on the unfunctionalised, even at the lower concentration of 85 ppm$_v$. Admittedly, for HSU 001-075.2 the calculated standard deviation at this concentration is relatively high, too. For both adsorbents, the standard deviations overlap. So, statistically there is a certain probability that the unfunctionalised adsorbent performs better than the silanised adsorbent at a CO concentration of 85 ppm$_v$. For 10,000 ppm$_v$ in difference, the standard deviation is relatively low for both investigated adsorbents. At this concentration, the relative loading of HSU 001-075.2 is with a value of 16.4 µg m^{-2} without statistical limitation, clearly higher than the loading of HSU 001-075 which results in 11.5 µg m^{-2} on average. In case of the highest two investigated concentrations of carbon monoxide as adsorptive, the surface of the adsorbents can be considered as totally covered by a monomolecular layer. This is indicated by the almost identical loads at the latter two CO concentrations. Thus, the maximum load for both adsorbents is already reached at comparably low concentrations, possibly even for concentrations below 85 ppm$_v$.

For the Merck material HSU 031-295 and the functionalised HSU 031-295.2, the results are slightly different. This might be due to the different characteristics of the base supports. HSU 031-295 particles have diameters from 2000 µm to 5000 µm and thus are ten times larger than the particles of HSU 001-075 with diameters of 200 µm to 500 µm. Their pore diameters differ as well. For HSU 031-295, the pores are in average 33 Å wide, whereas HSU 001-075 offers diameters which are three times larger with an average value of 100 Å. This could lead to different adsorption behaviour of the silica supports. HSU 031-295 as base material behaves like the above described base HSU 001-075 in terms of the shape of the isotherm curve, although the relative loads are generally significantly lower.

HSU 031-295.2 as a functionalised version is comparably loaded to the base material even at a concentration of 85 ppm_v. Considering the implemented deviations, it can be assumed that the loading with carbon monoxide at this concentration is for both adsorbents at the same level. At the highest concentration of 1 vol.-%, i.e. 10,000 ppm_v in contrary, the load for HSU 031-295.2 with 14.5 µg m^{-2} is significantly higher by more than 70 % compared to the unfunctionalised base support HSU 031-295 with an average value of 8.4 µg m^{-2}.

From these equilibrium measurements, it can be concluded that he separation performance concerning CO can be improved at least for the higher and more dangerous concentrations for both base materials. The pore sizes and the particle sizes, on the other hand, seem to have an influence on the improvement achievable through functionalisation.

For isotherms, which are of the Langmuir type, as mentioned in Chapter 2.1.1, Markham and Benton postulated that the inverted load over the inverted concentration should result in a straight line. This method is very well suited to determine whether a Freundlich isotherm is present. Basically, it can be assumed that the respective isotherm is not an ideal form. To find out what this ideal form would look like, a straight line can be constructed. Such a straight line can be translated back and then shows the corrected optimal Freundlich isotherm. The comparison of the corrected isotherm with the measured isotherm shows visually how close the measured corresponds to the Freundlich type. The measured adsorption isotherm of HSU 001-075 translated into a Markham-Benton-function is close to a straight line, but also reveals minor deviations. This can be seen in Figure 23, where the inverted relative load is plotted

over the inverted concentration. HSU 001-075 values are shown as black filled circles. On the other hand, black filled triangles represent the values for the theoretical ideal straight line according to Markham and Benton. The measurement points at the lowest and the highest concentration help as fixed parameters in the construction. Apparently, the distances between filled triangles and filled circles as measuring point markings are relatively small. This also applies to HSU 001-075.2 whose values are represented in parallel by white filled circles and triangles. In contrast, especially the value pair at an inverted concentration of 8.5^{-1} ppm_v^{-1} (the second group of values from the right) is comparatively far apart.

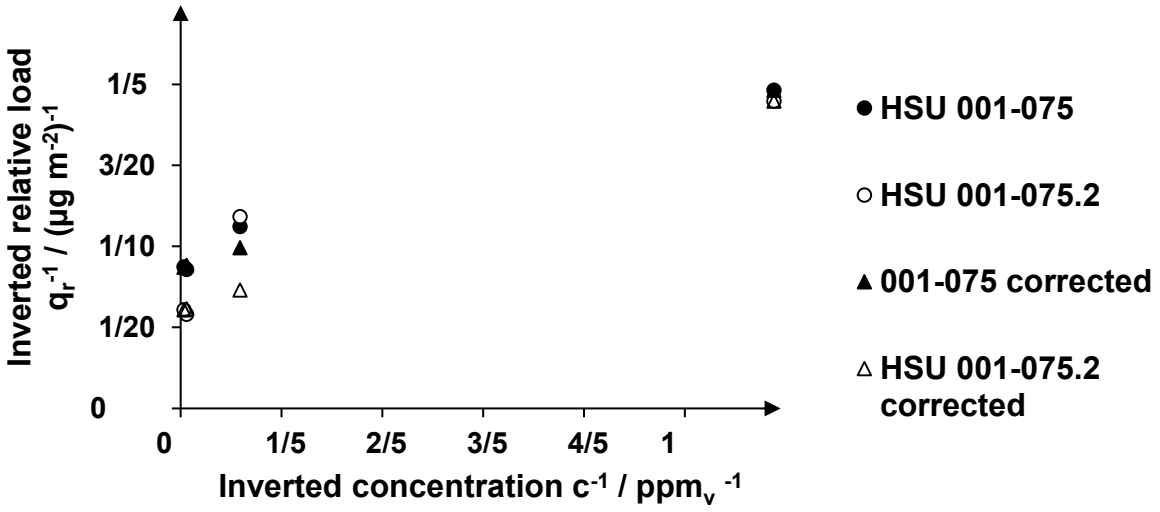

Figure 23: Markham and Benton functions for HSU 001-075 and its functionalised version HSU 001-075.2 caused by different concentrations of CO

Figure 24 shows the straight lines optimally modelled according to Markham and Benton translated back into Freundlich isotherms in comparison to the previously measured values.

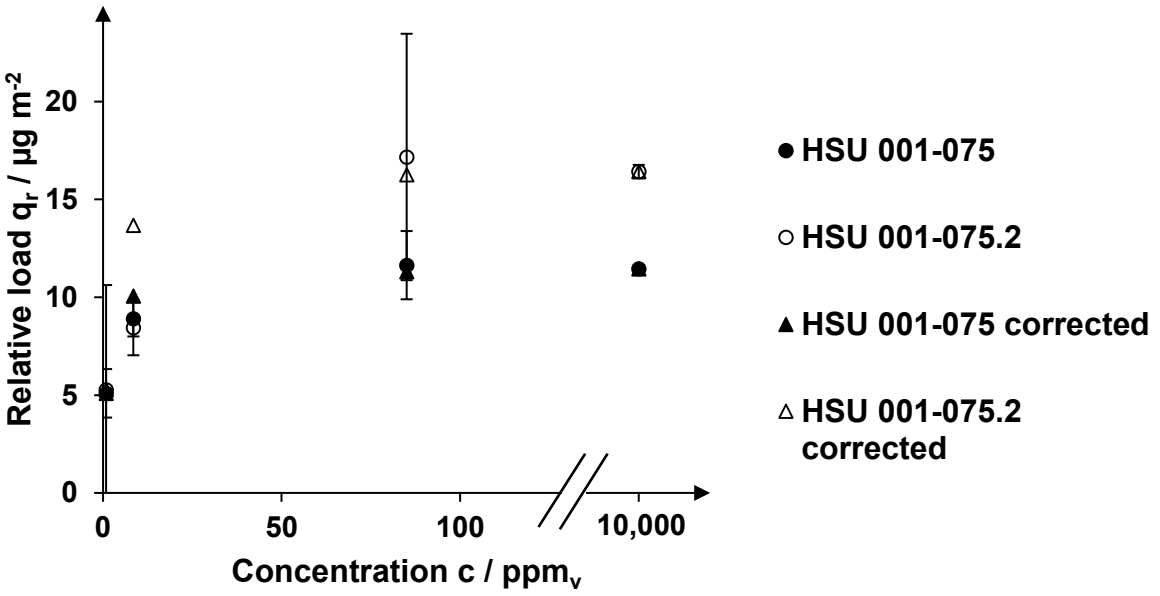

Figure 24: Isotherm of CO onto HSU 001-075 and HSU 001-075.2 as measured and as expected following Chapter 2.1.1

In case of HSU 001-075, the measured isotherm and the isotherm modelled according to an optimised Markham-Benton function run almost in parallel. All modelled points are covered by the measured values at least within the standard deviation, although, especially at the lowest concentration, the measurement deviations are comparably large. This is caused by the very small loads, where the smallest deviations have a large impact on the results. Calculations showed that a correction of the relative load to a smaller value would lead to an even better fit of the calculated isotherm to the measured isotherm. HSU 001-075.2 does not clearly achieve this ideal form of a Freundlich isotherm, especially at lower concentrations. For a concentration of 8.5 ppm$_v$ CO, a measured load of 8.4 µg m^{-2} results, which is significantly below the expected value of 13.7 µg m^{-2} as modelled. The load for the functionalised variant is therefore not quite as good as the model suggests. Instead, the isotherm can rather be interpreted as a relatively flat Henry form, especially at small and smallest concentrations, which changes relatively late into the Freundlich form and thus runs below the optimal Freundlich isotherm. This can also be explained by the obviously increased capacity compared to HSU 001-075. Such a linear fraction at the beginning of the isotherm can be prolonged by providing more adsorptive sites for the adsorptive.

In addition to the investigations concerning equilibria, kinetic investigations with a duration of 10, 30 and 60 minutes were conducted. For selected adsorbents, these

measurements were also executed over 120 and 180 minutes. Figure 25 shows the progressing load over time of CO in a concentration of 1 vol.-% or 10,000 ppm_v in synthetic air onto the adsorbent HSU 001-075 and its functionalised versions HSU 001-075.1 and HSU 001-075.2. Very clearly, the .2 functionalised silica support is superior to the other two versions over time. Already after 10 min, the relative loading of HSU 001-075.2 is 10.9 µg m^{-2}. After the same time interval, the loading of the basic version HSU 001-075 is only 5.4 µg m^{-2}. Thus, after a short interval, the loading of the functionalised material is with a difference of 5.5 µg m^{-2} twice as high as that of the unfunctionalised material. After 60 min, however, this difference decreases. The loading for the starting material HSU 001-075 then reaches 11.6 µg m^{-2}. For HSU 001-075.2, the relative loading results only in 3.1 µg m^{-2} more, namely 14.7 µg m^{-2}.

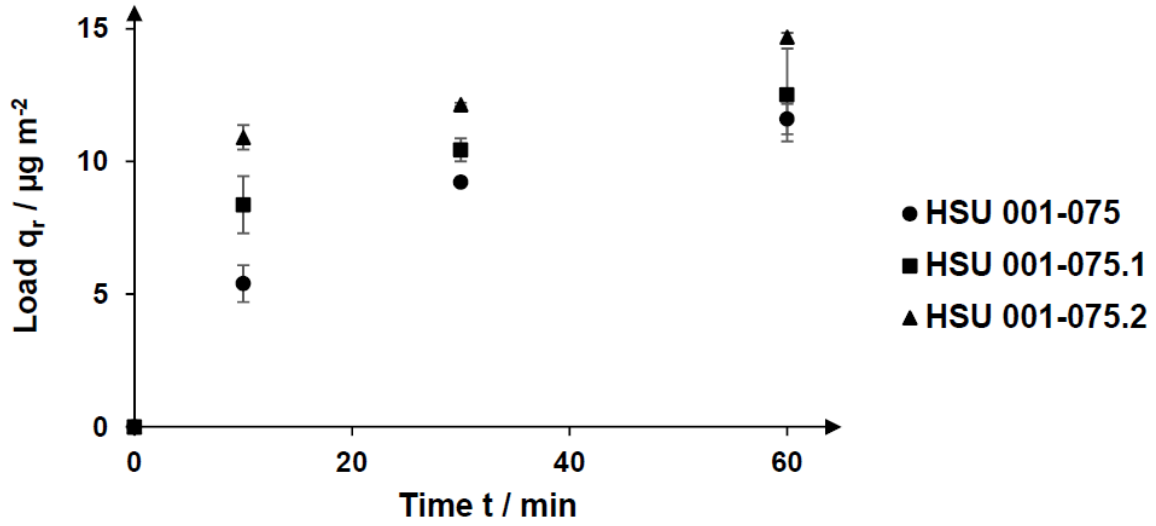

Figure 25: Kinetics of HSU 001-075 and differently functionalised derivates with an applied adsorptive concentration of 10,000 ppm_v

As soon as 10 min have elapsed, HSU 001-075.1 is loaded with 8.4 µg m^{-2}, which is 3.0 µg m^{-2} more than HSU 001-075. Compared to HSU 001-075.2, this results in a negative difference of 2.5 µg m^{-2}. Accordingly, the difference between the two functionalised variants is smaller than their distance to the unfunctionalised variant. Regarding the relatively weak degree of functionalisation for HSU 001-075.1 compared to HSU 001-075.2, as shown in Table 6, the separation success at this early point in time is very high and speaks for the great effectiveness of the functionalisation. After 30 minutes, HSU 001-075.1 with a load of 10.4 µg m^{-2} is still superior to the base silica

support with 9.2 µg m^{-2}, but clearly loses advantage with only 1.2 µg m^{-2} more load of carbon monoxide on the surface of the adsorbent. Thus, the distance to the base material is smaller than to the further functionalised variant HSU 001-075.2, which binds an amount of 1.7 µg m^{-2} more on its surface. When 60 minutes have elapsed, the values of HSU 001-075 and HSU 001-075.1 are within the standard deviation of each other. This form of kinetics is to be expected for HSU 001-075.1 just as it is shown. The maximum load differs only to a limited extent from HSU 001-075. Obviously, however, the affinity for carbon monoxide is increased in comparison to the base material by this functionalisation investigated, which results in a higher adsorption rate especially at the beginning of the exposure. The free places are thus occupied earlier by the adsorbent. Consequently, the still free capacities decrease progressively faster, so the adsorption rate seems to be reduced in relation to the initial variant HSU 001-075.

In Figure 26, the Merck material HSU 031-295 and its functionalised versions HSU 031-295.1 and HSU 031-295.2 are depicted. For HSU 031-295.2, the initial kinetics are significantly slower than for the other two, although the maximum load of HSU 031-295.2 is the highest in comparison to the others. HSU 031-295.1 offers the fastest loading rates within the first 30 minutes.

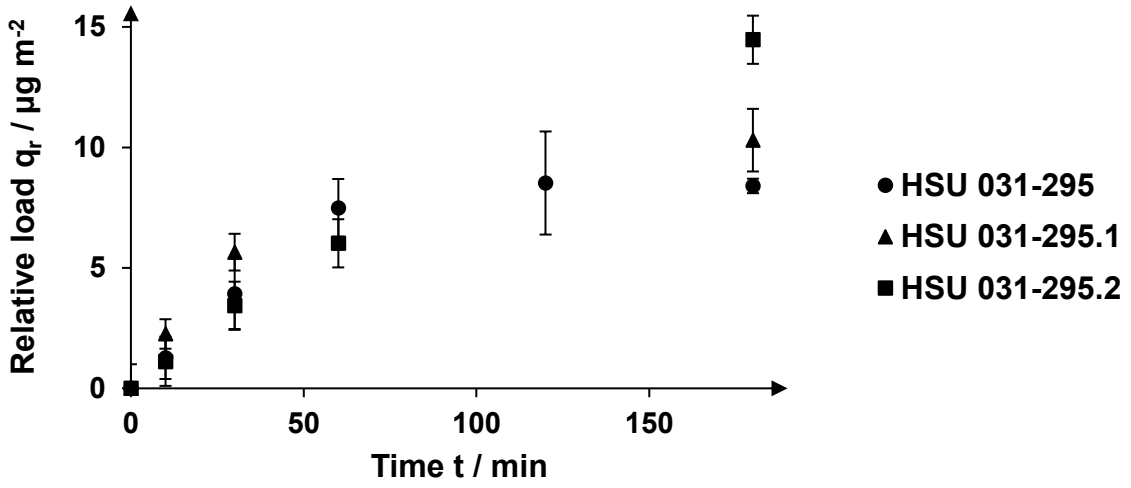

Figure 26: Kinetics of HSU 031-295 and differently functionalised derivates at a carbon monoxide concentration of 10,000 ppm_v

The ligands applied as well as their concentrations in the solvent for the functionalisation process are identical to those used for HSU 001-075. This reinforces

the assumption regarding the effect of the functionalisation. A .1-functionalisation basically does not lead compulsorily to a higher load. On the other side, supposedly dependent on pore size and particle size, it can enforce the kinetics of the adsorption process. When a .2 functionalisation is conducted, however, this also does not increase the adsorption rate fundamentally, but the amount adsorbed in total independent from time.

This is exemplified and confirmed in Table 11, where the loading of CO onto the named adsorbents after 10 minutes, 30 minutes and after infinite time is listed as comparable figures. In addition, kinetics is recorded as the mean adsorption rate r_a, which is calculated as the relative load in weight per surface divided by time

$$r_a = q_r \, t^{-1} \qquad (36)$$

after 10 and 30 minutes. The values are given in Table 11

Table 11: Comparison of the loading of different adsorbents at a CO concentration of 10,000 ppm_v after 10 and 30 minutes as well as maximum load

	10 minutes		30 minutes		Maximum
	Rel. load	Kinetics	Rel. load	Kinetics	load
Adsorbent	q_r / µg m^{-2}	r_a / µg m^{-2} min^{-1}	q_r / µg m^{-2}	r_a / µg m^{-2} min^{-1}	q_r / µg m^{-2}
HSU 001-075	5.4 ± 0.7	0.54 ± 0.07	9.2 ± 0.1	0.31 ±0.01	11.5 ± 0.2
HSU 001-075.1	8.4 ± 1.1	0.84 ± 0.13	10.4 ± 0.4	0.35 ± 0.02	15.7 ± 1.9
HSU 001-075.2	10.9 ± 0.5	1.09 ± 0.05	12.1 ± 0.1	0.40 ± 0.01	16.4 ± 0.3
HSU 031-295	1.2 ± 0.9	0.12 ± 0.09	3.9 ± 1.5	0.13 ± 0.05	8.4 ± 0.3
HSU 031-295.1	2.3 ± 0.6	0.23 ± 0.06	5.5 ± 0.3	0.18 ± 0.01	10.3 ± 1.3
HSU 031-295.2	1.1 ± 0.2	0.11 ± 0.02	3.4 ± 0.2	0.11 ± 0.01	14.5 ± 0.8

The values for the kinetics shown in the table are derived from the mean value of the loads reached after the respective time has elapsed. A comparison between the calculated kinetics for 10 and 30 minutes provides valuable information for the adsorption behaviour. The adsorption capacity and its rate at the beginning of the adsorption process are of especially decisive importance and a measure for the effectiveness of the adsorbent in the application. In fact, these values allow to deduce the separation ability per time at a specific moment. In addition, it can be determined to what extent the temporary loading capacity decreases with increasing adsorption of

the adsorptive. The values in the two kinetic columns were calculated from the corresponding load columns.

HSU 001-075, which is coarser-pored, and its functionalised variants obviously achieve higher relative area loads compared to HSU 031-295 and its efficiency-enhanced versions. This goes so far that the unfunctionalised HSU 001-075 achieves on average higher relative loading values than the functionalised HSU 031-295.1. Including the standard deviation, which is just under 13 % for HSU 031-295.1, both materials are in the same effectiveness range. A comparison of the respective unfunctionalised variants shows that HSU 001-075 with 11.5 µg m^{-2} adsorbed carbon monoxide achieves an adsorptive value 37 % higher than HSU 031-295 with 8.4 µg m^{-2}. For the two variants 001-075.2 and HSU 031-295.2, this comparison is significantly less severe with an increase of 13 % to 16.4 µg m^{-2} from 14.5 µg m^{-2} for the later mentioned adsorbent.

The differences in loading between HSU 001-075, HSU 031-295 and their variants improved by ligand binding are even more pronounced after short adsorption times of 10 and 30 minutes. HSU 001-075 is already coated with an average of 5.4 µg m^{-2} CO after 10 minutes, which corresponds to almost 47 % of the total load. HSU 031-295 adsorbed only about 1.2 µg m^{-2} CO within the same time, i.e. about 22 % of the value achieved by HSU 001-075 and only 14 % of its later total load. After 30 minutes, the ratio shifts in favour of HSU 031-295, which at that time was loaded with 3.9 µg m^{-2} of the adsorptive, or 42 % of the load reached by HSU 001-075. Relative to the totally achieved load, these values are 80 % for HSU 001-075 and 46 % for HSU 031-295. This already shows for the starting materials, that HSU 001-075 with its three times larger pore diameters but ten times smaller particle diameters, allows considerably faster adsorption kinetics in the first minutes of the adsorption process. This effect becomes even clearer with the functionalised variants HSU 001-075.2 with a relative load of 10.9 µg m^{-2} and HSU 031-295.2 with 1.1 µg m^{-2}. Consequently, adsorption by the fine-pored HSU 031-295 and its derivatives proceeds considerably slower than by the reference material HSU 001-075, but over a longer period with a more constant adsorption rate.

Another observation is of outstanding interest. For HSU 001-075, the functionalisations to HSU 001-075.1 and HSU 001-075.2 are accompanied by an increase in the adsorption rate. After 10 minutes, the adsorptive uptake per time unit for

HSU 001-075.2 with 1.09 µg m^{-2} s^{-1} is twice as high as for HSU 001-075 with 0.54 µg m^{-2} s^{-1}. After 30, the adsorption rate is still 29 % higher with 0.40 µg m^{-2} s^{-1} in comparison to 0.31 µg m^{-2} s^{-1}. This effect is not fully detectable for HSU 031-295 and its variants. The results obtained for HSU 031-295.2 also show that functionalisation can also lead to a slowdown in adsorption, or at least not to further acceleration. Compared to the adsorbent HSU 031-295.1, the adsorption rate is lowered by 0.11 µg m^{-2} s^{-1} for HSU 031-295.2 in both time periods investigated. However, HSU 031-295.1 has an increased adsorption rate compared to its base material HSU 031-295. Considering that the ligand for HSU 031-295.1 and HSU 031-295.2 is the same but bound in different concentrations on the surface, it is likely that an increased ligand concentration will slow down adsorption. Since this effect occurs with larger particles combined with smaller pore diameters, it must be assumed that pore diffusive effects due to smaller diffusion channels within the pores favour lower kinetics.

Both functionalisations offer benefits for the adsorption behaviour of the adsorbents. With a view to industrial application, the amount of a special ligand necessary to achieve a certain effect is of utmost interest. It could be shown that the increase in efficiency is comparable for both standard materials, HSU 001-075 and HSU 031-295, applying these functionalisations. Furthermore, it is important to quantify the additional loading success that a certain amount of the ligand on the surface of the silica gel allows in contrast to the base material. This success can be computed by employing the following formula, where the relative load additionally achieved by a functionalisation q_{r+} is calculated and divided by the allocation with the ligand on the surface of the corresponding base adsorbent q_l.

$$f_{le} = q_{r+}\, {q_l}^{-1} \qquad (37)$$

The result of such a calculation is the mass of the adsorptive, which was adsorbed per substance amount of the bound ligand in addition to the adsorption success of the unfunctionalised silica gel.

Table 12: Relative loads and additional effect by functionalisations of different silica supports at a concentration of 10,000 ppm_V

	30 minutes		180 minutes	
Adsorbent	Rel. load q_r / µg m^{-2}	Add. load f_{le} / µg mol^{-1}	Rel. load q_r / µg m^{-2}	Add. load f_{le} / µg mol^{-1}
HSU 001-075.1	10.4 ± 0.4	0.18	15.7 ± 1.9	0.72
HSU 001-075.2	12.1 ± 0.1	0.11	16.4 ± 0.3	0.18
HSU 031-295.1	5.5 ± 0.3	0.48	10.3 ± 1.3	0.57
HSU 031-295.2	3.4 ± 0.2	0	14.5 ± 0.8	0.55

When using this calculation method for the maximum load of HSU 031-295.1 and HSU 031-295.2, it is found that 0.57 g mol^{-1} and 0.55 g mol^{-1} adsorptive which corresponds to 20.3 mmol mol^{-1} (adsorbent per ligand bound onto the surface) and 19.6 mmol mol^{-1}, respectively are additionally adsorbed per ligand. It can therefore be assumed that there is a linear relationship between the amount of ligand bound and the additional adsorption success in comparison to the base material HSU 031-295. When looking at the same materials after 30 minutes, the results differ. With HSU 031-295.1, an improvement value of 0.48 µg mol^{-1} is achieved by functionalisation. HSU 031-295.2, by contrast, does not produce an improvement. Instead, the value, including the measurement deviations, approaches 0. For HSU 001-075.1 and HSU 001-075.2, the measurement results after 30 minutes with 0.18 µg mol^{-1} and 0.11 µg mol^{-1} are considerably closer to each other. This confirms the above-mentioned assumption that a stronger loading of the adsorbent surface with the used ligand can lead to a slowing down of the adsorption rate, which is probably due to a worse accessibility of the pores. The ligand appears to increase the access barrier for the adsorptive, which affects HSU 031-295 and its variants with larger particle but smaller pore diameters more than the smaller but relatively large-pored HSU 001-075.

Derivations can be derived from the measurements considered, which show which savings in adsorbents are possible by specific functionalisations. The demand for an adsorbent quantity depends in particular on the loadability, i.e. the predominant kinetics. As already mentioned, a physically hard-working person has a time-related air requirement of 95 L min^{-1}. This corresponds simultaneously to the air requirement

of three resting persons. The example of a concentration of 10,000 ppm_v, which is lethal very quickly, and a comparison of the adsorbents HSU 001-075 and the silanised variant HSU 001-075.2 show that there is a considerable improvement in the absorption capacity. It must be assumed that a concentration above 8000 ppm_v is deadly for humans after only 10 minutes. A concentration of 10,000 ppm_v used here is therefore very suitable for an exemplary consideration. For the model calculation, this threatening concentration must be reduced to harmless 30 ppm_v, which corresponds to the maximum permissible workplace load (34).

Assuming that a physically hard-working person is exposed to the aforesaid carbon monoxide load for 10 minutes, the adsorption rate drops within these first 10 minutes to a value of 0.54 µg m^{-2} s^{-1} or 1.09 µg m^{-2} s^{-1} for HSU 001-075 and HSU 001-075.2, respectively. At the named concentration, 1184 mg min^{-1} CO must be separated from the breathing air. In the case of the unsilanised material HSU 001-075, this means a calculated material requirement of 7973 g. HSU 001-075.2 is required here in much smaller quantities, namely only 4893 g, and thus only 61.4 % of the necessary base material mass. This clearly shows which improvements in adsorption capacity can be achieved by a favourable functionalisation.

5.1.4 Hydrogen Sulphide

Compared to carbon monoxide or the investigated hydrocarbons, hydrogen sulphide is highly corrosive. This complicates the circumstances not only for the measurement set-up but also for the adsorbents themselves. For comparison, the equilibrium measurements of three different but unfunctionalised adsorption materials, HSU 031-279, HSU 031-295 and HSU 001-075, at four different concentrations, namely 10 ppm_v, 70 ppm_v, 140 ppm_v and 5000 ppm_v are presented in Figure 27.

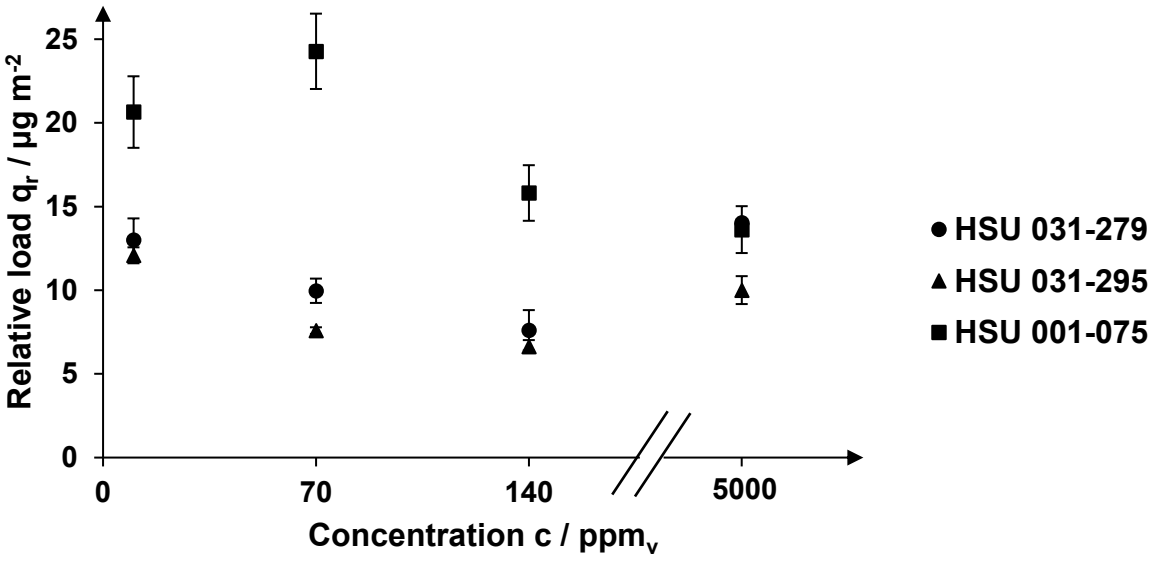

Figure 27: Comparison of load caused by H_2S on various unfunctionalised silica gels with different physical characteristics over three hours

The measurement results obtained do not show the expected course of a continuous and finally stagnating increase in loading as a function of increasing adsorptive concentrations. In fact, HSU 031-295 reaches the highest measured relative loading already at a concentration of 10 ppm_v with 12.1 µg m^{-2} adsorptive bound on its surface. With a relative load of 14.0 µg m^{-2}, the mean value of the maximum loading for HSU 031-279 is highest at 5,000 ppm_v but lies within the standard deviation of the relative loading at a concentration of 10 ppm_v. Thus, the gravimetrically determined loads achieved for both adsorbents at the next higher concentrations of 70 ppm_v and 140 ppm_v are lower for both adsorbents, also taking the standard deviations into account. HSU 001-075 behaves differently; for this adsorbent, the highest loading is achieved with 24.3 µg m^{-2} adsorpt at a concentration of 70 ppm_v, whereby the standard deviations for the concentration of 10 ppm_v overlap with those at 70 ppm_v. HSU 001-075 achieves relative loads of 15.8 µg m^{-2} and 13.6 µg m^{-2} for concentrations of 140 ppm_v and 5000 ppm_v, which are considerably smaller than those achieved for the lower concentrations. Thus, for all three materials, a peak is already reached at low adsorptive concentrations, and higher concentrations lead to a lower loading. In particular, the increase in load at higher concentrations indicates a reaction at the surface. It is reported in the literature that moisture is irreversibly adsorbed by silica gels in a single layer at room temperature. Desorption of this layer is therefore not possible (95 pp. 38-39). This humidity could be available for a reaction with H_2S. It is

likely that it will be removed by a sufficiently high hydrogen sulphide concentration which leads to a loss of weight. The adsorbent then could adsorb the following hydrogen sulphide in the next step, which could explain why higher concentrations lead to an increase in weight, again.

HSU 001-075 was considered best suitable for the separation of hydrogen sulphide in comparison to the other materials, at least when the base and not functionalised adsorbents are employed. Compared to the reference adsorbents HSU 031-295 and HSU 031-279, it is always superior in its relative adsorption capacity per surface regarding hydrogen sulphide. In relation to HSU 031-279, whose performance is second best, the adsorption of H_2S is 58 % higher at a concentration of 10 ppm_v and 150 % higher at 70 ppm_v, whereas for the next higher concentrations measured, this superiority is significantly reduced again. At 140 ppm_v the relative load for HSU 031-279 is on average 7.6 µg m^{-2}, while for HSU 001-275, the load is with 15.9 µg m^{-2} still 109 % higher than for the previous mentioned. For concentrations above 5,000 ppm_v, a superiority can no longer be recognised. Both values lie with a relative load of 14.0 µg m^{-2} for HSU 031-279 and 13.6 µg m^{-2} for HSU 001-075 within the standard deviation of the other. Consequently, it was decided to use HSU 001-075 in further investigations, especially with functionalised versions. A comparison of the measured results between the unfunctionalised HSU 001-075 and its specially functionalised version HSU 101-075-10 is depicted in Figure 28.

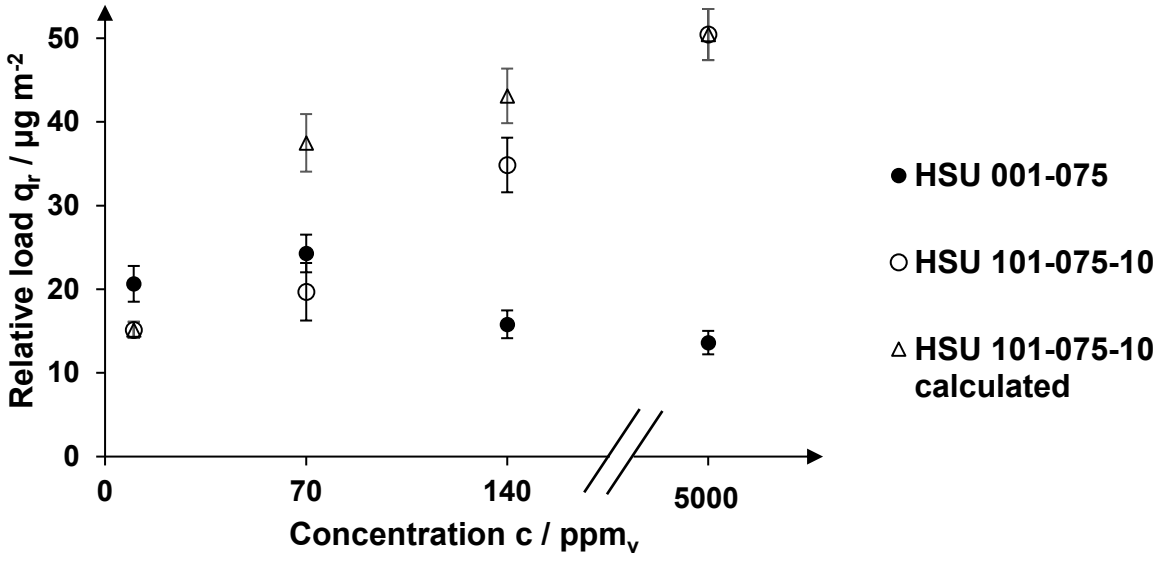

Figure 28: Comparison of relative load of hydrogen sulphide on the surface of HSU 001-075 and the functionalised version HSU 101-075-10 over three hours

At lower concentrations, the functionalised version is even less effective in the separation of hydrogen sulphide, as obvious from Figure 28. In contrast, for higher concentrations of 140 and 5,000 ppm, the efficiency of HSU 101-075-10 clearly exceeds the performance of HSU 001-075. Apparently, the base material HSU 001-075 is increasingly attacked at higher hydrogen sulphide concentrations and loses mass. HSU 101-075-10 on the contrary is stable to hydrogen sulphide, and the load increases steadily between the concentrations of 10 ppm_v to 10,000 ppm_v. The load of the unfunctionalised variant drops in the same range of concentrations. At a concentration of 140 ppm_v, HSU 001-075 achieves a relative loading on its surface of 15.8 µg m^{-2}, but the functionalised variant already achieves a loading of 34.8 µg m^{-2}. This difference becomes even clearer at the concentration of 5,000 ppm_v hydrogen sulphide in synthetic air, where the values of the relative loads achieve 13.6 µg m^{-2} for HSU 001-075 and 50.4 µg m^{-2} for HSU 101-075-10. The adsorption of adsorptive per area can therefore be increased to 371 % of the base material at this highest measured concentration. In difference to the base material, the load of HSU 101-075-10 is increasing over all measured concentrations. Thus, it can be concluded that the functionalised material is barely destroyed by the corrosive atmosphere.

Ideally, the adsorption isotherm should describe the Langmuir form. For the verification of this assumption, the Markham and Benton method was employed again. It can be concluded from Figure 29 that the graph resulting from the inverted relative loading over the inverted adsorptive concentration does not result in a straight line.

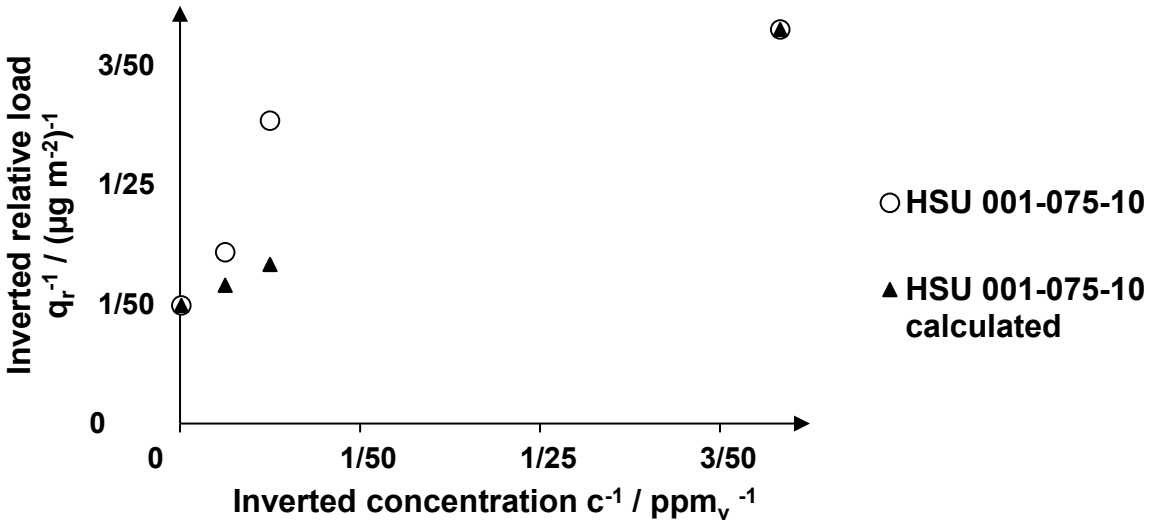

Figure 29: Markham and Benton function for HSU 001-075-10 resulting from H_2S containing atmospheres

Like for carbon monoxide, an inversion of the measured values according to Markham and Benton can be utilised very well to determine whether an Freundlich isotherm is given. The white circles, which represent the measured and then inverted values, show very clearly that HSU 001-075-10 does not describe a straight line after the Markham-Benton inversion. In particular, the point caused by the value pair at 70 ppm_v (the third pair of points from the left side) is clearly too high in the inversion. For 140 ppm_v (the second pair of points from the left side), the two points approach each other again clearly. With the black triangles, a straight line is constructed, which represents the ideal form of an inverted Freundlich isotherm. All points which are inverted following Markham and Benton and describe values above this, indicate too small initial values for an optimal Freundlich isotherm. This applies to the measured values of HSU 101-075-10 in two out of four measured cases. The inverted values, which are shown as black triangles in Figure 29, lead to the optimal calculated Freundlich isotherm in Figure 28, which is also shown as black triangles there.

For concentrations of 70 ppm_v and 140 ppm_v, the experimentally determined load is too small compared to the calculated loading to represent a Langmuir isotherm. In this section, the isotherm is more like the form described by Henry. A corresponding straight line can be described briefly taking the standard deviations into account. The most important insight from the aforementioned results is that commercially available silica gels are not necessarily appropriate for the separation of H_2S from the air but can

be improved by specific functionalisations to stabilise them against hydrogen sulphide and thus, to improve the adsorption's effectivity.

HSU 101-075-10 was the most effective adsorbent investigated out of a group of different functionalisations. For this reason, the kinetics were also compared with this material. In the following Figure 30, the corresponding loads of HSU 031-279, HSU 031-295 and HSU 101-075-10 after 10, 30, 60 and 180 minutes with H_2S are presented.

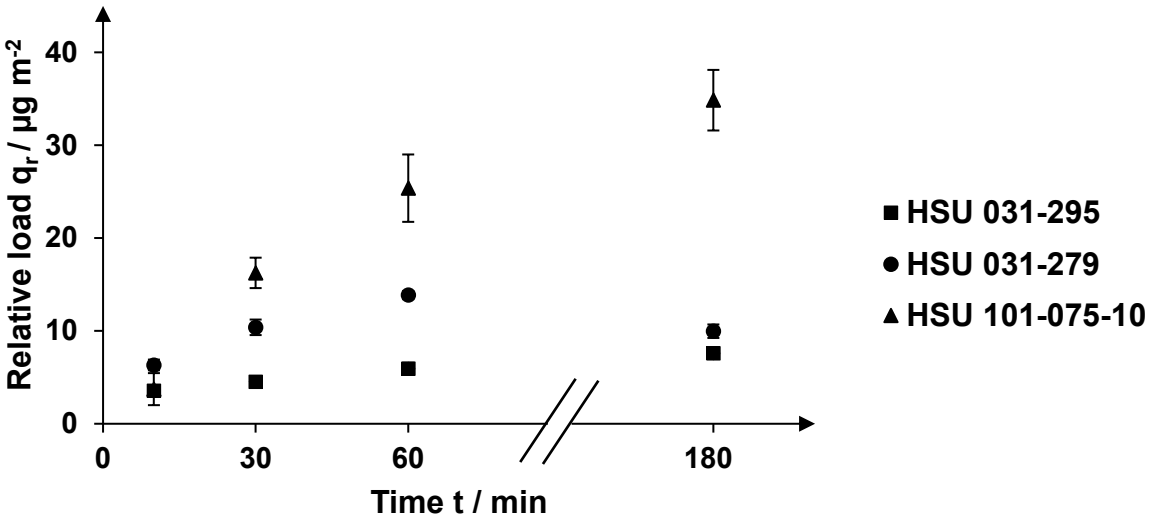

Figure 30: Comparison of kinetics caused by 70 ppm_v H_2S in synthetic air on different silica gels

As expected, HSU 101-075-10 is superior in comparison to the other adsorbents over all executed measurements, except after 10 minutes, where HSU 031-279 with a relative load of 6.3 µg m^{-2} is very efficient as well. However, all resulting curves provide a form as one might expect. It is remarkable that HSU 031-279 loses weight after 180 minutes compared to the measurement after 60 minutes and reaches 1.9 µg m^{-2} less loading. This symbols a valid trend for the material and is due to starting corrosive effects caused by H_2S on the unfunctionalised base material, employed as adsorbent. Furthermore, several measurements were conducted to prove the results. Generally, as can be seen by Figure 30, there is a very small standard deviation, especially for the unfunctionalised adsorbents, of maximal 10 %, which is a sign for precise sampling and measurements. The standard deviations for the silanised supports are expected to be higher due to the functionalisation in the prototype stage and amount to 14.5 % in the maximum case. Obviously, it needs some time, before the unfunctionalised silica

gel is erased by the aggressive atmosphere. In principle, the shown functionalisation has succeeded in improving the stability against an atmosphere containing hydrogen sulphide and at the same time in increasing the connection rate and the maximum load capacity. Compared to other experimental series in which adsorption was controlled by pure hydrogen sulphide atmospheres at different pressures, similar results are obtained. HSU 101-075-10 adsorbs up to 0.4 wt.-% of the initial mass of hydrogen sulphide in the studies presented. The investigated silica gels in the comparative measurement from the literature with a magnetic suspension balance achieve up to 0.35 wt.-%, whereby one stands out with a weight increase of 1.0 wt.-% (70 p. 76). It is likely that a pure hydrogen sulphide atmosphere, despite lower prevailing pressures due to the lack of competition with oxygen and nitrogen, has a positive effect on adsorption. This in turn underlines the performance of the newly developed silanisation HSU 101-075-10.

A model calculation for an application case shows the considerable added value that silanisation provides in combination with the most favourable starting material. This becomes clear at an initial concentration of 70 ppm_v, which is almost unbearable for a human being and which can already lead to severe disorders of the central nervous and the cardiovascular system. Corresponding input concentrations would have to be lowered to 5 ppmv in order to comply with the applicable occupational health and safety regulations (34). A physically hard-working person generates a mass flow of 9.51 mg min^{-1} hydrogen sulphide by breathing. After 30 minutes, the relative absorption capacity per time unit for the adsorbent HSU 031-295 is 0.151 µg m^{-2} min^{-1}. For the silanised HSU 101-075-10, this value is considerably better at 0.541 µg m^{-2} min^{-1}, and thus 3.6 times as high. This does not have such a significant effect on the weight of the required amount of adsorbent due to the relatively small area per weight of the basic material HSU 001-075. However, for the described application of the material HSU 101-075-10, only 68.9 g are required, whereas under the same conditions, almost 110 g of the material HSU 031-295 would be necessary. This clearly shows the potential that lies in the directed selection and functionalisation of the corresponding adsorbents.

5.1.5 Ammonia

For the adsorption of ammonia, especially activated carbon in industrial applications as well as clinoptilolite tuffs in scientific research are utilised (39 p. 220 ff.; 40 p. 151 ff.). In this research, another method based on selected variants of the synthetic support HSU 9000 was chosen. These variants were compared to HSU 001-075 utilised for the other investigated target compounds.

For the measurements, three different concentrations of dry ammonia in synthetic air were applied; these were 137 ppm_v, 274 ppm_v and 10,000 ppm_v. The concentrations delivered by Linde as test gases offered a high storage stability and thus were perfectly suitable for the conducted experiments.

Surprisingly, HSU 9000-2 does not behave similar to HSU 001-075. It was expected that the new material would bind more of the targeted ammonia onto the surface compared to HSU 001-075 at every concentration. But this is not the case. HSU 9000-2 is obviously superior to HSU 001-075 at very high concentrations but less effective at lower concentrations. Respective results can be seen in Figure 31.

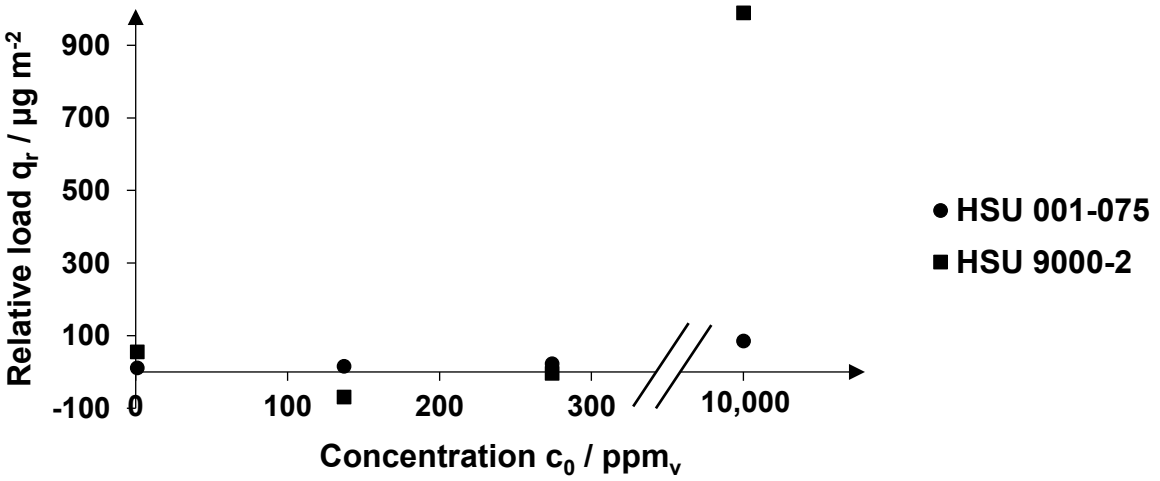

Figure 31: Relative load of dry ammonia on different separation materials at different concentrations over 180 minutes

In this case, the affinity for ammonia is obviously stimulated by higher concentrations. A similar effect, although with significantly lower loads, can be seen for the material HSU 9000-5, which was investigated as well. Due to the particle size of 5 to 10 mm and the impossibility to crush HSU 9000-5 into a smaller size, it was not possible to investigate its pore size and surface area. It is therefore compared by weight with HSU 9000-2, as depicted in Figure 32.

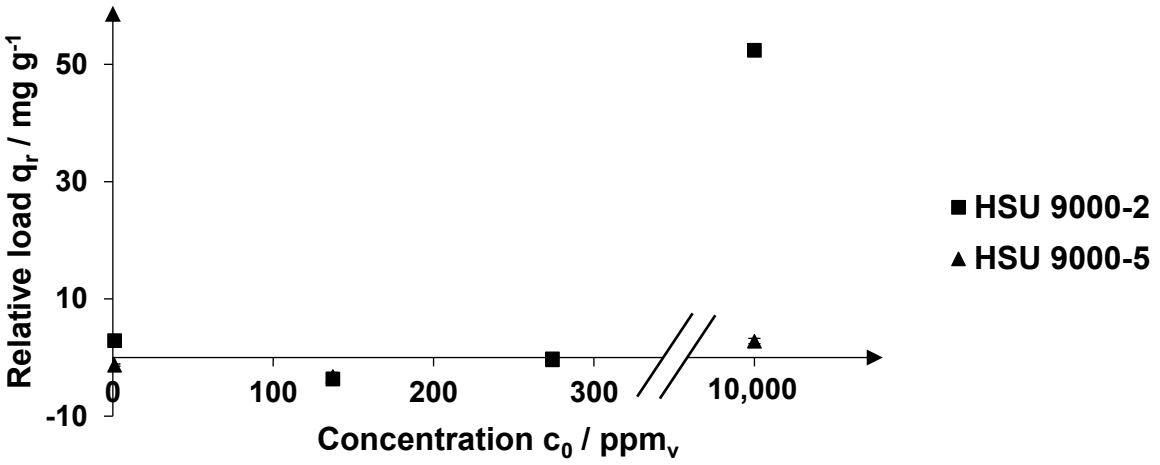

Figure 32: Comparison of HSU 9000-2 and HSU 9000-5 in their efficiency in the separation of ammonia from synthetic air at different concentrations over 180 minutes

Due to their special nature, the adsorbents of the 9000 series must not be dried completely, as they then lose their ability to separate substances. Therefore, there is at least some residual moisture on their surface. For measurements with low concentrations, it can be assumed that the effect of a possible further drying of the corresponding adsorbents superimposes the effect of loading by a low concentration of ammonia, giving the impression that the target substance is not separated. This effect then vanishes at higher concentrations when there are surplus amounts of NH_3 in the air and the drying effects lose their impact. As a result of the measurements carried out, especially with regard to the higher and therefore more interesting concentrations, HSU 9000-2 has proven to be the material of choice for the separation of NH_3.

In a next step, the kinetics were investigated. A concentration of 1 vol.-% gaseous ammonia in synthetic air was used with otherwise unchanged parameters. The loading, caused by the charging of the separation material with ammonia, were investigated after 10, 30, 60 and 180 minutes. For HSU 001-075 and HSU 9000-2, the results are depicted in Figure 33.

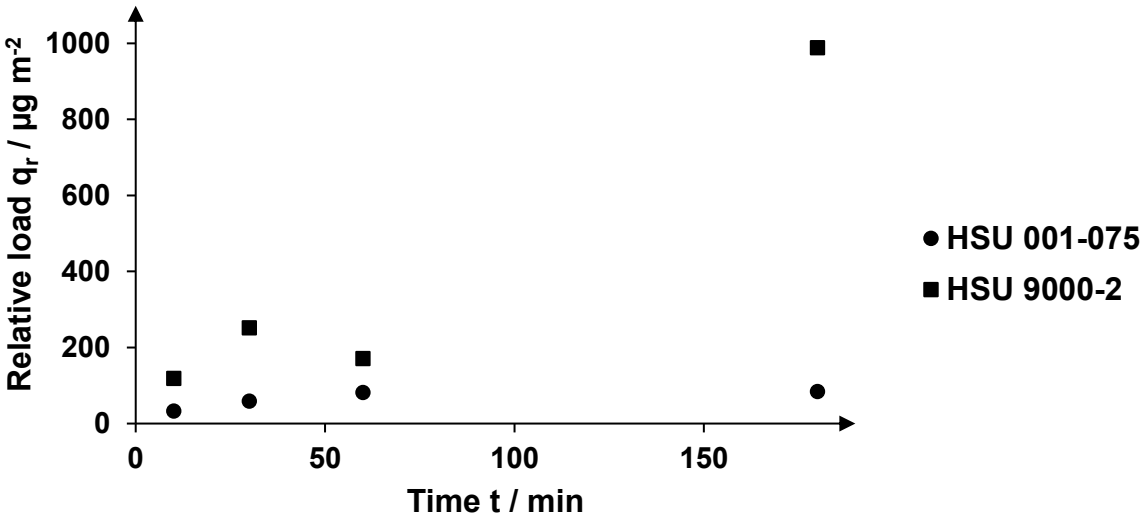

Figure 33: Adsorption kinetics of 1 vol.-% ammonia in synthetic air on different adsorption materials

In case of HSU 001-075, kinetics describes a very plausible curve. The deviations over all measurements were very small, and the gradient decreases over time. For HSU 9000-2, the results are not as clear. Although there is an obvious tendency in the first 30 minutes, which is comparable to HSU 001-075, for 60 minutes, the weight is actually decreasing, which was not expected. After 180 minutes, however, HSU 9000-2 is far superior to HSU 001-075. Consequently, for a final understanding of the potential efficiencies of these materials, the results from the breakthrough measurements must also be considered. Chapter 5.3.4. presents further findings that are of crucial importance for understanding the adsorption behaviour of HSU 9000-2.

An input concentration of 1,000 ppm_v ammonia is no longer bearable for a human being, the tolerability threshold is exceeded at 300 ppm_v at the latest. The concentration considered here can therefore be regarded as harmful to health. From 1,700 ppmv on, the ammonia concentration is lethal (34). The concentration value shown is therefore very suitable for a model-like consideration of a successful separation by a specifically applied adsorbent, since the initial value of the concentration in a real scenario would represent a considerable danger to potential workers. For example, the limit values for jobs are set to 20 ppm_v in Europe. In order to reduce an initial concentration of 1,000 ppm_v for a physically hard-working person with an air consumption of 95 L min^{-1} to a safe level even after half an hour of use, HSU 001-075 theoretically requires 36,456 m^2 of adsorbent surface. In contrast, the improved material HSU 9000-2 only requires an active surface area of 8.539 m^2.

Consequently, the more suitable material HSU 9000-2 requires less than a fourth of the area required by silica gel HSU 001-075. Thus, for the assumptions made here, a fundamental improvement could be achieved by an appropriate choice of adsorbent. This is also confirmed by the breakthrough experiments described in Chapter 5.3.4.

5.2 Multi Component Measurements

In the previous chapters, the focus was essentially on single-substance adsorption. In the remaining chapters, multi-component adsorption will also be dealt with. A highly probable multi-component adsorption always results from the separation of the target substance and humidity from the ambient air. Experiments with undried silica-based adsorbents have shown that slightly less adsorption was achieved for cyclohexane than for dried silica gels.

In case of carbon monoxide and hydrogen sulphide, it is decisive that the humidity of the atmosphere is known, as the weight increase caused by these compounds is small compared to organic compounds and could be superposed by adsorbed humidity from the air.

Two different set-ups were used for the multi-component experiments. Ammonia was employed in the form of ammonia water in different concentrations as adsorptive. Accordingly, the arrangement described in Chapter 4.1.1 was used for the associated measurements. For carbon monoxide, hydrogen sulphide and cyclohexane, the experimental set-up described in Chapter 4.1.4 was used. In principle, moist air was always fed into the measuring room with the adsorbents for more than 24 hours. It was then mixed with a certain concentration of the target substance for 5 hours at a constant total humidity content. The adsorbents were weighed after loading with moist air and after loading with the added adsorptive. The weight difference is then a measure of the separation success from a multi-component gas mixture.

5.2.1 Cyclohexane with Humidity

According to Chapter 5.1.4, the best results, both in terms of maximum loading and kinetics under dry conditions, were obtained for HSU 101-075-07. For this reason, this material is compared to an activated carbon already used in the industry.

In the experiments carried out, the activated carbon used for the research always proved to be superior to the silica gels investigated in the separation of cyclohexane at lower concentrations. This is illustrated in Figure 34, where the relative loads of

HSU 001-075-07 and activated carbon are compared. At higher partial pressures starting from 0.53 p_0 and the onset of pore condensation, the adsorption behaviour of the silica gels is clearly superior. However, this also shows that a mixed bed of both adsorbents can make sense. In the context of an appropriate air purification, at low concentrations of the air pollutant cyclohexane, the activated carbon can thus ensure the main part of the separation of the target substance. If the concentration continues to rise, the newly developed silanisation of the silica gel HSU 101-075-07 can remove cyclohexane from the ambient air with considerably greater efficiency. This results in a considerably increased range of applications.

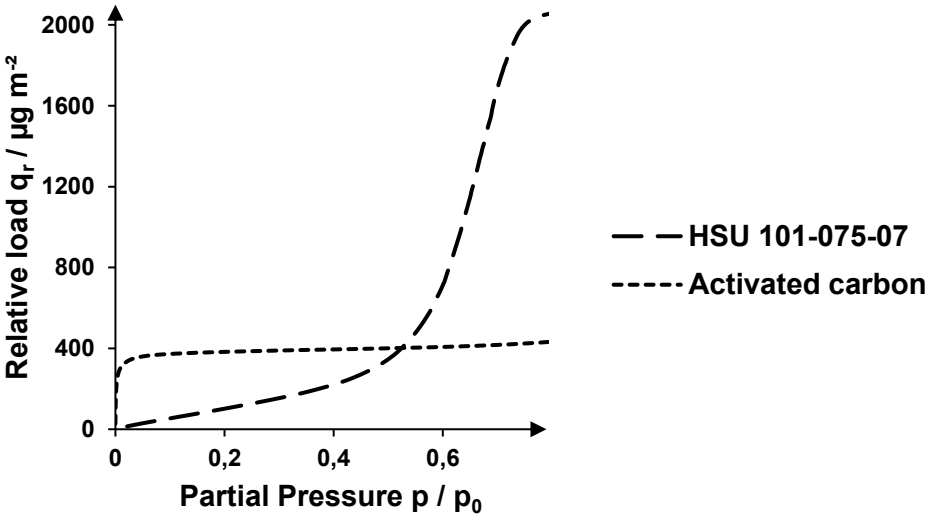

Figure 34: Comparison of relative loads in dry atmosphere caused by cyclohexane on HSU 101-075-07 and activated carbon

Activated carbon is commonly known for its hydrophobic character (96 p. 329). For this reason, it is used e.g. in waste water for the elimination of organic trace substances (97 p. 6 ff.). The results of the measurements in humid air can be found in Figure 35.

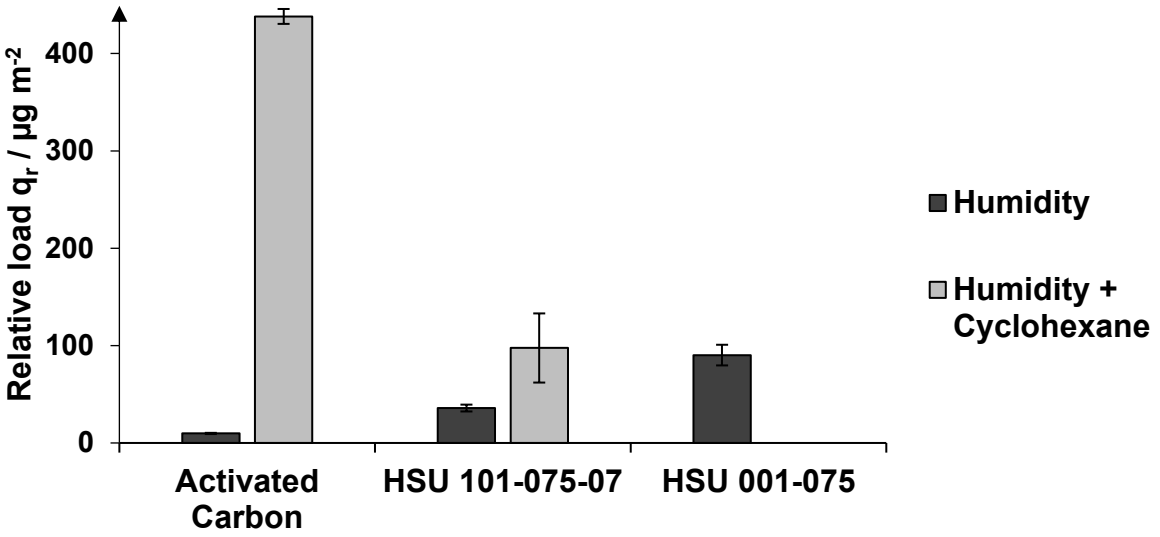

Figure 35: Comparison of relative load on HSU 101-075-07 and an industrial used activated carbon caused by humidity and cyclohexane

With reference to the surface of the materials, the affinity of water to bind on the surface of the silica is much higher than for the activated carbon, which was expected. Within the first 24 hours, when the adsorbents are only exposed to humid air, HSU 101-075-07 binds moisture on its surface in an amount of 35.9 µg m^{-2}. The relative loading of the activated carbon is 9.8 µg m^{-2} at the end of the same period. Therefore, the loading of the activated carbon by air humidity is only 27 % of the comparative value for the functionalised silica gel HSU 101-075-07. Compared to the unfunctionalised variant HSU 001-075, HSU 101-075-07 is significantly lower in its capacity to adsorb water, which is proven when the relative loading of HSU 001-075 after 24 hours in defined humid air is 90.2 µg m^{-2}. HSU 101-075-10 thus adsorbs 60 % less moisture than the base material, which emphasises the selectivity of the functionalised adsorbent. Compared to the adsorbent HSU 101-075-10 for example, there is no significant difference, since the standard deviations for HSU 101-075-10 overlap the measured values for HSU 101-075-07.

After another 5 hours, in which the adsorbents are loaded with cyclohexane in addition to humidity, the superiority of activated carbon is once again evident. It achieves a total loading of 438.0 µg m^{-2} in the produced atmosphere, while HSU 001-075-07 only reaches a total loading of 97.5 µg m^{-2}. On the other hand, the functionalised silica gel also has a comparatively large standard deviation. For both materials, it is shown that in addition to the previously adsorbed humidity, cyclohexane was also adsorbed significantly. The difference and thus guaranteed amount of adsorbed cyclohexane is

for HSU 101-075-07 61.6 µg m^{-2}, and for the activated carbon used even 428.2 µg m^{-2}. Compared to the isotherms in Figure 34, the adsorption capacity of the activated carbon is practically not restricted by humidity. The amount of adsorbed cyclohexane on the surface corresponds to the values achieved by dry activated carbon in a dry atmosphere, considering the standard deviation. HSU 101-075-07 also achieves values that are at least close to adsorption processes from the dry gas phase. Chapter 5.3.1 shows that moisture nevertheless has an influence on the load.

5.2.2 Carbon Monoxide and Humidity

Figure 36 shows the relative loads of HSU 001-075, HSU 001-075.1 and HSU 001-075.2 caused by the summation of a humid atmosphere and the same humid atmosphere supplemented with CO. The measurement results for each of the three adsorbents are displayed as stacked columns. Therefore, the columns below represent the loading of the adsorbents with moisture from the air. A complete equilibrium loading can be assumed after 24 hours in a constantly humid atmosphere. The additional loading with CO is represented by the column above. Since the adsorbent is already completely loaded with humidity, the additional loading must be caused by the CO added. Therefore, a resulting total column is the sum of the mean values of two discrete measurement series for each adsorbent under consideration.

HSU 001-075 as base silica support adsorbs on average 129 µg m^{-2} moisture from the incoming gas mixture. HSU 001-075.1 in difference already achieves an average relative load of 203 µg m^{-2}. Thus, the load of HSU 001-075.1 with air humidity is 58 % higher than with the base material. HSU 001-075.2 even reaches a relative load of 390 µg m^{-2} in the same 24-hour period. This corresponds to an increase of 203 % in the ability to adsorb humidity. It can therefore be seen that the ability to adsorb moisture is considerably increased by the selected functionalisations. However, the resulting expectation that free adsorption sites for the target substance CO are blocked by humidity already adsorbed has not been confirmed. The results in Figure 36 clearly show that CO from humid air can also be separated by adsorbents already loaded with moisture.

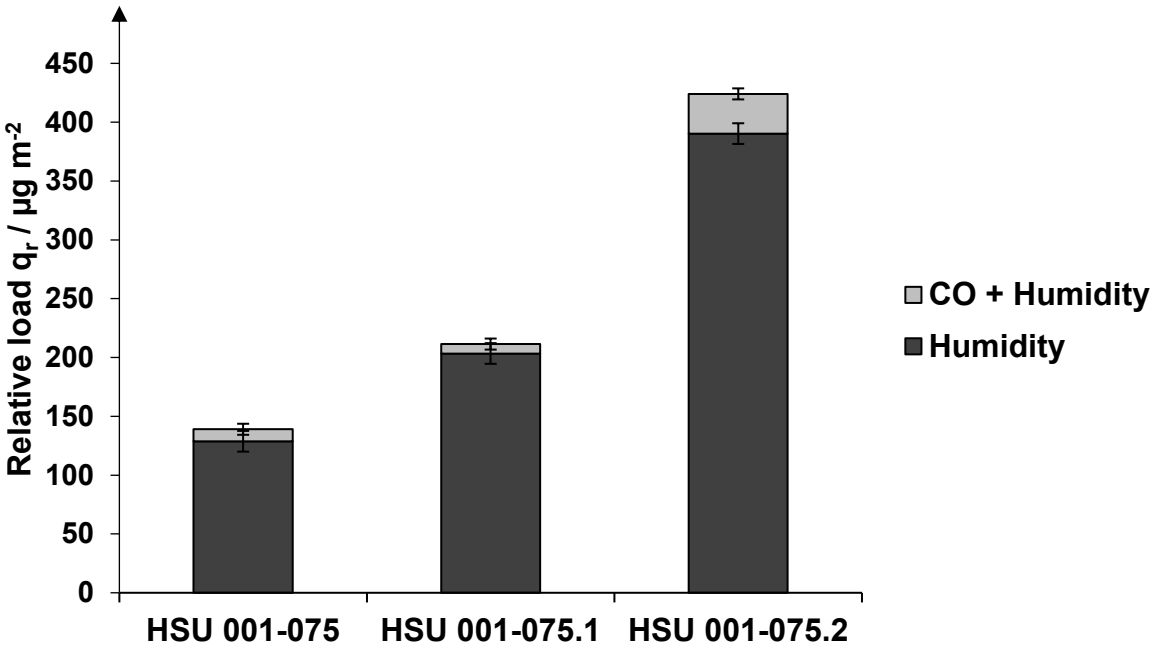

Figure 36: Load by multi component adsorption of humidity and CO in a concentration of 10 vol.-% in synthetic air

A superior load with CO, after loading with humidity, cannot be detected for HSU 001-075.1 with a relative extra load of 8.0 µg m^{-2} CO in comparison to the base material HSU 001-075 with a load of 10.2 µg m^{-2} CO. In this case, the standard deviations of the associated measurement series overlap over a sufficiently large range, such that on average, the observed values of both adsorbents can be regarded as equal. HSU 001-075.2, on the other hand, reaches a relative load of 33.8 µg m^{-2} CO, which is significantly higher than the comparative values of the base support and exceeds them by 231 %. It is proven that the .2 functionalisation has a positive impact on the capacity for carbon monoxide as a compound to be separated, although the adsorbent was already affected by humid air. For HSU 001-075.1, it is at least shown that the cumulated relative load of all adsorbed compounds is higher compared to the unfunctionalised material. Major benefits can only be expected using HSU 001-075.2. This can also be determined in comparison to dry loading with CO as adsorptive. Both, HSU 001-075 and HSU 001-075.1 are considerably restricted in their capacity to adsorb CO by moisture in the air. In a dry atmosphere and a concentration of the target substance of 1 vol.-%, relative loads of 11.5 µg m^{-2} for HSU 001-075 and 15.7 µg m^{-2} for HSU 001-075.1 are achieved. In humid air and with the significantly higher concentration of 10 vol.-% CO, the values decrease to 10.2 µg m^{-2} and 8.0 µg m^{-2}, respectively. For HSU 001-075.2, the values even double from 16.4 µg m^{-2} to

33.8 µg m^{-2}. Obviously, the elevated air humidity is the trigger for an intensified interaction of the adsorbent with the target substance, which further increases the adsorbent's absorption capacity for carbon monoxide. However, this effect does not seem to be effective with lower densities of the bound ligand on the surface of the adsorbent HSU 001-075.1. The measurement data even indicates that a reduction of the adsorption capacity could occur, although it must be noted that the standard deviations clearly overlap each other.

For multi-component adsorption, especially related to humidity, decisive insights were discovered and published (98) during the measurements. Further results are presented in the following for the first time. In order to gain insights into the adsorption kinetics of carbon monoxide in combination with humid air, another experiment was established. The experimental set-up corresponds to that described in Chapter 4.1.2 for single-component adsorption. At the beginning of the experiment, a relative humidity of 40 % was set in the interior. This inner atmosphere was then exposed to carbon monoxide. After 10, 30 and 60 minutes, the load on the adsorbent was determined. The corresponding measured values were then compared with the values obtained in a dry CO-containing atmosphere as shown in Figure 37. Thereby, the squares represent the loading of the adsorbent over time in a dry atmosphere, and the triangles indicate the loading over time in the corresponding humidified atmosphere.

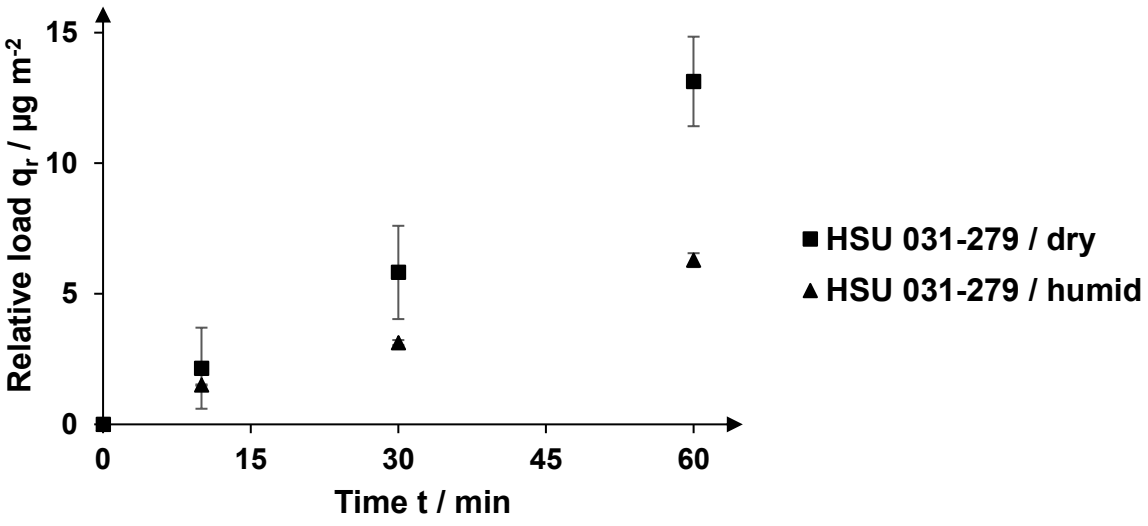

Figure 37: CO loads by a concentration of 1 vol-% at certain times for HSU 031-279 influenced by a humidity containing atmosphere of φ_{rh} = 40 % and without influence of humidity

It turns out that after 10 minutes, there is almost no difference between the measurements in humid and dry air. The results obtained for dry air with 2.1 µg m^{-2} do not differ from those for humid air with 1.5 µg m^{-2} if the associated standard deviations are considered. However, after 30 minutes, there is a clear difference. Although the standard deviations, especially of the measurement series with dry gas mixture, are very pronounced, they do not overlap. The mean relative load in dry air is now 5.8 µg m^{-2}. Therefore, the load in dry CO-containing air after 30 minutes is on average 87 % higher than in humid air with 3.1 µg m^{-2}. After one hour, this relative distance increases further to 108 %. The corresponding values here are 6.3 µg m^{-2} in humid air and 13.1 µg m^{-2} in dry air. After a sufficiently long adsorption time, both values approach each other again. In a comparison of the two measuring methods used, the measured values for the relative loading per area within the standard deviation are the same after 24 hours.

Due to the oversupply of air humidity with moist air, a faster loading of the adsorbent would have been expected in this experiment. Instead, CO from dry air is obviously adsorbed more quickly. Apparently, a higher air humidity impedes the adsorption of CO. At the same time, this adsorption behaviour also shows that humidity cannot be adsorbed unhindered either. The competitive situation among the two adsorptives leads to an overall slowdown of the process.

For the understanding of the separation efficiency, it is also reasonable to calculate the corresponding kinetics. The relevant values for HSU 031-279 are noted in Table 13.

Table 13: Relative load of CO with a concentration of 1 vol.-% after certain times onto HSU 031-279 and relevant average values for r_a

	Completely dry air		Air with 40 % humidity	
t / min	$q_r(t)$ / µg m^{-2}	r_a / µg m^{-2} min^{-1}	$q_r(t)$ / µg m^{-2}	r_a / µg m^{-2} min^{-1}
10	2.2 ± 1.5	0.22	1.5 ± 0.2	0.15
30	5.8 ± 1.8	0.19	3.1 ± 0.3	0.10
60	13.1 ± 1.7	0.22	6.3 ± 0.4	0.10

Obviously, the values of the adsorption rate r_a hardly change over the first 60 minutes for HSU 031-279 in dry air. For all three measuring points, the kinetic comparison value remains in a range between 0.19 µg m^{-2} s^{-1} and 0.22 µg m^{-2} s^{-1}. Due to the standard

deviations of the relative load, which serves as the essential variable for calculation, it can therefore be assumed that the load does not change per time in the first 60 minutes. As a result, there is a linear load increase on the adsorbent, and consequently, a constant capacity for the removal of the incoming threatening substance. In humid atmosphere, the factor is smaller over all the time and even decreases with the measurement point at 30 minutes for the first time. In other words, the capacity per time decreases as well for the target substance. Therefore, a possible adsorber bed would have to be planned to be longer. This would then require significantly more adsorbent, Furthermore, the maximum load was nearly identical in both situations, as explained before. It was achieved after 120 minutes at the latest for a completely dry atmosphere. For the humid atmosphere, the maximum load was achieved within a period of 24 hours. It can therefore essentially be said that air humidity has less of a decisive influence on the maximum load but has a considerable effect on the adsorption rate.

5.2.3 Hydrogen Sulphide and Humidity

The experimental set-up described in Chapter 4.1.4 was also used for the experiments with hydrogen sulphide and humidity. To enrich the humid air with the target adsorptive, a pressurised gas cylinder with a concentration of 0.5 vol.-% was connected to the system. Chapter 5.1.4 already shows that higher concentrations do not necessarily mean higher relative loads on the surface of the adsorbents. For this reason, the results for hydrogen sulphide in a higher concentration combined with water are of utmost importance and measurements of those combinations delivered surprising results, as can be seen in Figure 38 (99 p. 63 ff.).

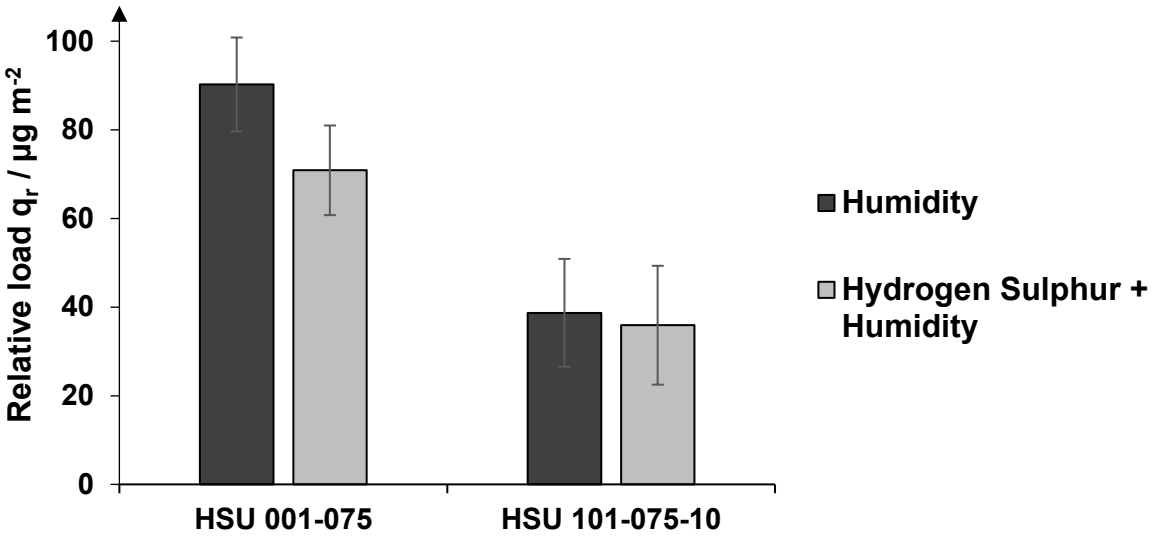

Figure 38: Relative load q_r on HSU 001-075 and HSU 101-075-10 caused by humidity and humidity combined with hydrogen sulphide in a concentration of 0.5 vol% in synthetic air

The relative loads of HSU 001-075 and the functionalised variant HSU 101-075-10 are shown, and the mass increase for both adsorbents after 24 hours of loading with humid air and the subsequent five-hour loading with air of the same humidity and additional hydrogen sulphide is depicted.

There is a clear trend which confirms the superiority of the functionalised silica gel. HSU 001-075 as base version is affected by humidity significantly more than the functionalised version. It is noticeable that the starting material HSU 001-075 with 90.2 µg m^{-2} achieves 2.3 times the surface loading with moisture of the functionalised variant HSU 101-075-10 with 38.7 µg m^{-2}. HSU 101-075-10 thus adsorbs considerably less moisture than the unfunctionalised HSU 001-075, which confirms its improved selectivity towards humidity, as it is the aim to adsorb as little moisture as possible.

Mainly, the ability to adsorb hydrogen sulphide in this defined humid atmosphere is of interest. Although the concentration of water is not lowered, additionally brought in hydrogen sulphide does not lead to a gravimetrically measurable increase of the load on the adsorbent's surface. For HSU 101-075-10 with 35.91 µg m^{-2} the load keeps nearly constant in comparison to the achieved load by an H_2S free atmosphere. Even the relevant standard deviations caused by the different atmospheres overlap for the most part in case of this adsorbent. Thus, both averages of the measurement results can be regarded as equal. It therefore appears that hydrogen sulphide in humid air has

no significant influence on HSU 101-075-10, if it is already loaded with defined moisture.

For the unfunctionalised version, the effect of weight loss is much more pronounced. Added hydrogen sulphide reduces the calculated average surface load from 90.3 µg m^{-2} to 70.9 µg m^{-2}. This corresponds to a reduction of 21.5 %, although even here, the boundaries of deviation of the measurements with only humidity and with humidity and hydrogen sulphide overlap each other. These results are a valid sign that HSU 101-075-10 is a better choice for the separation of H_2S. Other chapters in the book concerning H_2S also show a measurable positive effect of the functionalisation. Although the described experiments are not appropriate as singular evidence for the postulated theory, they fit into those other observations. Consequently, these experiments support the theory that the functionalised version is the better choice for the separation of hydrogen sulphide. Finally, this is proven with the breakthrough experiments of Chapter 5.3.3.

5.2.4 Ammonia in Water

The experiments for ammonia water were carried out with the set-up according to Chapter 4.1.1 as it must always be multi component adsorption. For the considerations, the adsorbents were exposed to an atmosphere saturated with a defined concentrated ammonia water in a range between 0 vol.-% and 25 vol.-% for 5 days or 120 hours. As could be seen in Chapter 5.1.5, higher concentrations of gaseous ammonia do not necessarily lead to higher loading. There seems to be a breakeven point, where the ammonia starts to destroy and thus erode the adsorbent. There is a similar effect for ammonia water.

In Figure 39, single points of two isotherms are depicted. HSU 001-075, produced by Silicycle (Québec, CA), and HSU 9000-2, which base is produced by Sigma-Aldrich (St. Louis, MO, USA) were compared concerning the separation of ammonia water. The graph shows the relative loading that the respective material is affected by, as a function of the concentration of the target substance.

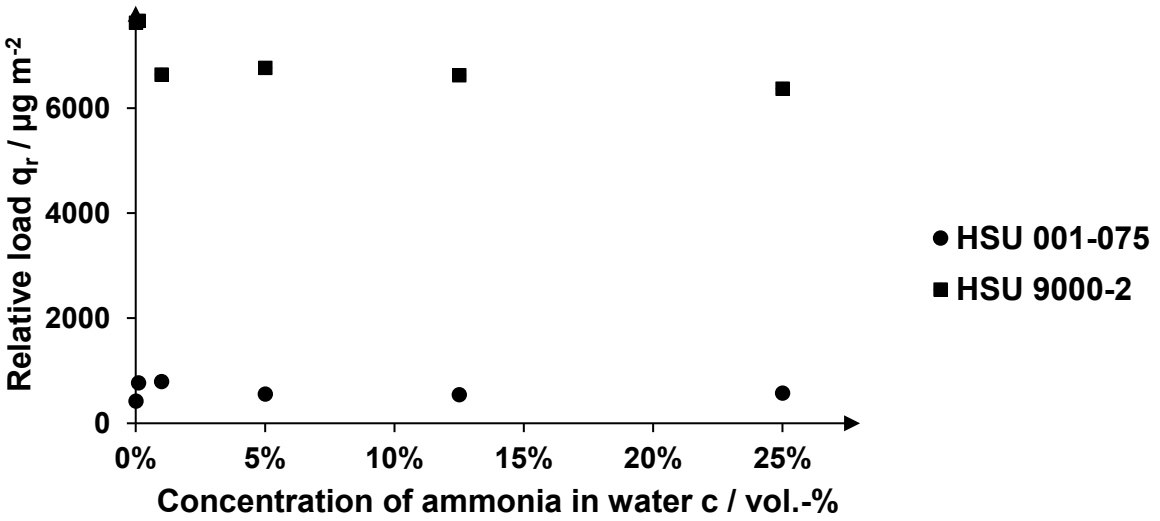

Figure 39: Measurement results for isotherms of ammonia water on different separation materials in the static set-up

Clearly, there is a significant difference regarding the amount of ammonia bound on the surface for both investigated adsorption materials. HSU 9000-2 is much more effective for all measured concentrations. The maximum relative load achieved for HSU 001-075 is 798 µg m^{-2} at a concentration of ammonia in water of 1 vol.-%. For HSU 9000-2, the maximum value is reached earlier, namely at 0.1 vol.-% with a relative load of 7.67 * 10^3 µg m^{-2} and thus 9.6 times the maximum value of HSU 001-075 relative to the surface. Differences in the relative loading at certain concentrations between the two materials can be quantified between 6.90 * 10^3 µg m^{-2} at a concentration of 0.1 vol.-% and 5.80 * 10^3 µg m^{-2} at a concentration of 25 vol.-%.

For both materials, HSU 001-075 and HSU 9000-2, the maximum load decreases at higher concentrations. At an adjusted ammonia concentration of 1 vol.-%, HSU 9000-2 receives a loading relative to the surface of 6.64 * 10^3 µg m^{-2}. This corresponds to a decrease of 13.4 % compared to the value reached at a concentration of 0.1 vol.-%. At the next higher concentrations of 5 vol.-% and 12.5 vol.-%, the relative loads reached do not deviate as much and are also within the error tolerance. For a concentration of 25 vol.-%, however, the value falls below the tolerance range and is averaged over all measured values at 6.37 * 10^3 µg m^{-2} and thus 4.1 % lower than at a concentration of 1 vol.-% and 16.9 % lower than the highest load achieved.

HSU 001-075 has increasing loads up to a concentration of 1 vol.-%, where the average load at a concentration of 0.1 vol.-% is 771 µg m^{-2}. At a concentration of

0 vol.-%, which represents pure moisture without ammonia, the relative load reaches 427 µg m^{-2}. For higher concentrations, the loads decrease again but stagnate at a constant level. The deviations in the load at concentrations of 12.5 vol.-% and 25 vol.-% lie within the standard deviations compared to the load of 5 vol.-% with a value of 560 µg m^{-2}.

The materials are clearly attacked by ammonia-containing air humidity and thus lose part of their mass. In contrast, the abrasive effect on the adsorbents does not seem to increase significantly with higher concentrations of ammonia in the water. In principle, however, it can also be concluded that air humidity containing ammonia is nevertheless adsorbed. The determined weight after adsorption is always higher than the initial weight of the prepared adsorbents before the experiment.

In this research, ammonia water cannot be divided into its two phases. Therefore, the measurements concerning the adsorption kinetics were carried out with the experimental set-up described in Chapter 4.1.2. An extended measurement set-up for multi-component adsorption, as described in Chapter 4.1.4, is not necessary. Measurements were taken at 10, 30, 60 and 120 minutes with an ammonia concentration in the water of 1 vol.-%. The results are shown graphically in Figure 40.

As suspected, based on the findings from the isothermal measurements, HSU 9000-2 is loaded significantly faster than HSU 001-075. After 120 hours, a total load of 6640 µg m^{-2} is obtained for HSU 9000-2 using ammonia water with a concentration of 1 vol.-%. This is 8.3 times as high as the loading of 799 µg m^{-2} for HSU 001-075. Looking at the average relative loads after 10, 30 and 120 minutes respectively, the distance between the material separation sequences is constantly increasing. After 10 minutes, HSU 9000-2 reaches a loading of 44 µg m^{-2}, which is 2.9 times the loading achieved by HSU 001-075 within the same time with 15 µg m^{-2}. After 120 minutes, this difference has increased over-proportionally. HSU 9000-5 is loaded with 210 µg m^{-2}, which corresponds to 3.9 times the loading of HSU 001-075 with 54 µg m^{-2}.

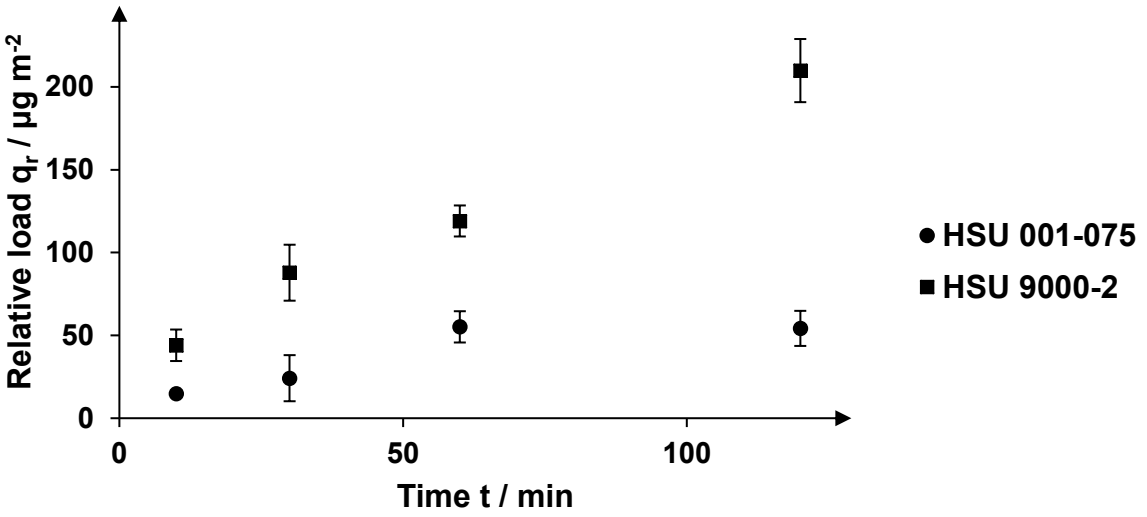

Figure 40: Comparison of HSU 001-075 and HSU 9000-2 regarding loading rate caused by ammonia water with a concentration of c = 1 wt.-%

The obvious tendency of HSU 9000-2 to become more superior to HSU 001-075 in the adsorption of ammoniacal humidity over time can also be well proven by kinetics, as shown in Table 14.

Table 14: Adsorption kinetics of HSU 001-075 and HSU 9000-2 in an atmosphere enriched with ammonia water with a concentration of c = 1 wt.-%.

	Adsorption rate r_a / µg m^{-2} min^{-1}		
	10 minutes	30 minutes	120 minutes
HSU 001-075	1.50	0.80	0.45
HSU 9000-2	4.40	2.93	1.75

Here, the values specified for the kinetics are calculated from the loads at the corresponding points in time. Basically, the calculated adsorption rate decreases with increasing time for both adsorbents. For HSU 001-075, it declines from 1.50 µg m^{-2} s^{-1} to 0.45 µg m^{-2} s^{-1}. Thus, the value decreases by 70 % within 110 minutes. During the same period, the kinetics of HSU 9000-2 decrease from 4.40 µg m^{-2} s^{-1} to a value of 1.75 µg m^{-2} s^{-1} after 10 minutes, which corresponds to a reduction of 60 %. Accordingly, the kinetics of HSU 001-075 decrease disproportionately compared to HSU 9000-2. This is of special interest for the durability of the materials, which is investigated in more detail in the breakthrough experiments in Chapter 5.3.4.

5.3 Breakthrough Measurements

In the application of adsorbents by the end-user, the focus of interest is on the material's specific retention against selected compounds. Especially the adsorptive substances mentioned so far are known to be toxic to humans. Hence the interest in keeping these substances out of the air as long as possible and as effectively as feasible. The substances cyclohexane, carbon monoxide, hydrogen sulphide and ammonia were all used. Additionally, different adsorbent combinations were studied regarding their efficiency, especially against combinations of ammonia water and cyclohexane.

The flow rate for the research was adjusted to 300 mL min^{-1}. Two different cross-sections were used for the employed material separation cells. In the first and smaller case, the cross-section was 19.6 cm^2, in the second and larger case, 176 cm^2. The larger cross-section is thus nine times as large as the smaller one. This difference in size also influences the flow velocity and thus has an impact on the residence time of the gas mixture in the cell at a constant flow rate. In this way, kinetic limitations in the adsorption capacity of individual adsorbents are partially circumvented in the larger cell, which also has a modular design. It can be extended in length and thus in the resulting interior space. Consequently, adsorber beds of different lengths can be implemented.

5.3.1 Cyclohexane

Cyclohexane is very well separated from air by the adsorbents investigated as already described in Chapters 5.1.1 and 5.2.1. With the data from the experiments concerning kinetics and maximum loading, excellent results can be expected regarding the breakthrough experiments as well. Furthermore, the various adsorption cells available allow conclusions to be drawn about the effects of reduced flow velocities and thus longer residence times.

Figure 41 compares several set-ups. On the one hand, this concerns the adsorption cells used. The larger cell with an inner diameter of 150 mm and the smaller cell with an inner diameter of 50 mm are considered. For both cells, the breakthroughs are investigated without filled adsorbent and for comparison with an adsorber bed length of 1.5 mm. Results are obtained which are presented as concentration after a certain time at the exhaust of the respective adsorption cell. The inflowing gas phase

corresponds to dry synthetic air (Alphagaz 1.0 by Airliquide), which is loaded by gas washing bottles with cyclohexane. With a concentration at the entrance of the adsorption cell of 39,000 ± 1,500 ppm_V, the experimental set-up corresponds to that presented in Chapter 4.3.1.

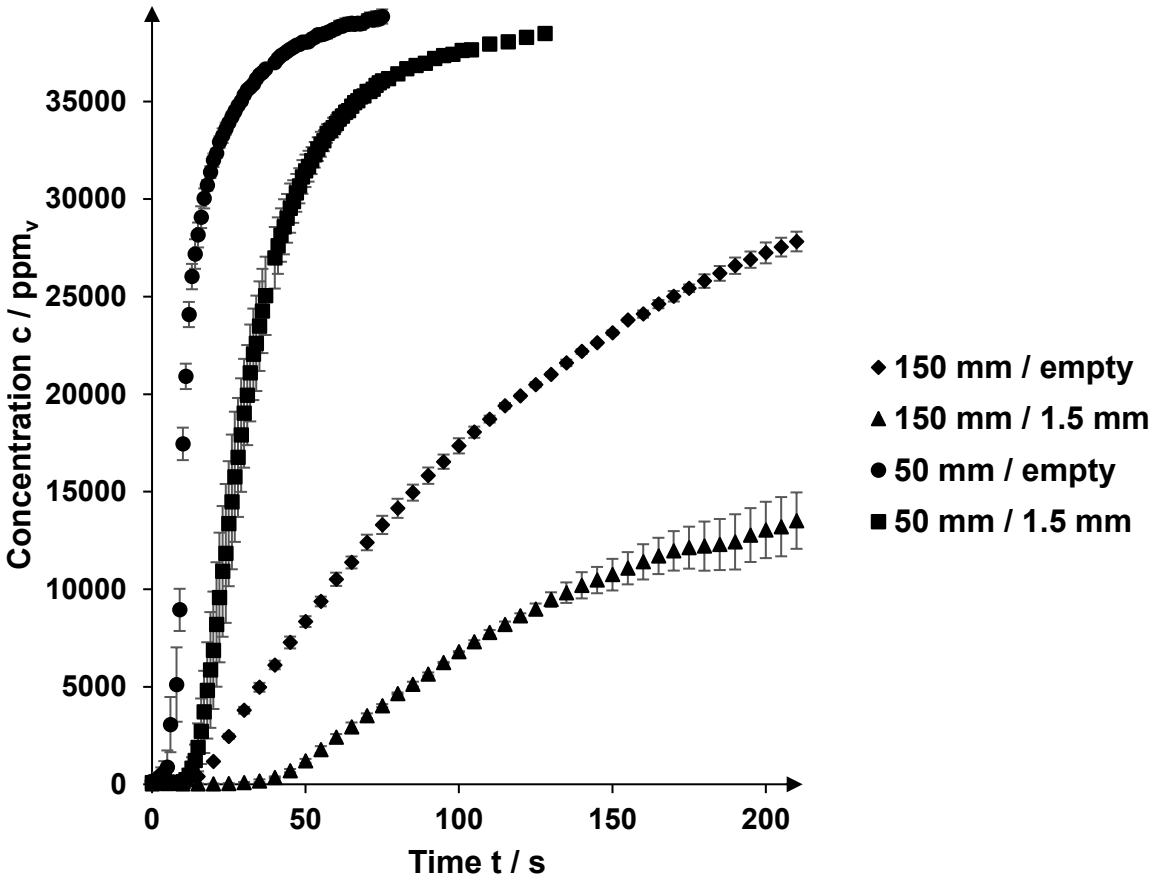

Figure 41: Comparison of breakthrough behaviour through an atmosphere fully saturated with cyclohexane on HSU 001-075 at different sizes of the used adsorption cell

Two things can be seen very clearly in the figure. First, the use of a very short adsorber bed for both cross-sections, such as the one employed here with a length of 1.5 mm, leads to a significant delay in the breakthrough. It also becomes clear that the shape of the breakthrough curve is significantly flattened both by the influence of the adsorbent and by the influence of the cell diameter, making the breakthrough less sharp. Reasons for this behaviour with regard to internal space of the reactor have already been described in Chapter 4.3.2.

A high separation success in the breakthrough experiment can be seen in particular from the time period over which the target substance cannot be detected at the exhaust

of the adsorber bed. Figure 42 focuses on the initial phase of the considered breakthrough experiment in order to show more clearly, after which period which combination of bed length and diameter allows the target substance to pass.

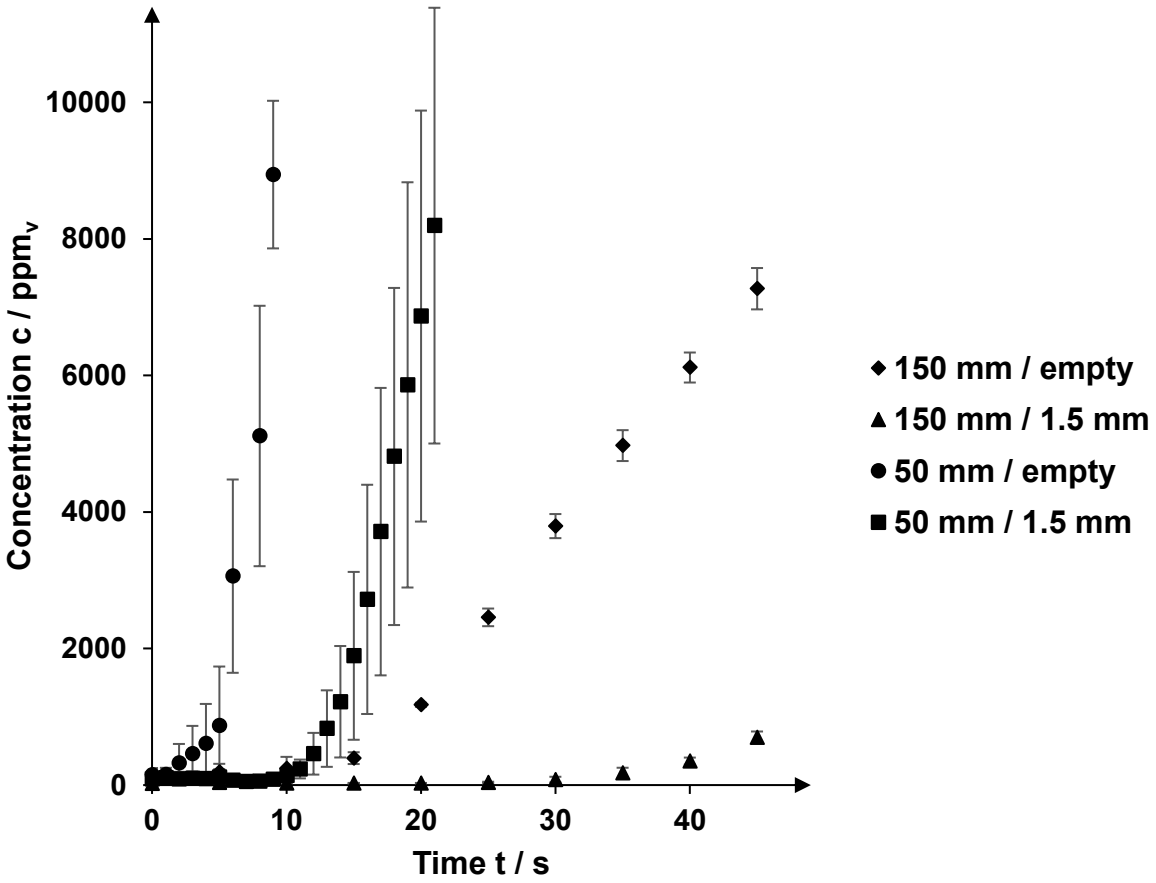

Figure 42: Magnified initial phase of breakthrough curves as depicted in Figure 41

For the breakthrough in the small empty cell, an average concentration of the target substance at the cell exhaust of 151 ± 112 ppm_v can be detected immediately after the start of the measurement. Permanently increasing concentrations for the same adsorption cell with an adsorber bed of 1.5 mm length can only be detected after 10 s. At this point, the concentration of the adsorptive cyclohexane at the exhaust of the cell is 142 ± 95 ppm_v. A significant breakthrough occurs in the large cell with an adsorber bed of 1.5 mm length only after 30 s, and this with a considerably lower concentration compared to the smaller cell of 80 ± 51 ppm_v. After 35 s, the concentration already rises to 177 ± 95 ppm_v. The breakthrough at the large cell without an inserted adsorber bed must also be included in these considerations. For this combination, as for the small cell without adsorbent, a breakthrough is measured immediately as well. The initial concentration is already 152 ± 119 ppm_v at the beginning of the

measurement (0 s). Thus, the initial concentrations of the empty cells are identical. However, it becomes quite clear in the further course that the larger cell contributes to the delay of the further breakthrough. Reference is made to Table 15,which shows which combination achieves an interpolated breakthrough concentration of 8,000 ppm_v after which time. This set point is defined arbitrarily since its value corresponds to about one fifth of the measurable maximum value and is thus still a low concentration. At the same time, a concentration of this level means a beginning toxicity with lasting health consequences (34), so that it is basically relevant for later applications. Corresponding time values were interpolated from the existing values.

Table 15: Interpolated point in time, when 8000 ppm_v are first passed for different adsorber bed lengths

Combination diameter / bed length	Time t / s
50 mm / empty	9
50 mm / 1.5 mm	21
150 mm / empty	48
150 mm / 1.5 mm	113

As can be clearly seen from Table 15, the influence of the reactor room is quite relevant. To reach the outlet concentration of 8,000 ppm_v, only 9 s elapse in the small, empty adsorption cell. In the larger cell, the increase to the same concentration requires 48 s and takes just over five times as long. With an inserted adsorber bed with a length of 1.5 mm, values of 21 s for the small cell and 113 s for the large cell result. The increase to the mentioned concentration takes just over five times as long when the larger cell is interposed. However, the decisive factor is the extension of the breakthrough time with the same reactor size by using an adsorbent. Under the given experimental conditions, the time to reach the concentration of 8,000 ppm_v is more than doubled for the small cell from 9 s to 21 s, and for the large cell from 48 s to 113 s. To gain further insights here, the smaller of the two cells was equipped with another adsorber bed with a length of 7.5 mm and the values were plotted accordingly. For the small adsorption cell, the breakthrough curves shown in Figure 43 result, whereby the breakthrough curves without adsorbent and with a bed length of 1.5 mm are already known.

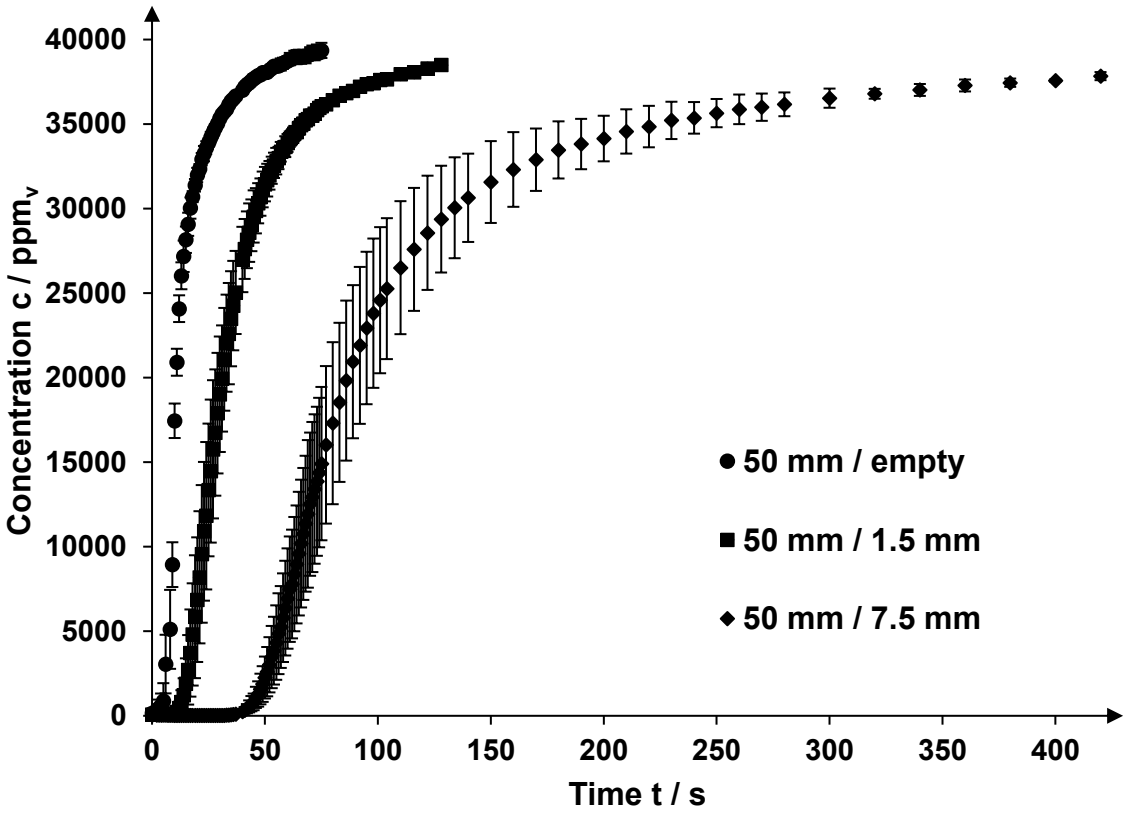

Figure 43: Comparison of retention time by different bed lengths in the larger adsorption cell through an atmosphere fully loaded with cyclohexane

An extension of the adsorber bed leads to a further delay of the breakthrough. As expected, however, the retention time difference compared to the empty cell does not increase to the fivefold difference between the short bed and the empty cell. One reason for this approach is, that a greater filling of the reactor interior with the adsorbent simultaneously reduces the reactor volume, which inevitably leads to a reduction in the residence time. This has a negative effect on the adsorption success because the different diffusion steps in adsorption basically require a certain amount of time, which may no longer be reached. Table 16 shows the times at which 5 %, 50 % and 95 % of the initial concentration of 39,000 ppm_v are measured as breakthrough concentration using linear interpolation for the three adsorbent placements shown.

Table 16: Interpolated times at which cyclohexane concentrations of 5 %, 50 % and 95 % of the input concentration are reached at the cell exit

	$t_{0.05}$ / s	$t_{0.5}$ / s	$t_{0.95}$ / s
l = 0 mm	5.5	10.7	48.7
l = 1.5 mm	16.1	32.0	118.6
l = 7.5 mm	49.3	86.5	422.6

After 16.1 s, the first defined concentration threshold of 0.05 c_0 is exceeded with a bed length of 1.5 mm. This delays the breakthrough by a delta of 10.4 s compared to the empty cell. A five times as long adsorber bed with 7.5 mm, delays the breakthrough by 43.8 s compared to the empty cell. Thus, the longer bed delays the breakthrough 4.1 times as long as the short bed. An optimal value of a fivefold delay is not reached, which was to be expected. For the time up to the breakthrough value of 0.5 c_0, this ratio is even worse. It is achieved with a bed length of 7.5 mm after 86.5 s, with a bed length of 1.5 mm after 32.0 s. For the empty cell, this value is already reached after 10.7 s. Thus, the breakthrough via the short bed length is delayed by a delta of 21.3 s, via the long bed length by 75.8 s, and the added value in the retention capacity for the long adsorber bed is 3.6 times higher than for the short adsorber bed. Reaching the concentration of 0.95 c_0 can be delayed by the longer adsorber bed by 5.3 times compared to the shorter bed length. Such an effect seen for $t_{0.05}$ and $t_{0.5}$ can be explained with the minimization of the room inside the adsorption cell. This is caused by the increasing volume of the adsorbent, while the cell as well as the volume flow, keep the same. Consequently, the reaction room for the flow of atmosphere decreases, which leads to a shorter residence time for the atmosphere and thus worse results. For the highest concentrations at $t_{0.95}$, this effect does not seem to be as relevant. As an explanatory approach, probably due to dispersion effects, there are more possibilities for the hazard to settle on one of the last free adsorption spaces. That means a long fade out, especially at the highest concentrations.

In further measurements, the influence of humidity was also investigated. Incoming air was not only saturated with cyclohexane but also with moisture and had a humidity of 80 % rh. Corresponding results concerning HSU 001-075 are depicted in Figure 44. A comparison of all previously used adsorber bed lengths and their respective breakthrough curves is shown as black filled symbols. In addition to the breakthrough

curves with cyclohexane in dry air, the corresponding breakthrough curves with cyclohexane in moist air are also depicted as white symbols. Due to the set-up of the experiment, the concentration of cyclohexane was lower in the measurements with humidity in comparison to the measurements without humidity. It decreased from approximately 39,000 ppm_v to approximately 32,000 ppm_v. For this reason, with the objective of improved comparability, the measured concentration was standardised to the input concentration.

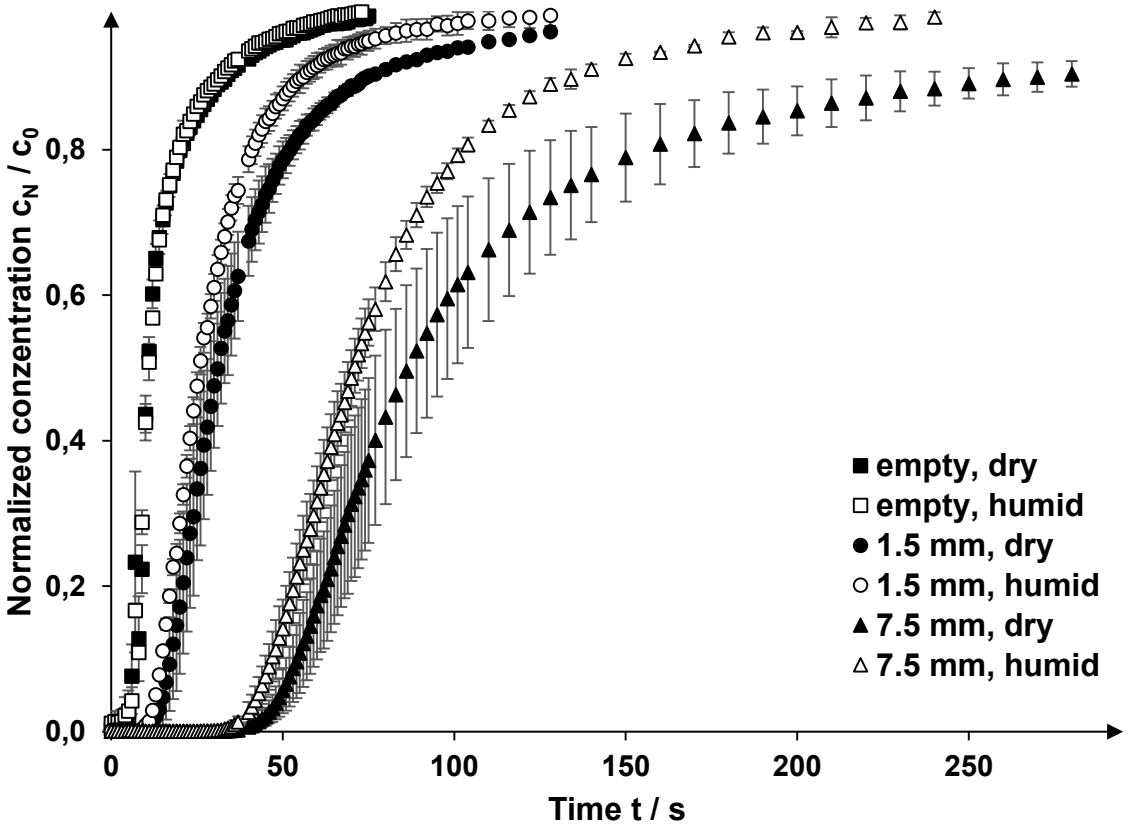

Figure 44: Comparison of breakthrough behaviour on HSU 001-075 in the smaller adsorption cell by dry and humid atmosphere of 80 % rh with cyclohexane

For an empty adsorption cell, it obviously does not matter for the breakthrough, whether additional moisture is present in the atmosphere or not. On the other hand, as soon as there is adsorbent in the cell it is becoming decisive, as indicated by Figure 44. This confirms not only the expectations regarding the adsorption behaviour but also the suitability of the measuring method. Humidity leads to a clearly worse behaviour concerning the breakthrough of cyclohexane. In Table 17 below, the times are interpolated, at which 5 %, 50 % and 95 % of the input concentration are measured at the exhaust of the adsorption cell for the different adsorbent fillings.

Table 17: Times for different concentrations after passing the adsorbent applying dry and humid air

	$t_{0.05}$ / s	$t_{0.5}$ / s	$t_{0.95}$ / s
Empty, dry	5.5	10.7	48.7
Empty, humid	6.1	10.9	46.7
1.5 mm, dry	16.1	32.0	118.6
1.5 mm, humid	13.0	25.7	75.2
7.5 mm, dry	49.3	86.5	422.6
7.5 mm, humid	42.7	70.8	175.8

Differences in the breakthrough times for the empty cells between the humid and the dry atmosphere are clearly around the standard deviation. Within this deviation, the interpolated average concentrations of 5 % and 95 % with 5.5 s and 46.7 s are reached 0.6 s and 2.0 s, respectively, earlier in humid air than in dry air. In purely mathematical terms, only half of the input concentration in dry air is reached slightly earlier at 10.7 s, but the standard deviations for all measured values are so high that simultaneity can be assumed.

Moisture contained in the incoming air leads at a bed length of 1.5 mm to an increase of the concentration at the exit of the cell to 0.05 c_0 within 13.0 s. Without the influence of humidity, the corresponding breakthrough time of 16.1 s is 24 % longer. Very similar conditions arise for the times until half of the input concentration, which is reached at 25.7 s in humid air and 32.0 s in dry air, where the corresponding concentration at the exit of the adsorber cell is thus reached 25 % later.

For the longer beds investigated with a length of 7.5 mm, values in the same order of magnitude result, whereby an even smaller influence of the humidity seems to exist. A first concentration mark of 0.05 c_0 is reached with dry air after 49.3 s, which is 1.15 times later than with humid air ($t_{0.05}$ = 42.7 s). To reach the concentration of 0.5 c_0 in humid air, 70.8 s elapse, while in dry air with 86.5 s almost 16 s more pass. This corresponds to a delay of 22 %. In most cases, the range of low to medium concentrations is relevant. In this range, the breakthrough for dry air with cyclohexane occurs 15-25 % later than the breakthrough for humid air with cyclohexane. Thus, humid air has a significant influence on the adsorption capacity, but in the low to medium concentration ranges this influence is well calculable and limited. At higher

concentrations of 0.95 c_0, additional moisture has a much stronger effect. The adsorption of water compared to the used adsorptives seems to be slower. With progressing time, the effect of air humidity increases to the disadvantage of the target substance to be adsorbed. For longer beds, this effect is more pronounced than for shorter ones. In case of cyclohexane, with a bed length of 1.5 mm, the time for a breakthrough with a concentration of 0.95 c_0 is shortened from 119 s to 75.2 s, which corresponds to a reduction of the breakthrough time to 63 %. With a bed length of 7.5 mm, cyclohexane is retained up to the target concentration for 423 s, and the fed humidity causes the value to shrink to 176 s, which corresponds to 42 %.

5.3.2 Carbon Monoxide

In comparison to the other investigated adsorptives, the breakthroughs of CO are the fastest. Consequently, the measurements were all conducted with the larger adsorption cell. With the smaller cell, however, it was not possible to reliably measure a separation success outside the standard deviation. HSU 001-075 as basis material and its functionalised versions HSU 001-075.1 and HSU 001-075.2 were used. As the measurement success in cases of HSU 001-075.1 were not as good as expected, the focus is on HSU 001-075.2. The concentration of CO in the otherwise synthetic air was 1 vol.-%. In contrast to the other presented breakthrough experiments, the measurements were conducted with a reduced flow rate of only 100 mL min^{-1}.

It could be proven, even for the not functionalised silica support HSU 001-075, that an obvious adsorption process took place by using the investigated adsorbents. Figure 45 shows the results of different bed lengths of HSU 001-075 in comparison to an empty cell. In this example, the depiction of the results is cut after eleven and a half minutes or an outlet concentration of 1,550 ppm_v in order to fit the standard deviation of the smaller bed length into the graph. The standard deviations are relatively high and partially touch each other for the different bed lengths. However, there clearly is a difference between the different bed lengths. The longer the adsorbent bed length, the smaller the uncertainty, which is in harmony with the reaction engineering findings (3 p. 147 ff.).

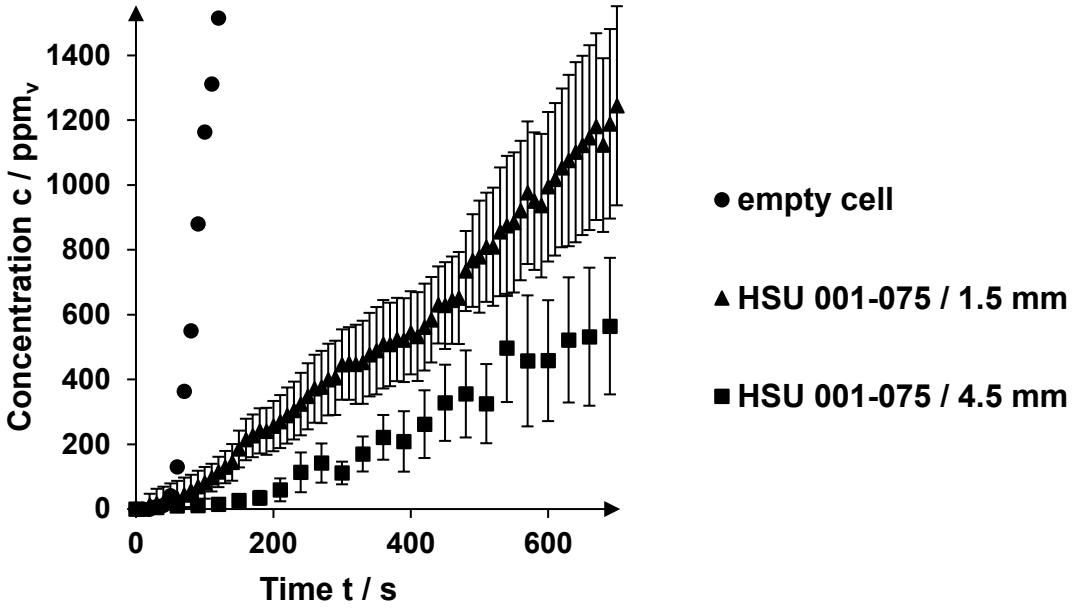

Figure 45: Comparison of breakthrough curves caused by a CO concentration of 1 vol.-% on HSU 001-075 with different bed lengths

After an interval of 60 s, the influence of the adsorbents can be read off very well. At the exhaust of the empty adsorption cell, the concentration of carbon monoxide increases to 130 ppm_v. For bed lengths of 1.5 mm and 4.5 mm, concentrations of 34 ppm_v and 10 ppm_v, respectively, result. The effect is considerably intensified after 120 s, when the concentration at the exhaust of the empty adsorption cell reaches 1,516 ppm_v and is thus more than ten times the measured concentration after flowing through a bed of 1.5 mm length, where a concentration value of 115 ppm_v is reached. A bed length of 4.5 mm ensures that a concentration value of 15 ppm_v is not exceeded. After 300 s, only the concentration values for the cell with the adsorber beds can be recorded. In case of the shorter bed length, the measured average concentration is then 446 ppm_v and thus about four times higher than for the longer bed length, for which the concentration reaches 111 ppm_v. This large difference in the concentration at the cell exhaust decreases due to the incipient breakthrough with time. A creeping breakthrough is shown in the graph, which can be due to flow inhomogeneities. These could be caused by an enhanced flow between the wall of the device and the adsorbent bed. Additionally, the adsorber bed itself could be inhomogeneous. A longer bed obviously leads to a significantly better proven separation result. After 600 s, the concentration after the short bed is 995 ppm_v, after the long bed it is 458 ppm_v. In absolute figures, the longer bed thus causes a reduction in concentration of 537 ppm_v. In relative terms, the concentration is reduced by more than half.

Table 18 notes the times in which 500 ppm_v and 1,000 ppm_v are reached depending on the bed length. These values were chosen to fit into the existing experimental set-up. As the input concentration has a value of 1 vol.-%, 500 ppm_v corresponds to a fraction of 0.05 c_0, and 1,000 ppm_v is the equivalent to 0.1 c_0. The higher concentration already represents a hostile gas composition. It can be assumed, that a concentration of 1,500 ppm_v is lethal after 60 min. The used measurement devices can cope with concentrations up to 2,000 ppm_v. Table 18 shows interpolated values of the next directly measured values.

Table 18: Special retention times in seconds for different bed lengths of CO on HSU 001-075 at a concentration of 1 vol.-%

	t_{500ppm_w} / s	$t_{1000ppm_w}$ / s
l = 0 mm	77	94
l = 1.5 mm	356	602
l = 4.5 mm	606	906

As can already be seen in Figure 45, the breakthrough curve at the empty adsorption cell comes very close to the ideal form with its very steep increase in concentration. The mean measured time to reach the first concentration of 500 ppm_v is 77 s. It takes 94 s to reach twice the concentration of 1,000 ppm_v, which is only 17 s longer. A successful adsorption can also be shown by comparing the breakthrough times for the mentioned different bed lengths with those for an empty cell. With a bed length of 1.5 mm, a concentration of 500 ppm_v can be detected after 356 s. This is 4.6 times as long as the time for the compared empty cell. For the bed length of 4.5 mm, the increase up to the mentioned concentration takes 606 s and thus is 7.9 times as long as at the time interval for the empty cell. For a concentration of 1,000 ppm_v, these comparative factors increase again significantly for the short adsorber bed with 602 s to 6.4 times the time of 94 s for the empty cell and with 906 s for the long adsorber bed to 9.6 times the time of the empty cell.

The benefit of a functionalisation can also be proven at least for HSU 001-075.2. Comparably to Figure 45, the success of different set-ups is compared in Figure 46. For these experiments, a bed length of 1.5 mm was used. Similar comparisons from the research results described here, but for bed lengths of 4.5 mm, have already been published in the scientific literature (98). Corresponding measurements were

conducted with the base material HSU 001-075 as well as the functionalised materials HSU 001-075.1 and HSU 001-075.2. These adsorbents were expected to perform best in case of carbon monoxide as stated before. For HSU 001-075.1, however, with regard to Chapter 5.1.3 and 5.2.1, it seemed likely that an improvement could not be proven, as the enhancements are relatively small and the deviations relatively large.

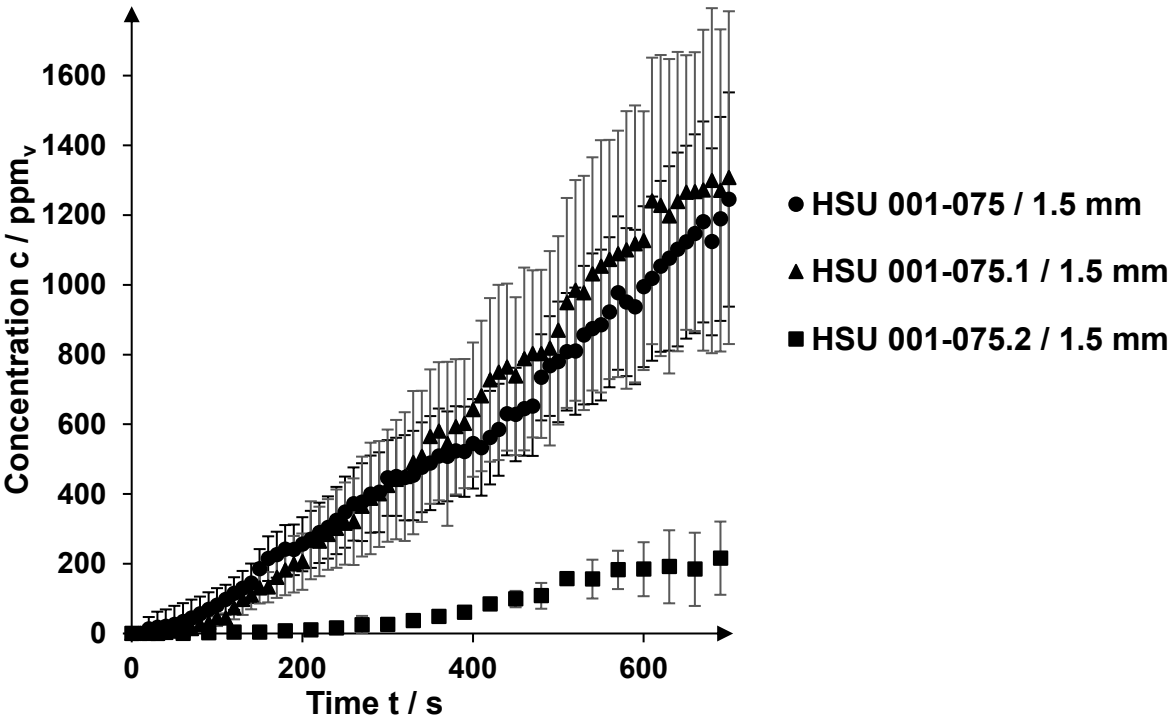

Figure 46: Comparison of breakthrough behaviour of differently functionalised adsorbents with a bed length of 1.5 mm at a CO concentration of 1 vol.-%

Obviously, the breakthrough curves of the unfunctionalised adsorbent and the .1 functionalised adsorbent are on nearly the same track. For the first 200 seconds, it seems that HSU 001-075.1 is slightly more successful in separation compared to the base material but then loses the superiority, and the base material becomes more effective, although both average curves are within the standard deviations of each other. Thus, it could be concluded that there is hardly any difference at all. On the other hand, it could be proven before that HSU 001-075.1 offers faster adsorption kinetics. This is emphasised by the results shown here. Fast kinetics mean that free adsorption spaces are filled and consequently blocked after a relatively short time. Assuming, the capacity of HSU 001-075.1 is not superior to the capacity of HSU 001-075, after a certain time, the ability to hold back further amounts of the target substance must decrease, and thus, the base material must become more efficient.

Functionalised silica gel HSU 001-075.2, which is marked as squares in Figure 46, shows a significantly better performance in comparison to both other adsorbents. After 240 s, a concentration of 16 ppm_v, and thus a two-digit concentration is measured for HSU 001-075.2 for the first time. At the same point in time, the unfunctionalised material HSU 001-075 already passes an averaged concentration of 324 ppm_v, and HSU 001-075.1 passes an averaged concentration of 301 ppm_v, whereby the standard deviations of the latter two largely overlap each other. This strong difference is clearly confirmed once again after 600 s. At this point, the concentrations for HSU 001-075 and HSU 001-075.1 are already 995 ppm_v and 1,127 ppm_v, respectively, while the concentration for HSU 001-075.2 using the same bed length is comparatively low at 184 ppm_v.

Based on these considerations, the possible improvement of silica gels becomes obvious. In fact, an adsorber bed of HSU 001-075.2 with a length of 1.5 mm is on average at least as powerful in the separation of CO as a bed with a length of 4.5 mm made of the unfunctionalised HSU 001-075. Therefore, the values of both adsorbent set-ups lie in each other's standard deviations. This data emphasises the known results of kinetics and maximum loading, where the superiority of HSU 001-075.2 was already proven.

5.3.3 Hydrogen Sulphide

Hydrogen sulphide is problematic concerning measurements of kinetics and equilibrium loading as could be seen in the relevant Chapter 5.1.4. However, the adsorbents are working, as could be proven not only by the former described experiments, but also by the breakthrough curves described in this chapter. In comparison to the measurements of cyclohexane and ammonia, the retention capacity of the materials, on the other hand, has much less impact. In Figure 47, the measurements shown concerning the breakthrough behaviour were conducted with the smaller adsorber cell and an input concentration of 70 ppm_v of hydrogen sulphide in synthetic air and an adjusted flow rate of 300 mL min^{-1}.

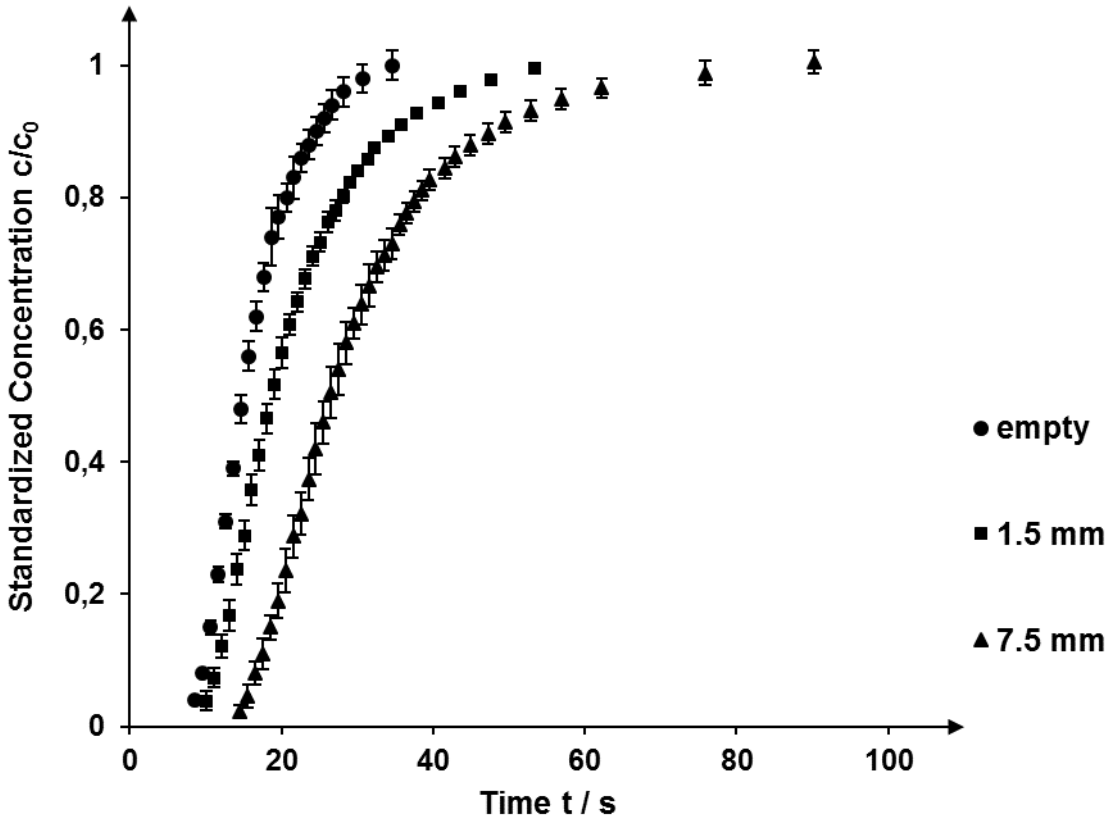

Figure 47: Retention behaviour concerning hydrogen sulphide with an input concentration of 70 ppm_v in dry synthetic air caused by different bed lengths of HSU 001-075 in the smaller adsorption cell

A first detectable value with 2 ppm_v was measured after 9 s for the empty adsorber bed and after 10 s for the short bed. The time difference in this case is very small with only 1 s. In the long bed, however, the first value is recorded after 15 s with 1 ppm_v. Consequently, it is shown that the adsorbent causes an obvious delay in the breakthrough. This is also evident for the time of the complete breakthrough when the cell entry concentration of 70 ppm_v is reached at the cell exhaust. The respective highest concentration values are measured for the empty cell after 35 s, for the short and the long adsorber bed after 53 s and 90 s, respectively. In order to make the shown course numerically more tangible, Table 19 shows for all three settings of the adsorber bed an interpolation of the times at which 5 %, 50 % and 95 % of the input concentration c_0 are reached at the exhaust of the adsorber cell.

Table 19: Times for relative concentrations of H_2S after passing different bed lengths of HSU 001-075 at an H_2S concentration of 70 ppm_v

	$t_{0.05}$ / s	$t_{0.5}$ / s	$t_{0.95}$ / s
l = 0 mm	8.9	14.9	27.2
l = 1.5 mm	10.4	18.8	41.0
l = 7.5 mm	16.1	26.9	57.1

Particularly significant is the extension of the breakthrough time caused by the long adsorber bed compared to the short bed in relation to the breakthrough time at the empty cell. On average, the breakthrough to 0.05 c_0 is delayed by the short adsorber bed by 1.5 s, and by the long adsorber bed by 7.2 s. This means that the fivefold longer adsorber bed extends the breakthrough time by a factor of 4.8, which meets the expected value of 5 very well. A very favourable ratio, which decreases for the measuring points at 0.5 c_0 and 0.95 c_0. For concentrations of 0.5 c_0, the result for the short adsorber bed is 3.9 s, and 12.0 s for the long bed, which is equivalent to a 3.1-fold breakthrough time for the longer bed. Looking at concentrations of 0.95 c_0, this value is further reduced to 2.2. Lowering effects may be due to flow inhomogeneities as described in Chapter 5.3.2. Nevertheless, it can also be seen that the absolute time gain increases. The lowest given concentration 0.05 c_0 is reached after the long bed 5.5 s later than after the short bed. At the concentration of 0.95 c_0, the additional time is already 16.1 s.

With a broader diameter of the adsorber bed, this steep ascent is not possible as can be seen in Figure 48, which is due to the consequently strengthened pore diffusion. In this case, the standard material of the silica gel, HSU 001-075, was compared with its functionalised version HSU 101-075-10. For these measurements, the input concentration was doubled to 140 ppm_v. A higher concentration had to be used, because the lower concentrations led to results with too wide of a spread. Significantly higher concentrations, on the other side, were also impractical. These led, assumedly caused by the very quickly occurring overcharging, to very steep but undifferentiated

breakthroughs with high overlaps between both investigated materials. This is also a sign for the importance of a high affinity, which leads to fast kinetics.

The large cell itself allows the increase in concentration at the cell exit to be considerably delayed while the bed lengths remain the same. For this reason, minutes instead of seconds were selected as the time unit for the abscissa.

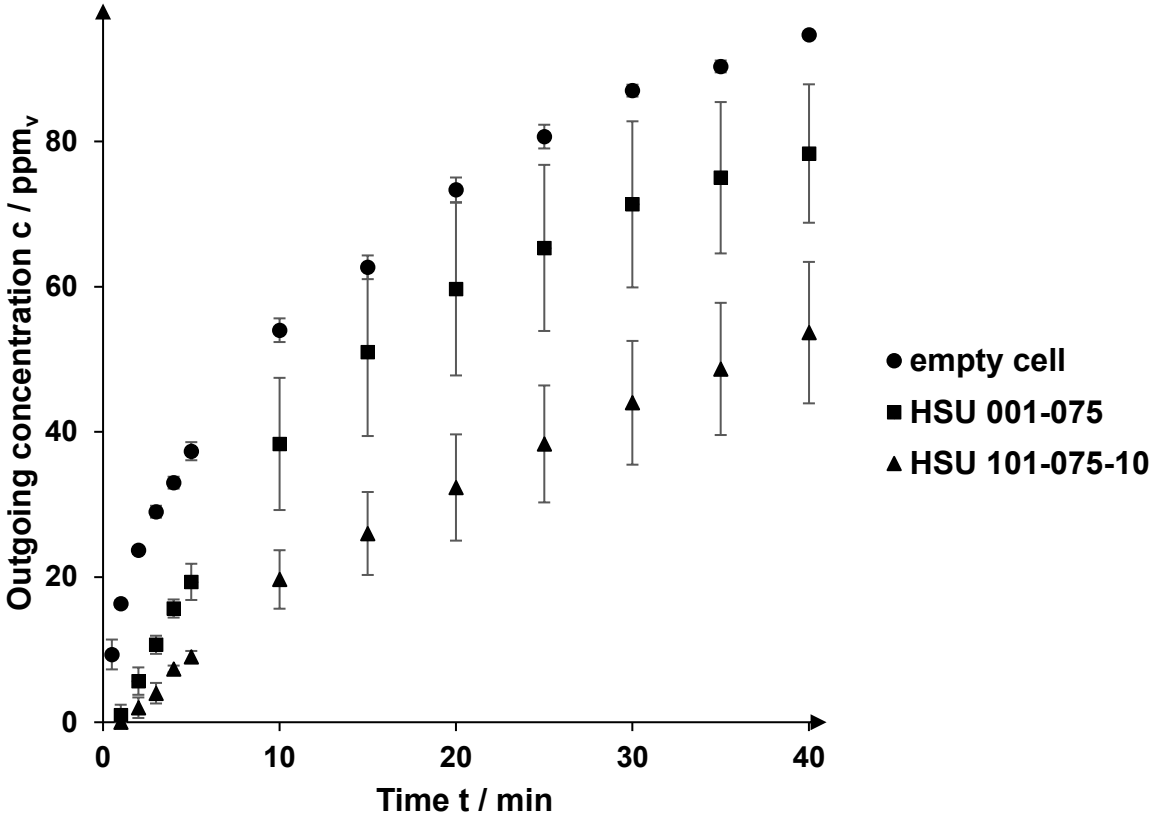

Figure 48: Comparison of retention capability of HSU 001-075 and HSU 101-075-10 against hydrogen sulphide in a concentration of 140 ppm_v

A concentration of 9 ppm_v can already be measured at the exhaust of the empty adsorber device after 30 seconds. Thus, the enlargement of the adsorber cell hardly influences the residence time. For the cells equipped with adsorber beds of the different materials HSU 001-075 and its functionalised version HSU 001-075-10, no hydrogen sulphide concentrations can be measured at this time. Table 20 gives an overview of the time at which a concentration value of 1 ppm_v is reached for these three investigated set-ups.

Table 20: Times until a concentration of 1 ppm_v is detected at the exhaust of the adsorption cell with an input concentration of 140 ppm_v

Used adsorbent	t (c = 1 ppm_v) / s
Empty cell	14 ± 3
HSU 001-075	53 ± 11
HSU 101-075-10	106 ± 38

For the empty cell, a concentration of 1 ppm_v is reached after 14 ± 3 s, while for HSU 001-075 it takes 53 ± 11 s. However, this value is even doubled to 106 ± 38 s for the functionalised HSU 001-075-10. Thus, after 2 min, corresponding concentrations of a beginning hydrogen sulphide breakthrough can be reliably detected for all investigated materials, e.g., at the exhaust of the empty cell 24 ppm_v. For HSU 001-075 and HSU 001-075-10, the values after 2 min are 6 ppm_v and 2 ppm_v, respectively. After 5 min, clear concentration values can be measured for all three variants. 37 ppm_v are already reached after the empty cell, whereas for the functionalised HSU 001-075-10, a significantly lower value of 9 ppm_v is obtained. With the measured values for 10 min and longer intervals, the standard deviations increase significantly. This applies to the measured data of the cell equipped with adsorbents. For the empty cell, the standard deviations for all measured values are less than 2 ppm_v. In contrast, for HSU 001-075 and HSU 001-075-10, the standard deviations increase up to 12 ppm_v and 9 ppm_v, respectively. In case of both adsorbents, the standard deviations always exceed a value of 4 ppm_v after a measuring time of 10 min. Nevertheless, they only overlap after 15 min and 20 min between the empty cell and the one equipped with HSU 001-075. It can be proven that the adsorbent significantly delays the breakthrough. The measurement curve for HSU 001-075-10 never touches one of the other two curves, even if measurement deviations are considered. Therefore, the effectiveness of the functionalisation of the silica gel HSU 001-075-10 is very well proven.

Another investigated aspect is the influence of humidity on the breakthrough behaviour. The results induced by an additionally applied humid atmosphere are depicted in Figure 49. For these measurements, humidity was set to 40 % rh and the used concentration of hydrogen sulphide to 10 ppm_v, which is relatively low (100 p. 50). For the presented measurements, the smaller adsorption cell and a bed length of 1.5 mm were used. In contrast to the other breakthrough measurements with normally

much higher concentrations of the compound to be separated, the period was investigated after which an initial breakthrough of a certain concentration could be determined. In all other cases presented in this book, the concentration after selected times was investigated. Consequently, the standard deviations are parallel to the abscissa and not to the ordinate. The experimental set-up used for these experiments corresponds to the one described in Chapter 4.1.4.

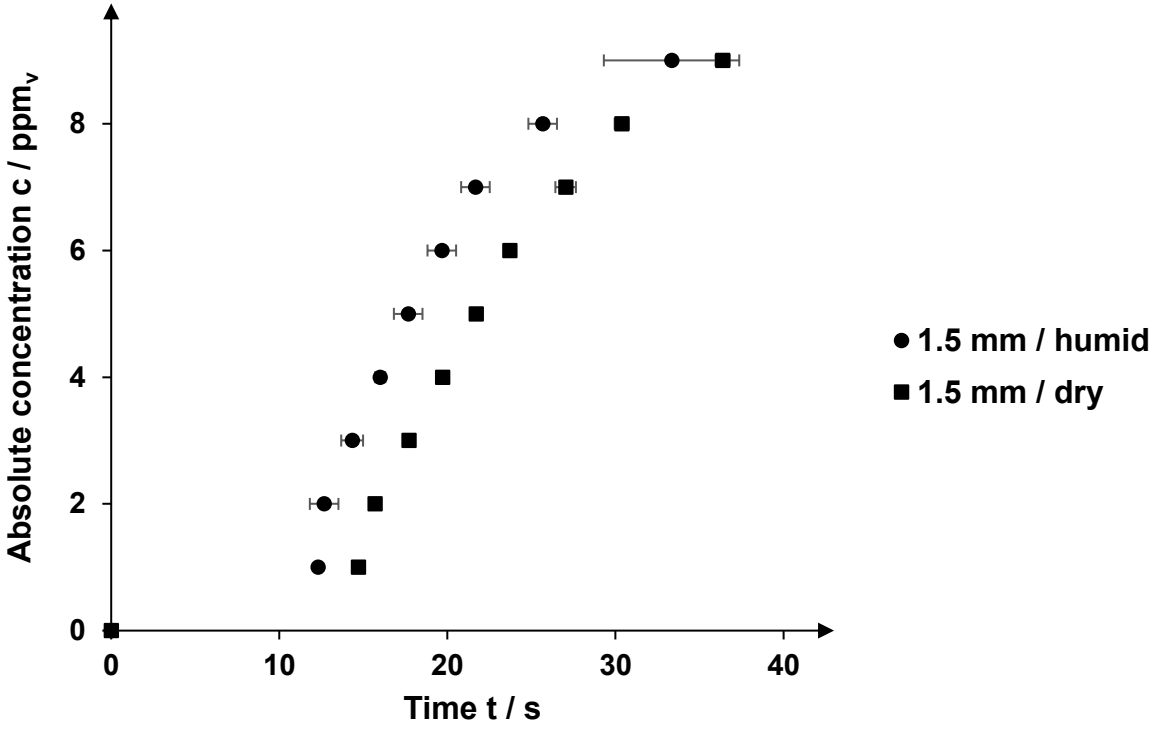

Figure 49: Comparison of breakthrough behaviour at HSU 001-075 caused by a concentration of 10 ppm_v H_2S in dry and humid atmosphere of 40 % rh

Obviously, the addition of humidity to the introduced atmosphere leads to an accelerated breakthrough. It takes 12 s to reach a hydrogen sulphide concentration of 1 ppm_v in humid air, while in dry air this value is measured 3 s later after 15 s. This is equivalent to a reduction of the retention time to 80 %. For the further course of the measured values, it becomes clear that the curve in humid air is steeper than its counterpart in dry air. Such an effect was to be expected since the humidity caused additional adsorption onto the adsorbents. Consequently, time differences increase as well until a certain concentration is reached. At a concentration of 5 ppm_v, this time difference amounts to 4 s, whereas at a concentration of 7 ppm_v the time difference increases to 5 s, which still means a reduction of the retention time in humid atmosphere to a level of 81 % of the reference value in dry air. Starting from

concentration values of 9 ppm_v and higher, no such sharp distinction can be made for measurements in humid air due to the large standard deviation. Fundamentally, it can be very well deduced from the measured values obtained that the influence of humidity on the adsorption of the target substance is certainly present but not as pronounced as expected. Conclusively, the basic material HSU 001-075 is also suitable for significantly delaying the breakthrough in humid atmospheres despite its sensitivity to hydrogen sulphide.

5.3.4 Ammonia

Dry ammonia is a very good example for the improvement of the separation efficiency due to the selection of an appropriate adsorbent. Compared to e.g. carbon monoxide, it is held back significantly longer - even by the base material. For the results shown in Figure 50, an ammonia concentration of 10,000 ppm_v and the adsorber cell with the larger diameter of 150 mm in conjunction with a bed length of 4.5 mm for both investigated materials was used. However, the breakthrough curve for HSU 001-075 shows a comparably steep ascent. The lowest known toxic concentration of 20 ppm_v on average was reached in this set-up first after more than 15 minutes. With a continuously increasing gradient, 100 ppm_v are reached shortly after the mark of 30 minutes; and after 60 minutes, even 300 ppm_v are reached. But although these results seem to indicate an inefficient material for the separation of ammonia from air, the comparison to an empty cell allows a different assessment. Without any material, 20 ppm_v are reached after less than 20 s, depending on the measurement deviations, potentially even after less than 10 seconds. After one minute, the latest, 300 ppm_v are reached. This data is not shown in Figure 50, as this would appear only as points on the ordinate, but emphasises the already high effectivity of the commercially available silica gel HSU 001-075 for the separation of ammonia. Nevertheless, HSU 9000-2 obviously is the much more efficient material.

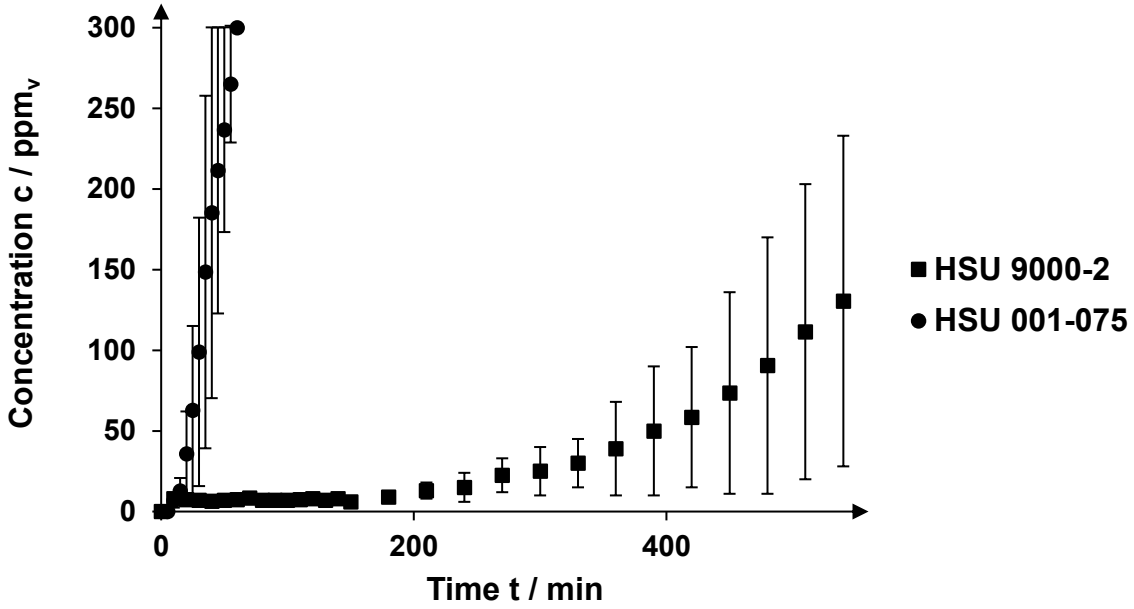

Figure 50: Comparison of breakthrough of dry ammonia at an initial concentration of 1 vol.-% against HSU 001-075 and HSU 9000-2

For HSU 9000-2, the ascent is by far not as steep as that for HSU 001-075. With 20 ppm_v, the lowest toxic concentration is first reached after more than 240 minutes. Not shown as it would negatively affect the readability of the Figure, 300 ppm_v were reached after 10 hours at the earliest. This value represents the most unfavourable measurement result achieved. On average, it took 13.5 h before the named concentration was reached. For a potential application, the difference in the performances of the material has a far-reaching meaning. The more convenient HSU 9000-2 delays the increase to this concentration of ammonia by a factor of 16 compared to HSU 001-075, which is also of high interest, as HSU 9000-2 normally should be expected to be less effective with the same bed-lengths. As stated in Chapter 3.1.1 in Table 5, the relative surface of HSU 9000-2 is relatively small in comparison, whereas the pore sizes are comparably large.

It must be mentioned that the standard deviations in the measurements presented in Figure 50 are relatively high. The flow inhomogeneities probably have a significant influence due to the short bed length of the adsorbent of only 1.5 mm.

Exemplary measurements were also conducted with ammonia water in a concentration of 1 wt.-%. The corresponding results are shown in Figure 51.

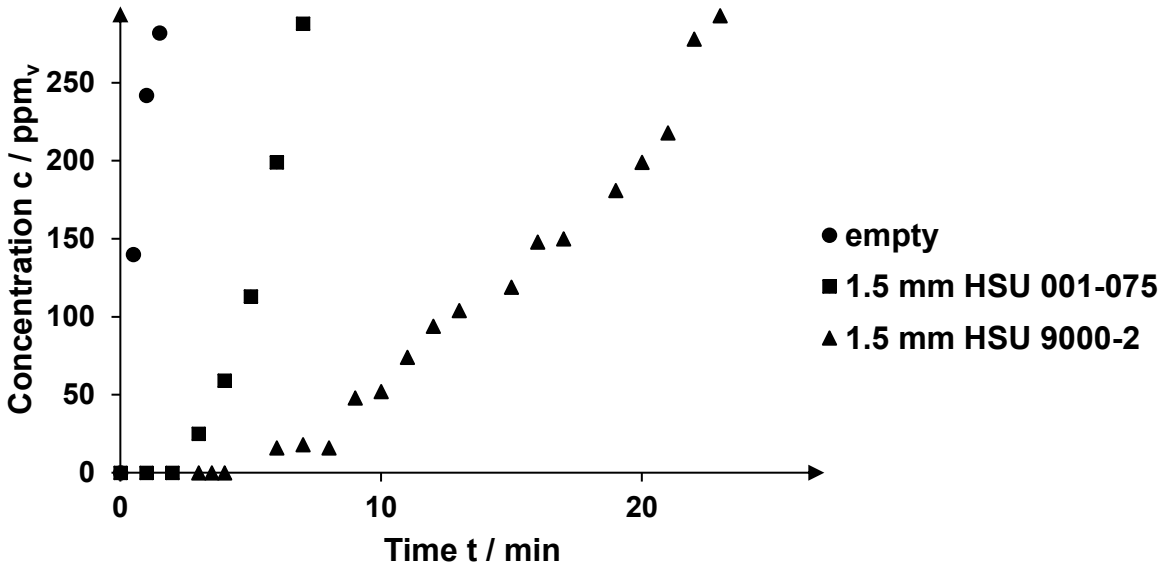

Figure 51: Breakthrough curves of ammonia water with a concentration of 1 wt-% on different separation materials

After 1.5 min, a concentration of 282 ppm_v can be measured at the exit of the empty cell. This is in clear contrast to the materials investigated for the separation of ammonia, which were used as adsorbent in the separation device. For both, HSU 001-075 and HSU 9000-2, no ammonia concentration is detectable at the cell exit after the same time interval. However, there is a considerable difference in the breakthrough behaviour between the two materials. The graph shows very clearly that HSU 9000-2 leads to a considerably delayed breakthrough compared to HSU 001-075. According to HSU 001-075, a concentration of 199 ppm_v is already reached at the exhaust of the adsorber cell after 6 min. However, for HSU 9000-2, a time of 20 min elapses until the identical concentration is reached. The time difference here is therefore 14 min. Overall, it can be seen, that by using HSU 9000-2 compared to HSU 001-075, the course of the breakthrough curve is considerably flatter, but the breakthrough is also very much delayed.

In comparison to the breakthrough measurements with dry ammonia, the breakthrough by ammonia water occurs earlier. This effect appears as expected because moisture is also adsorbed in the process under investigation. Consequently, humidity, which is adsorbed very well, is also occupying the free spaces on the surface of the adsorbents. A selectivity, which fully excludes the adsorption of water, is not given for both materials as already demonstrated in Figure 39 in Chapter 5.2.4.

In further experiments, the combination of the investigated materials was investigated as well. The results in this case are surprising. An exemplary measurement is represented in Figure 52, where the concentration at the exhaust of the cell with the adsorber bed is given in weight proportions over time. Since the individual materials used as adsorbents show considerable differences in the breakthrough behaviour against ammonia water, a logarithmic representation was chosen for the abscissa.

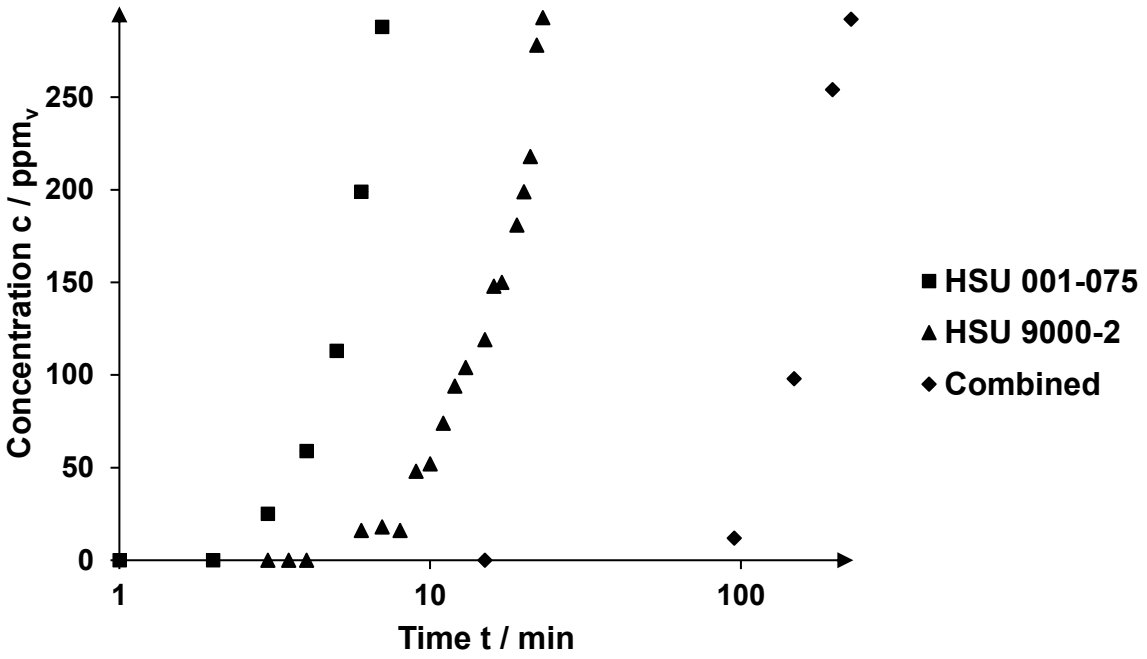

Figure 52: Comparison of breakthrough-curves of ammonia water with a concentration of 1 wt-% on HSU 001-075, HSU 9000-2 and a combination of both materials

For the bed lengths of the single materials again 1.5 mm were chosen in the adsorption cell with a diameter of 150 mm. When the materials were combined, the length was doubled, which is 3 mm in this case. With the knowledge of the results described above, a breakthrough time between the double of HSU 001-075 and HSU 9000-2 would be expected for the combination of both materials. Surprisingly, this assumption could not be confirmed. The first concentration of ammonia appeared after 95 min with a value of 12 ppm_v. This is 89 min later compared to HSU 9000-2, where a concentration of 16 ppm_v appeared after 16 min, and 92 min later compared to HSU 001-075 with a concentration of 25 ppm_v after 3 min. Consequently, the combination of the materials HSU 001-075 and HSU 9000-2 compared to the pure HSU 9000-2 results in a 16-fold delay of the breakthrough. Compared to pure HSU 001-075, the breakthrough is 32 times delayed until the first reading. This can be

assumed, because the first measured concentration with the combined bed is lower than both first measured concentrations of the pure adsorbents. The absolute time difference for the highest measured values is even clearer. After 226 min, a concentration of 292 ppm_v is measured at the exhaust of the cell filled with both materials. With the simple HSU 9000-2, a concentration of 293 ppm_v is reached after 23 min. This results in a delay of the breakthrough up to a concentration of 300 ppm_v of at least 203 min. Compared to HSU 001-075 as the sole material for substance separation with a concentration of 288 ppm_v after 7 min, the difference even amounts to 219 min. As a result, the additional breakthrough time achieved is many times higher than expected and clearly demonstrates the added value that selected material combinations can produce for the adsorption of certain target substances.

This behaviour could be explained by the separation of water and ammonia in the adsorber. Most likely, HSU 001-075, which is passed first by the atmosphere, separates only few of the ammonia but seems to adsorb most of the incoming water. As most of the humidity is separated from the gas phase before the section of HSU 9000-2, it does not block free adsorption places for the ammonia. Therefore, the ability to adsorb ammonia is increased. This explanation leans on the results depicted in Figure 50, where the breakthrough of ammonia in dry atmosphere occurred even later. Furthermore, it can be explained by the theories of multi-component adsorption, as described in Chapter 2.1.4. In addition, with a selectivity in favour of water for HSU 001-075, the described adsorbent system is an excellent example for the possibilities of powerful combinations of different adsorption materials.

6 Conclusion and Outlook

Adsorption is a powerful method for the separation of different compounds from the ambient air. Earlier works at the chair of “Process Engineering, especially Separation Technologies” dealt with these topics mainly in conjunction with restaurants, food producing or other industries (9; 86; 101). In the previous chapters of this scientific paper, cyclohexane as well as carbon monoxide, hydrogen sulphide and ammonia were discussed. It was investigated how these substances can be adsorbed by silica gels and how the performance of these silica gels can be improved by adequate functionalisation.

For the research, gravimetric measurement set-ups were designed, which alone represent a significant scientific progress. The experimental installations are not only equally suitable for measuring maximum loads and kinetics but also completely insensitive to corrosive materials. In addition, multi-component mixtures can be investigated, regardless of whether they are present in the gas phase or must be vaporised.

For very corrosive adsorptives, the measurements showed that it is possible to make the adsorbents substantially more resistant by a targeted functionalisation. The example of hydrogen sulphide in particular shows that it is also possible to considerably improve the possible maximum load. When the basic material HSU 001-075 is increasingly attacked and degraded at higher hydrogen sulphide concentrations, HSU 101-075-10 obviously remains stable, and the load increases steadily from 15.1 µg m^{-2} at 10 ppm_v to 50.4 µg m^{-2} at 5,000 ppm_v in comparison to 20.6 ppm_v and 13.6 ppm_v for the base material affected by the same concentrations, respectively.

A corresponding increase in the maximum loading capacity could also be observed for the other adsorptives. For cyclohexane at a partial pressure of 0.5 p_0, the functionalised adsorbent HSU 101-075-10 is 20 % more efficient with a relative loading of 393 µg m^{-2} than the unfunctionalised silica gel HSU 001-075 with a relative loading of 326 µg m^{-2}. At a concentration of 10,000 ppm_v, the possible uptake of CO for the functionalised HSU 001-075.2 is 43 % higher with a value of 16.42 µg m^{-2} than for HSU 001-075 with 11.45 µg m^{-2}. Measurements for ammonia at the identical concentration were even clearer with 85 µg m^{-2} for the starting material HSU 001-075 and 989 µg m^{-2} for the

improved material HSU 9000-2, which is equivalent to a 10-fold increase in performance at this point.

Kinetics for all adsorptives considered could also be improved. This results in smaller amounts of adsorbents, which are necessary for the separation of the corresponding adsorptive. For example, to reduce a carbon monoxide concentration from 10,000 ppm_v to 30 ppm_v for a physically hard-working person over 10 minutes there is a need for 7973 g of HSU 001-075 but only 4893 g of HSU 001-075.2. For hydrogen sulphide, the active surface required for a reduction of the concentration from 70 ppm_v to 5 ppm_v over 30 min is for HSU 031-295 at a value of 62,980 m^2. for HSU 101-075, the value decreases to 17,580 m^2. In case of ammonia, the necessary area for a reduction of the concentration from 1,000 ppm_v to 20 ppm_v over 30 min could be reduced from 36,456 m^2 to 8,539 m^2.

Furthermore, an increase in selectivity could be observed. In a loading experiment with air humidity over 24 hours, it was found that HSU 001-075 achieved a loading of 129 µg m^{-2}, whereas the functionalised HSU 101-075-07 was only loaded with 36 µg m^{-2}. This effect is very desirable since cyclohexane was the targeted component. In the investigations concerning the loading of adsorbents with CO in humid air, a considerable improvement could also be achieved for HSU 001-075.2 with 33.8 µg m^{-2} compared to HSU 001-075 with 10.2 µg m^{-2}. However, it also showed that the rate of loading with the target material in humid air decreases considerably.

The breakthrough behaviour has also been largely improved. Utilizing the adsorber cell with a cross-section of 19.6 cm^2 under a volume flow of 100 mL min^{-1}, for an input carbon monoxide concentration of 10,000 ppm_v an outgoing concentration of 100 ppm_v was already achieved after 130 s using HSU 001-075, and after 450 s, if HSU 001-075.2 was used. For hydrogen sulphide under a volume flow of 300 mL min^{-1} into the larger adsorption-cell with a cross-section of 176 cm^2, a reference concentration of 1 ppm_v in dry air with HSU 001-075 was reached on average after 53 s, and for HSU 101-075-10 after twice the time of 106 s. The greatest development leap in this respect under the last named experimental conditions could be demonstrated for ammonia water. Using both supports, HSU 001-075 and HSU 9000-2, the retention time to reach a concentration of 290 ppmv was increased more than 30-fold from 7 min to 226 min compared to the base material HSU 001-075.

The described investigations have shown that the separation of cyclohexane, carbon monoxide, hydrogen sulphide and ammonia can be significantly improved by a targeted functionalisation of the silica gels used. Both the absorption rate and the maximum load capacity could be significantly increased for all components described. Finally, it could be demonstrated that the breakthrough of these harmful substances could also be significantly delayed by appropriate functionalisation. This results in a considerable added value, especially for later applications.

List of References

1. **Umweltbundesamt.** Umweltbundesamt.de. [Online] 14 February 2018. [Cited: 25 April 2019.] www.umweltbundesamt.de/daten/luft/schadstoff-emissionen-in-deutschland.

2. **German Economic Institute.** deutschlandinzahlen.de. [Online] 1 June 2018. [Cited: 26 March 2019.] www.deutschlandinzahlen.de/tab/deutschland/volkswirtschaft/bruttoinlandsprodukt/bruttoinlandsprodukt-nominal.

3. **Kast, Werner.** *Adsorption aus der Gasphase.* Weinheim, GER : VCH Verlagsgesellschaft mbH, 1988.

4. **Kommission Reinhaltung der Luft im VDI und DIN.** *VDI 3674: Waste gas cleaning by adsorption; Process gas and waste gas cleaning.* Düsseldorf, GER : Beuth Verlag GmbH, 2013.

5. **VDI-Kommission Reinhaltung der Luft.** *VDI Richtlinien: Emissionsminderung Kakao- und Schokaladenindustrie VDI 3893.* Düsseldorf, GER : Verein Deutscher Ingenieure (VDI), 1987.

6. **Täffner, Tim, Birkenseer, Matthias and Niemeyer, Bernd.** Optimized Selective Adsorbents, Process Parameters and Catalytic Conversion. [ed. Niemeyer, Bernd, Berger, Ralf, Krüger, Klaus, Matz, Gerhard, Otterpohl, Ralf and Stegmann, Rainer]. *Hamburger Berichte 36, Abfallwirtschaft: Odour Control.* Stuttgart, GER : Abfall aktuell, 2010.

7. **Cartellieri, Ansgar, Thiesen, Peter, Birkenseer, Matthias and Niemeyer, Bernd.** Neue regenerierbare und katalytisch wirkende Adsorbentien sowie Verfahrensentwicklung zur vor Ort Regeneration. [ed. Niemeyer, Bernd, Matz, Gerhard, Otterpohl, Ralf, Stegmann, Rainer and Steinhart, Hans]. *Hamburger Berichte 30 AbfallRessourcenWirtschaft: Minimierung von Gerüchen.* Stuttgart : Abfall aktuell, 2006.

8. **Robers, Ansgar, Thiesen, Peter and Niemeyer, Bernd.** Innovative Adsorptionstrennverfahren zur Geruchsminimierung. [ed. Niemeyer, Bernd, Robers, Ansgar and Thiesen, Peter]. *Hamburger Berichte 23 Abfallwirtschaft: Messung und Minimierung von Gerüchen.* Stuttgart, GER : Abfall aktuell, 2004.

9. **Täffner, Tim.** *Adsorptive Abtrennung von Schadstoffen aus komplexen Rohgasen für Anwendungen in der Abluftbehandlung, Dissertation.* Hamburg, GER : Dr. Hut, 2011.

10. **Mersmann, Alfons.** Adsorption. [ed.: Bohnet, Matthias, Brinker, Jeffrey, Cornils, Boy, Evans, Trevor, Greim, Helmut, et al.]. *Ullmann's Encyclopedia of Industrial Chemistry Volume 1.* Weinheim, GER : Wiley-VCH Verlag GmbH & Co. KGaA, 2003.

11. **Bathen, Dieter and Breitbach, Marc.** *Adsorptionstechnik.* Heidelberg, GER : Springer, 2001.

12. **Wedler, Gerd.** *Adsorption: Eine Einführung in die Physisorption und Chemisorption.* Weinheim / Bergstraße, GER : Verlag Chemie, 1970.

13. —. *Lehrbuch der physikalischen Chemie.* Weinheim, GER : Verlag Chemie, 1982.

14. **Tien, Chi.** *Adsorption Calculations and Modeling.* New York, NY, USA : Butterworth-Heinemann, 1994.

15. **Henry, William.** Experiments on the Quantity of GasesAdsorbed by Water , at Different Temperatures, and under Different Pressures. *Philosophical Transactions of the Royal Society of London.* 1803, 93: 29-43.

16. **Markham, E.C. and Benton, Arthur F.** The Adsorption of Gas Mixtures by Silica. *Journal of the American Chemical Society.* 1931, Vol. 53, 2: 497-507.

17. **Brunauer, Stephen, Emmett, P. H. and Teller, Edward.** Adsorption of Gases in Multimolecular Layers. *Journal of the American Chemical Society.* 1938, Vol. 60, 2: 309-319.

18. **Zhdanov, V. P. and Kesemp, B.** Diffusion-limited reaction kinetics in nanofabricated porous model catalysts. *Catalysis Letters.* 1998, Vol. 50, 3-4: 131-134.

19. **Sattler, Klaus.** *Thermische Trennverfahren: Grundlagen, Auslegung, Apparate; Dritte, überarbeitete und erweiterte Auflage.* Weinheim, GER : Wiley-VCH Verlag, 2001.

20. **Baerns, Manfred, Hofmann, Hanns and Renken, Albert.** *Chemische Reaktionstechnik - Lehrbuch der Technischen Chemie, Band 1; 3rd revised edition.* Stuttgart, GER : Georg Thieme Verlag, 1999.

21. **Gorbach, A., Stegmaier, M. and Eigenberger, G.** Measurement and Modeling of Water Vapor Adsorption on Zeolite 4A - Equilibria and Kinetics. *Adsorption.* 2004, Vol. 10, 1: 29-46.

22. **Fick, Adolf.** Über Diffusion. *Poggendorff's Annalen der Physik.* 1855, Vol. 94, 59-86.

23. **Chinag, Hung-Lung, Tsai, Jiun-Horng, Chang, Gen-Mu and Hsu, Yi-Chun.** Adsorption Kinetic Characteristics of H2S on Activated Carbon. *Adsorption.* 2002, Vol. 8, 4: 325-340.

24. **Berg, Frederik, Pasel, Christoph, Luckas, Michael, Eckardt, Tobias and Bathen, Dieter.** Adsorption of Cyclic Hydrocarbons on Silica Alumina Gels in Natural Gas Processing. *Chemie Ingenieur Technik.* 2017, Vol. 89, 7: 935-943.

25. **Talu, Orhan.** Measurement and Analysis of Mixture Adsorption Equilibrium in Porous Solids. *Chemie Ingenieur Technik.* 2011, Vol. 83, 1-2: 67-82.

26. **Gun'ko, V. M.** Competitive Adsorption. *Theoretical and Experimental Chemistry.* 2007, Vol. 43, 3: 139-183.

27. **Pires, Joao, Borges, Susana, Carvalho, Ana P. and Silva, Ana R.** Porous Silicas and Respective Carbon Replicates for Adsorption and Catalysis. *Adsorption Science & Technology.* 2010, Vol. 28, 8-9: 717-726.

28. **Möller, Andreas, Guderian, Joachim, Möllmer, Jens, Lange, Marcus, Hofmann, Jörg and Gläser, Roger.** Kinetische Untersuchungen der adsorptiven Luftzerlegung an Kohlenstoffmolekularsieben. *Chemie Ingenieur Technik.* 2013, Vol. 85, 11: 1680-1685.

29. **Wei, Yajuan, Sun, Yan, Su, Wei and Liu, Jia.** Influence of Pore Size on Ethylene Hydrate Formation in Carbon Materials. *Adsorption Science & Technology.* 2014, Vol. 32, 9: 717-724.

30. **Rosenfeld, Henning, Peper, Stefanie, Täffner, Tim, Kötke, Matthias, Fonka, Moundih A., Temme, Heike and Niemeyer, Bernd.** Effektive Stofftrennung in Gas- und Flüssigphase durch selektive Adsorption. *Chemie Ingenieur Technik.* 2011, Vol. 83, 8: 1229-1236.

31. **Vargas Crespo, Cristiam Camilo.** *Entfernung von Organophosphat basierten Pestiziden mittels Adsorption; Dissertation.* Hamburg, GER : Helmut-Schmidt-University / University of German Federal Armed Forces, 2014.

32. **Helmholz, Heike, Cartellieri, Simone, He, Lizhong, Thiesen, Peter and Niemeyer, Bernd.** Process development in affinity separation of glycoconjugates with lectins as ligands. *Journal of Chromatography A.* 2003, Vol. 1006, 127-135.

33. **Normenausschuss Feinmechanik und Optik im DIN.** *DIN EN 14387: Respiratory protective devices - Gas filter(s) and combined filter(s) - Requirements, testing, marking; German version EN 14387:2004+A1:2008.* Berlin, GER : Beuth Verlag, 2008.

34. **IFA Institute for Occupational Safety and Health of the German Social Accident Insurance.** GESTIS Substance Database. [Online] 27 April 2018. [Cited: 16 May 2018.] http://gestis-en.itrust.de

35. **Usman, Tariq and Tan, Ming-qiu.** H2S adsorption and dissociation on Rh(110) surface: a first principles study. *Adsorption.* 2018, Vol. 24, 6: 563-574.

36. **González, Maria G., Ponzi, Esther N., Ferretti, Osmar A. and Quincoces, Claudia E.** Studies on H2S Adsorption and Carbon Deposition Over Mo-Ni/Al2O3 Catalysts. *Adsorption Science & Technology.* 2000, Vol. 18, 6: 541-550.

37. **Tran, Hoai-Lam, Kuo, Maw-Suey, Yang, Wein-Duo and Huang, Yu-Chang.** Hydrogen sulfide adsorption by thermally treated cobalt(II)-exchanged NaX zeolite. *Adsorption Science & Technology.* 2016, Vol. Vol. 34, 4-5: 275-286.

38. **Hartmann, Martin and Bischof, Christian.** Mechanical Stability of Mesoporous Molecular Sieves SBA-15 and MCM-48 Studied by Adsorption of Benzene, Cyclohexane and n-Heptane. *Chemie Ingenieur Technik.* 2001, Vol. 73, 6: 620.

39. **Ciahotný, Karel, Melenová, Lenka, Jirglová, Hana, Pachtová, Olga, Kocirík, Milan and Eic, Mladen.** Removal of ammonia from waste air streams with clinoptiloite tuff in its natural and treated forms. *Adsorption.* 2006, Vol. 12, 3: 219-226.

40. **Takahashi, Yusuke, Fujita, Hirotaka and Sakoda, Akiyoshi.** Adsorption of ammonia and water on functionalized edge-rich carbon nanofibers. *Adsorption.* 2013, Vol. 19, 1: 143-159.

41. **Mishin, I. V., Brueva, T. R. and Kapustin, G. I.** Heats of Adsorption of Ammonia and Correlation of Activity and Acidity in Heterogeneous Catalysis. *Adsorption.* 2005, Vol. 11, 3-4: 415-424.

42. **Barpaga, Dushyant and Le Van, M. Douglas.** In-pore synthesis of ZnCO3 in various adsorbents for NH3 and SO2 adsorption. *Adsorption.* 2017, Vol. 23, 1: 87-99.

43. **Meng, Bo, Shen, Wenzhong and Guo, Qingjie.** Preparation of Activated Carbons from Biomass and their Adsorption of Benzene, Ammonia, DIrect Red 23 and Iron Ions. *Adsorption Science & Technology.* 2008, Vol. Vol. 26, 3: 201-208.

44. **Gottfried, J. M., Schmidt, K. J., Schroeder, S. L. M. and CHristmann, K.** Adsorption of carbon monoxide on Au(1 1 0)-(1 x 2). *Surface Science.* 2003, Vol. 536, 206-224.

45. **Rohmann, C., Metson, J. B. and Idriss, H.** A DFT study on carbon monoxide adsorption onto hydroxylated alpha-Al2O3(0001) surfaces. *PCCP (Physical Chemistry Chemical Physics).* 2014, Vol. 16, 14287-14297.

46. **Itadani, Atsushi, Tanaka, Masashi, Abe, Takahiro, Taguchi, Hideki and Nagao, Mahiko.** Al-pillared montmorillonite clay minerals: Low-pressure CO adsorption at room temperature. *Journal of Colloid and Interface Science.* 2007, Vol. 313, 2: 747-750.

47. **De Haeck, Jorg, Veldeman, Nele, Claes, Pieterjan, Janssens, Ewald, Andersson, Mats and Lievens, Peter.** Carbon Monoxide Adsorption on Silver Doped Gold Clusters. *The Journal of Physical Chemistry A.* 2011, Vol. 115, 11: 2103-2019.

48. **Le, Hai Thuy, Lang, Sandra M., De Haeck, Jorg, Lievens, Peter and Janssens, Ewald.** Carbon monoxide adsorption on neutral and cationic vanadium doped gold clusters. *PCCP (Physical Chemistry and Chemical Physics).* 2012, Vol. 14, 9350-9358.

49. **Kessler, Hans Wolfram.** Krieg ohne Tränen? Reizstoff für die Bundeswehr. Zur Änderung des deutschen Ausführungsgesetzes zum Chemiewaffenübereinkommen. *Humanitäres Völkerrecht, Informationsschriften; Journal of International Law of Peace and Armed Conflict.* 2005, Vol. 18, 1: 4-10.

50. **Department of Employment.** *The Flixborough disaster: Report of the Court of Inquiry.* London, UK : Her Majesty's Stationery Office, 1975.

51. **Health and Safety Executive.** www.hse.gov.uk. [Online] [Cited: 15 May 2018.] http://www.hse.gov.uk/comah/sragtech/caseflixboroug74.htm.

52. **Barthelemy, Francois, Hornus, Henri, Roussot, Jaques, Hufschmitt, Jean-Paul and Rafoux, Jean-Francois.** *Report on the Grande Paroisse company's factory in Toulouse.* Paris, FR : Ministry for Regional Development and the Environment, 2001.

53. **Tse, Pui-Kwan.** The Mineral Industry of China. [ed.: Leahy, P. Patrick and Norton, Gale A.] *Minerals Yearbook, Area Reports: International 2003, Asia and the Pacific, Vol. III.* Washington, D.C., USA : United States Government Printing Office, 2006.

54. **Statistisches Bundesamt (Destatis).** *Fachserie 12 Reihe 4, Gesundheit, Todesursachen in Deutschland 2015.* Wiesbaden, GER : Statistisches Bundesamt (Destatis), 2017.

55. **Kaiser, G. and Schaper, A.** Akute Kohlenmonoxidvergiftung: Ein alter Hut in neuen Schachteln. *Notfall + Rettungsmedizin.* 2012, Vol. 15, 5: 429-435.

56. **Bliefert, Claus.** *Umweltchemie.* Weinheim, GER : VCH Verlagsgesellschaft, 1994.

57. **Baldauf, R., Watkins, N., Heist, D., Bailey, C., Rowley, P. and Shores, R.** Near-road air quality monitoring: Factors affecting network design and interpretation of data. *Air Quality, Atmosphere and Health.* 2009, Vol. 2, 1: 1-9.

58. **Azmi, Siti Zawiyah, Latif, Mohd Talib, Ismail, Aida Shafawati, Juneng, Liew and Jemain, Abdul Aziz.** Trend and status of air quality at three different monitoring stations in the Klang Valley, Malaysia. *Air Quality, Atmosphere and Health.* 2010, Vol. 3, 1: 53-64.

59. **Kim, H. S., Tans, P. P. and Novelli, P. C.** On the regional background levels of carbon monoxide observed in East Asia during 1991~2004. *Air Quality, Atmosphere and Health.* 2008, Vol. 1, 1: 37-44.

60. **Eberheim, Andreas.** *Qualifizierung von Halbleiter-Gassensoren für die Detektion spezifischer organischer Rauchgaskomponenten; Inaugural Dissertation.* Gießen, GER : Justus-Liebig-Universität Gießen, 2003.

61. **Lazaridis, M., Latos, M., Aleksandopoulou, V., Hov, Oe, Papayannis, A. and Toerseth, K.** Contribution of forest fire emissions to atmospheric pollution in Greece. *Air Quality, Atmosphere and Health.* 2008, Vol. 1, 3: 143-158.

62. **Zu, Ke, Tao, Ge, Long, Christopher, Goodman, Julie and Valberg, Peter.** Long-range fine particular matter from the 2002 Quebec forest fires and daily mortality in Greater Boston and New York City. *Air Quality, Atmosphere and Health.* 2016, Vol. 9, 3: 213-221.

63. **Basmer, Peter and Zwick, Gerhard.** *Forschungsbericht Nr. 137: Einsatzmöglichkeiten eines mobilen FT-IR-Gasanalysators bei der Feuerwehr Teile 1 und 2.* Karlsruhe, GER : Ständige Konferenz der Innenminister und -SenatorForschungsstelle für Brandschutztechnik an der Universität Karlsruhe (TH) und Ansyco Karlsruhe, 2004.

64. **Fischer, Toni, Weber, Anetta and Grandjean, Etienne.** Luftverunreinigung durch Tabakrauch in Gaststätten. *International Archives of Occupational and Environmental Health.* 1978, Vol. 41, 4: 267-280.

65. **Wiberg, Nils.** *Hollemann, Wiberg: Lehrbuch der Anorganischen Chemie.* Berlin, GER : de Gruyter, 1995.

66. **Kaltschmitt, Martin, Hartmann, Hans and Hofbauer, Hermann.** *Energie aus Biomasse: Grundlagen, Techniken und Verfahren, 3. aktualisierte und erweiterte Auflage.* Berlin, GER : Springer Vieweg, 2016.

67. **Barbosa, Vera L., Burgess, Joanna E., Darke, Kathryn and Stuetz, Richard M.** Activated sludge biotreatment of sulphurous waste emissions. *Reviews in Environmental Science & Bio/Technology.* 2002, Vol. 1, 4: 345-362.

68. **Tyndall, John and Coletti, Joe.** Mitigating swine odor with strategically designed shelterbelt systems: a review. *Agroforestry Systems.* 2007, Vol. 69, 1: 45-65.

69. **Wellburn, Alan.** *Luftverschmutzung und Klimaänderung: Auswirkungen auf Flora, Fauna und Mensch.* Berlin, GER : Springer, 1997.

70. **Dreisbach, Frieder, Täffner, Tim and Niemeyer, Bernd.** Application-oriented Assessment of Optimized Adsorbents for H_2S-Removal. [ed. Niemeyer, Bernd, Berger, Ralf, Krüger, Klaus, Matz, Gerhard, Otterpohl, Ralf and Stegmann, Rainer]. *Hamburger Berichte 36, Abfallwirtschaft: Odour Control.* Stuttgart, GER : Abfall aktuell, 2010.

71. **Wlotzka, Frank.** Untersuchungen zur Geochemie des Stickstoffs. *Geochimica et Cosmochimita Acta.* 1961, Vol. 24, 106-154.

72. **Decius, Maja.** *Prüfung der Funktionsweise und Effizienz einer biologischen Abluftreinigungsanlage unter Praxisbedingungen im Hinblick auf das Rückhaltevermögen für Bioaerosole; Inaugural Dissertation.* Hannover, GER : Tierärztliche Hochschule Hannover, 2016.

73. **Gronow-Schubert, Stephanie.** *Untersuchungen zum Emissionsgeschehen von Ammoniak und Methan in der Mastschweinehaltung; Dissertation.* Hohenheim, GER : Universität Hohenheim, 2017.

74. **Appl, Max.** *Ammonia: Principals and Industrial Practice.* Weinheim, GER : Wiley-VCH, 1999.

75. **Herwig, Heinz.** *Wärmeübertragung A-Z, Systematische und ausführliche Erläuterungen wichtiger Größen und Konzepte.* Hamburg, GER : Springer-Verlag, 1999.

76. **Philipp, Bertram and Stevens, Peter.** *Grundzüge der industriellen Chemie.* Weinheim, GER : VCH, 1987.

77. **Fujita, Eric M., Zielinska, Barbara, Campbell, David E., Sagebiel, John C. and Ollison, Will.** High-end exposure relationships of volatile air toxics and carbon monoxide to community-scale air monitoring stations in Atlanta, Chicago, and Houston. *Air Quality, Atmosphere and Health.* 2016, Vol. 9, 3: 311-323.

78. **Archibald, A.T., Ordónez, C., Brent, E. and Williams, M. L.** Potential impacts of emissions associated with unconventional hydrocarbon extraction on UK air quality and human health. *Air Quality, Atmosphere and Health.* 2018, Vol. 11, 6: 627-637.

79. **Egbers, Max.** *Analysis of Different Adsorbents to Separate Harmful Gas Components; Bachelor Thesis.* Hamburg, GER : Helmut-Schmidt-University / University of German Federal Armed Forces, 2015.

80. **Sánchez-Zambrano, Kléver Santiago, Duarte, Lairana Lima, Maia, Débora Aline Soares, Vilarrasa-García, Enrique, Bastos-Neto, Moisés, Rodríguez-Castellón, Enrique and Silva de Azevedo, Diana Cristina.** CO2 Capture with Mesoporous Silicas Modified with Amines by Double Functionalization: Assessment of Adsorption/Desorption Cycles. *Materials.* 2018, Vol. 11, 6: 887.

81. **Thiesen, Peter H., Robers, Ansgar, Praveen, Konidala and Niemeyer, Bernd.** Selection of Adsorbents for the Treatment of Malodours. [ed.: Chen, K., Tong, T. W. and Sarlos, G.] *Proceedings of the International Conference on Energy and the Environment; Volume 2.* Shanghai, CHI : Shanghai Scientific and Technology Publisher, 2003.

82. **Welsh, William A. and Chapman, David M.** Silica Gel. [ed.: Bohnet, Matthias, Brinker, Jeffrey, Cornils, Boy, Evans, Trevor, Greim, Helmut, et al.]. *Ullmann's Encyclopaedia of Industrial Chemistry Volume 32.* Weinheim, GER : Wiley-VCH, 2003.

83. **Analytical Methods Committee .** Evaluation of analytical instrumentation. Part XIX. CHNS elemental analysers. *Accreditation and Quality Assurance.* 2006, Vol. 11, 11: 569-576.

84. **Li, Yue, Täffner, Tim, Bischoff, Michael und Niemeyer, Bernd.** Test Gas Generation from Pure Liquids: An Application-Oriented Overview of Methods in a Nutshell. *International Journal of Chemical Engineering.* 2012.

85. **Linde Gas Deutschland.** *HiQ Spezialgase. Kompetenz für zukunftsorientierte Lösungen.* Pullach, GER : Linde AG, 2014.

86. **Cartillieri, Ansgar.** *Entwicklung von Adsorptionstrennverfahren zur Geruchsminimierung; Doctor Thesis.* Hamburg, GER : VDI Verlag, 2005.

87. **Silviana, Kareth, S. and Petermann, M.** Durability assessment and physical properties investigation of modified petung bamboo (Dendrocalamus asper) as resulted on acetylation, assisted by supercritical CO2. *Procedia Chemistry.* 2014, Vol. 9, 273-283.

88. **Bel Japan Inc.** *Instruction Manual Belsorp-Aqua 3.* Osaka, JPN : Bel Japan Inc., 2012.

89. **Nierobisch, Paul.** *Erarbeitung einer Arbeitsanweisung zur Erstellung von Adsorptionsisothermen mit der "BELSORP-AQUA 3"; student research paper.* Hamburg, GER : Helmut-Schmidt-University / University of German Federal Armed Forces, 2014.

90. **Yadigaroglu, George.** Pressure Drop - Empirical Methods. [ed.: Yadigaroglu, George and Hewitt, Geoffrey F.]. *Introduction to Multiphase Flow; Basic Concepts, Applications and Modelling.* Cham, CH : Springer International Publishing, 2018.

91. **Emig, Gerhard and Klemm, Elias.** *Chemische Reaktionstechnik, 6. Auflage.* Berlin, GER : Springer Vieweg, 2017.

92. **Puerta, Johann, Blender, Karl and Niemeyer, Bernd.** *Naturwissenschaftlich-Technisches Praktikum: Chemische Reaktoren, Verweilzeit- und Mischungsverhalten, Umsetzung von Stoffen.* Hamburg, GER : Helmut-Schmidt-University / University of German Federal Armed Forces, 2016.

93. **Stephan, Peter and Stephan, Karl.** Thermodynamik. [ed.: Grote, Karl-Heinrich, Bender, Beate and Göhlich, Dietmar]. *Dubbel - Taschenbuch für den Maschinenbau, 25. Auflage.* Berlin / Heidelberg, GER : Springer Vieweg, 2018.

94. **Baehr, Hans Dieter.** *Thermodynamik - Grundlagen und technische Anwendungen; 11. Auflage.* Bochum, GER : Springer-Verlag, 2002.

95. **Hauffe, Karl and Morrison, S. Roy.** *Adsorption: Eine Einführung in die Probleme der Adsorption.* Berlin, GER : De Gruyter, 1974.

96. **Henning, Klaus-Dirk and Kienle, Hartmut v.** Activated Carbon. [ed.: Bohnet, Matthias, Brinker, Jeffrey, Cornils, Boy, Evans, Trevor, Greim, Helmut, et al.]. *Encyclopedia of Industrial Chemistry; Sixth, Completely Revised Edition; Volume 6 Butenes to Cellulose Ethers.* Weinheim, GER : Wiley-VCH, 2003.

97. **Benstöm, Frank.** *Granulierte Aktivkohle zur Elimination organischer Spurenstoffe aus kommunalem Abwasser; Doctor Thesis.* Aachen, GER : RWTH Aachen, 2017.

98. **Blender, Karl, Horn, Helena, Niemeyer, Bernd and Lassen, Stephan.** Carbon monoxide elimination for health and safety: new powerful silica-based adsorbents applied in continuous breakthrough experiments at elevated laboratory scale. *Air Quality, Atmosphere and Health.* 2018, Vol. 11, 9: 1049-1057.

99. **Dorn, Daniel.** *Researches for the Separation of Different Toxic Environmental Gases from the Air with Newly Developed Materials; Master Thesis.* Hamburg, GER : Helmut-Schmidt-University / University of German Federal Armed Forces, 2018.

100. **Boysen, Chris.** *Planning, Assembly and Commissioning of a Safety-Related Experimental Standard for the Investigation of the Efficiency of Integrated Air Purification Systems; Master-Thesis.* Hamburg, GER : Helmut-Schmidt-University / University of German Federal Armed Forces, 2017.

101. **Birkenseer, Matthias.** *Adsorptive Abtrennung und katalytische Oxidation von Geruchstoffen; Doctor Thesis.* Hamburg, GER : Shaker Verlag, Aachen, 2010.

List of Figures

List of Tables

Curriculum Vitae

For reasons of data protection, the curriculum vitae is not published in the electronic version of the paper.